



Department of Energy
Washington, DC 20585

APR 18 1994

Mr. Joseph J. Holonich, Director
Repository Licensing and Quality
Assurance Project Directorate
Division of High-Level Waste
Management
Office of Nuclear Material Safety
and Safeguards
U.S. Nuclear Regulatory Commission
Washington, DC 20555

Dear Mr. Holonich:

Enclosed for your information is a preliminary draft copy of Section VII, "Volcanic Risk Assessment for the Potential Yucca Mountain Site," which is a part of the draft Volcanism Status Report prepared by the Los Alamos National Laboratory.

The draft chapter of the volcanism report is being provided concurrently to members of the Advisory Committee on Nuclear Waste (ACNW), of the U.S. Nuclear Regulatory Commission (NRC), in advance of its 63rd meeting to be held on April 20-21, 1994, in which representatives from the Yucca Mountain Site Characterization Office and Los Alamos National Laboratory will provide presentations on the topic of volcanism studies underway in the characterization of the Yucca Mountain site on April 20, 1994. The purpose for providing Section VII of the preliminary draft volcanism status report to the ACNW members in advance of its meeting is to enhance the Committee members' knowledge of DOE's volcanism efforts to date.

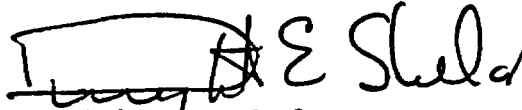
Presently, the preliminary draft volcanism status report (including Section VII) has not been reviewed or approved by DOE. As such, the contents of this report may not reflect the current position of DOE.

9404210080 940418
PDR WASTE
WM-11 PDR

102.8
wm-11
NHO3

If you have any questions, please contact Sharon Skuchko of my office at (202) 586-4590.

Sincerely,

A handwritten signature in black ink, appearing to read "Dwight E. Shelor". The signature is written in a cursive style with a large, stylized "S" at the end.

Dwight E. Shelor
Associate Director for
Systems and Compliance
Office of Civilian Radioactive
Waste Management

Enclosure:

Section VII, "Volcanism Risk Assessment
for the Potential Yucca Mountain Site,"
of the Preliminary Draft Volcanism
Status Report, prepared by the Los Alamos
National Laboratory

cc w/Enclosure:

R. Nelson, YMPO
T. J. Hickey, Nevada Legislative Committee
R. Loux, State of Nevada
D. Bechtel, Las Vegas, NV
L. Fiorenzi, Eureka County, NV
R. Williams, Lander County, NV
P. Niedzielski-Eichner, Nye County, NV
W. Offutt, Nye County, NV
L. Bradshaw, Nye County, NV
C. Schank, Churchill County, NV
F. Mariani, White Pine County, NV
V. Poe, Mineral County, NV
J. Pitts, Lincoln County, NV
J. Hayes, Esmeralda County, NV
B. Mettam, Inyo County, CA
M. Steinder, ACNW
L. Deering, ACNW

DRAFT

INFORMATION COPY

PRELIMINARY DRAFT
INFORMATION ONLY

1

SECTION VII: VOLCANIC RISK ASSESSMENT FOR THE POTENTIAL YUCCA MOUNTAIN SITE

I. SUMMARY

Section VII presents the status of volcanic risk assessment for the potential Yucca Mountain site focusing on estimating the occurrence probability of magmatic disruption of a repository. Probabilistic risk assessment is reviewed through evaluating the most likely, minimum, and maximum estimates of a range of alternative models of the geologic record of basaltic volcanism in the Yucca Mountain region (YMR). The purpose of these estimates is to explore the scientific basis for constraining and defining the distribution of data for a conditional probability model of potential repository disruption by magmatic processes. These studies provide the background foundation for formal probabilistic assessment of volcanic risk for the potential Yucca Mountain site in future reports by the Department of Energy (DOE).

The risk of future volcanism for the potential Yucca Mountain site is assessed as a conditional probability: $Pr_{dr} = Pr(E3 \text{ given } E2, E1)Pr(E2 \text{ given } E1)Pr(E1)$, where $E1$ denotes the recurrence rate of volcanic events, $E2$ denotes the probability of intersection of specified areas, and $E3$ is the probability of exceeding regulatory releases directly through volcanic eruptions or indirectly through changes in the waste isolation system. This conditional probability is expressed mathematically as an exponential or modified exponential equation on the basis of several assumptions: 1) a homogeneous, modified homogeneous, or nonhomogeneous Poisson distribution of volcanic events in time and space, 2) forward projection of past patterns of volcanic events, 3) use of current site characterization data for the identification and description of past volcanic events, and 4) incorporation of alternative interpretations of the eruption models of volcanic centers, and the chronology and structural controls of volcanic events in risk simulation to aid in the definition of uncertainty.

The strategy for assessing the issue of volcanism is to examine a series of questions focused on assessing the data needed for evaluating the risk of volcanism. There are four questions. (1) Is igneous activity a concern for the potential Yucca Mountain site? (2) What is the range of possible future volcanic events? (3) What is the occurrence probability of each type of volcanic or magmatic activity? (4) Where could future volcanic events occur? The presence of five Quaternary volcanic centers in the vicinity of Yucca Mountain is the primary basis for identifying the presence of the potentially adverse condition of future igneous activity. The range of possible future volcanic events includes the formation of a new volcanic center (λ_n), the formation of a cluster of volcanic centers (λ_c), the recurrence rate of magmatic intrusions (λ_i), the recurrence of polycyclic eruptions at an existing volcanic center (λ_p), and the probability of intra-cluster volcanic eruptions (λ_{cc}). Current site characterization information combined with simple logic require that $\lambda_i > \lambda_n > \lambda_c$, that $\lambda_i \approx \lambda_n$ and $\lambda_i, \lambda_n, \lambda_c$ are all $> 10^{-4}$ events yr^{-1} .

Pliocene and Quaternary volcanic activity in the YMR has been predominately mixed hawaiian and strombolian with minor hydrovolcanic eruptions. The occurrence frequency of hydrovolcanic eruptions is estimated to be $< 10\%$, particularly for areas of deep ground water. There is a very high probability ($> 95\%$) that future volcanic activity will occur within the distribution area of past volcanic events (the YMR), a high probability ($> 90\%$) that future events will occur within the Crater Flat volcanic zone (CFVZ), and a lesser probability of occurring in a northeast-trending structural zone (NESZ; 75%). Future volcanic events are about 6 times more likely to occur in an alluvial valley or range front than in a range interior.

Four time intervals are used to assess recurrence models of volcanic events (E1). One interval of emphasis is the Quaternary epoch; both the current geologic definition (1.6 Ma) and the regulatory definition (2.0) are used. A more appropriate and preferred approach to identifying time intervals for probabilistic assessment is to base them on recognized cycles of volcanic activity in the YMR (volcanic record). Two cycles are emphasized. The first is the duration of the Younger postcaldera basalt cycle (4.8 Ma). The second is a somewhat arbitrary interval in the Quaternary that corresponds to a time of possible increased frequency of volcanic events (1.0 Ma). The volcanic events λ_i , λ_v , λ_c are defined from the perspective of their impact on a geologic repository located about 300 m below the surface. A volcanic event is assumed to consist of the rapid emplacement of 1 to 3 dikes that feed surface volcanic eruptions. Any volcanic vent or center spaced over 5 km distance from another volcanic vent or center is presumed to represent a separate volcanic event. Events spaced less than 5 km are inferred to represent a single event unless field, geochronology or geochemical data indicate the vents formed from time-distinct events or separate pulses of magma. Polycyclic volcanism represents a special subclass of volcanic events. A polycyclic episode is defined as an eruption at a preexisting volcanic center that is separated in time from the preceding volcanic event by an interval exceeding the residence time of basaltic magma in the shallow crust (decades). It is dependent on the occurrence of a preceding event defined as the formation of a new volcanic center and is therefore a subclass of λ_c . Probabilistic assessment of polycyclic episodes will be considered in future volcanism studies.

The current data for the Pliocene and Quaternary volcanic record of the YMR are used in probabilistic risk assessment. The Quaternary volcanic record includes three groups of volcanic centers. The Quaternary basalt of Crater Flat consists of one cluster event or two to five center events. Each event is estimated to be 1.0 ± 0.1 Ma. Polycyclic episodes are suspected at the Red Cone and Black Cone centers. The basalt of Sleeping Butte is treated as two individual centers formed in one cluster event and one or two center events. Existing geochronology data have a mean age of 320 ± 50 ka but are not considered to be definitive. A Pleistocene episode of polycyclic activity may have occurred at the Hidden Cone center. The Lathrop Wells volcanic center is treated as a single-event volcanic center with three polycyclic episodes. The initiating event is estimated to be about 120 to 130 ka. The first polycyclic episode followed at 80 to 90 ka, the second at 40 to 60 ka, and the youngest at 4 to 9 ka. The estimated uncertainty of the initiating event and first polycyclic episode is ± 35 ka, and the uncertainty of the second polycyclic episode is ± 40 ka. The uncertainty of the youngest polycyclic episode cannot be estimated with current data. Pliocene volcanic centers include the basalt of Thirsty Mesa (4.8 ± 0.13 Ma), the aeromagnetic anomaly of the Amargosa Valley (3.85 Ma), the aeromagnetic anomalies (two anomalies) of central Amargosa Valley (undrilled but presumed to be the same age as the aeromagnetic anomaly of the Amargosa Valley), the basalt of southeast Crater Flat (3.74 ± 0.10 Ma) and the basalt of Buckboard Mesa (2.9 ± 0.13 Ma).

Revised estimates of E1, the recurrence rate of volcanic events, are examined systematically using time-series analysis, homogeneous Poisson and nonhomogeneous Poisson models, and magma-output rates. Time-series analysis is limited by the small record of Pliocene and Quaternary volcanic events. Some bounds on estimates can be approximated by assessing event repose times. The *minimum* repose interval during the last 4.8 Ma is 200 ka, and is equivalent to an eruptive recurrence rate of 5.2×10^{-6} events yr^{-1} . The mean estimate of the recurrence rate is 1000 ± 570 ka ($n = 6$) and provides little information. Homogeneous Poisson recurrence rates are examined for four time intervals, using event, cluster, and stress-dike event counts; estimates are obtained for the *minimum*, most likely and maximum recurrence rates. The mean recurrence rate for the *most likely* recurrence models is $3.5 \pm 1.3 \times 10^{-6}$ events yr^{-1} ; the mean of all *minimum* recurrence rates is $2.0 \pm 0.6 \times 10^{-6}$ events yr^{-1} and the *minimum* or best case estimate

is 1.5×10^{-6} events yr^{-1} . The mean of the *maximum* recurrence rates is $4.6 \pm 4.3 \times 10^{-6}$ events yr^{-1} and the *maximum* or worse case recurrence rate is 8.0×10^{-6} events yr^{-1} . The mean recurrence rate for the *most likely* recurrence models using nonhomogeneous Poisson models is $4.6 \pm 1.8 \times 10^{-6}$ events yr^{-1} . The mean of the *minimum* recurrence rate is $3.0 \pm 1.2 \times 10^{-6}$ events yr^{-1} and the minimum or best case recurrence rate is 1.4×10^{-6} events yr^{-1} . The mean of the *maximum* recurrence rate is $5.5 \pm 2.4 \times 10^{-6}$ events yr^{-1} and *maximum* or worse case recurrence rate is 8.4×10^{-6} events yr^{-1} . The β (fitting parameter for the Weibull distribution) is < 1 for all recurrence models using volcanic cycles, and is consistent with waning volcanism during both the last 4.8 Ma and the last 1.0 Ma. Volumes of volcanic eruptions during the last 4.8 Ma (DRE) have decreased by $>$ a factor of 30. Simple linear regression fits of magma volume versus time are unsatisfactory. Regression coefficients for different combinations of plots of magma volume versus time indicate strong correlations (squared multiple $R > 0.86$ for all but two cases). Linear regression models show that the basalt of Thirsty Mesa is an outlier. Residual plots show linearity and curvilinear structure. A log normalized regression model provides improved regression fits but the basalt of Sleeping Butte is an outlier, and there is structure to the regression residuals. Future work will examine event location and magma chemistry as variables in multiple regression. Two linear regression cases give marginally acceptable fits and have slopes (magma-output rates) of 270 and 300 $\text{m}^3 \text{yr}^{-1}$. These rates are used to calculate event recurrence times using different estimates of the volume of representative volcanic events. The only geological reasonable recurrence times are obtained for the mean volume of the *smallest* volume Quaternary eruptive events because of the 30-fold decrease in magma volumes through time. The mean estimate of the event recurrence rate is 3.4×10^{-6} events yr^{-1} for *preferred* models; *minimum* recurrence times are 3.2×10^{-6} events yr^{-2} and *maximum* recurrence times are 5.3×10^{-6} events yr^{-1} . Risk simulation is used to model recurrence rates for the YMR. The *median* estimates for eight recurrence models and five simulations using different boundary conditions (*minimum* and *maximum*) and distribution assumptions (trigen and normal distributions) vary from 3.6×10^{-6} events yr^{-1} to 5.5×10^{-6} events yr^{-1} .

Revised estimates of E2, the disruption probability, are examined systematically using spatial distribution models, structural models, and comparison with analog basaltic volcanic fields. Twenty-five spatial distribution models are evaluated. Eleven models are unlikely to result in repository disruption; three additional models are judged to have a low likelihood of resulting in repository disruption. The median estimate of the disruption probability for 14 spatial models (*including* the three unlikely models) is $3.1 \pm 1.5 \times 10^{-3}$ (dimensionless ratio). The median estimate for the 14 spatial models of the disruption probability is 4.6×10^{-4} if the models are weighted for the likelihood of volcanic events in range interiors. Seventeen structural models are used to estimate E2; four of the models include the potential Yucca Mountain site, one is judged to have a moderate likelihood of extending to the site, and the remaining 12 models are judged to have a low or improbable likelihood of extending to the potential site. The median estimate of the disruption probability for all models is $4.6 \pm 4.4 \times 10^{-3}$. The median estimate is 6.9×10^{-4} if the disruption probability is weighted for the likelihood of volcanic events in range interiors. The median estimate of intersection models (models that include the potential Yucca Mountain site) is $3.1 \pm 1.1 \times 10^{-3}$ ($4.7 \pm 1.6 \times 10^{-4}$ for range interiors). Structural models inferring northeast-trending structural controls of volcanic events *do not yield significantly higher* estimates for the disruption probability. Simple spatial analyses of the distribution of volcanic events in the Cima and Lunar Crater volcanic field show that the degree of dispersion of volcanic events orthogonal to the elongation direction of the fields is comparable to the observed dispersion of vents in the YMR. If these fields are overlain on the YMR with their long dimension oriented parallel to the CFVZ, the observed dispersion of events in the analog fields would not penetrate the potential Yucca Mountain site. Simulation modeling is used to assess the variability in E2. A simulation matrix is constructed using five sets of model estimations for E2 and two subclasses for each

model. The mean estimates of intersection models range from 3.1 to 4.6×10^{-3} ; the mean estimates of the range interior models range from 4.7 to 7.7×10^{-4} .

The cumulative probability distributions for E1 and E2 are combined through risk simulation to give the cumulative probability distribution for the probability of magmatic disruption of the repository [$\Pr(E2 \text{ given } E1)\Pr(E1)$]. Two sets of simulation matrices were evaluated. The first uses two distribution curves for E2 (intersection and range intersection) and a range of distribution models for E1. The second uses a single distribution curve for E1 and varies distribution models for E2. The median estimates for the first simulation matrix range from 2.1 to 2.6×10^{-8} events yr^{-1} for intersection models, and 3.2 to 3.9×10^{-9} for range intersection models. The median estimates of the second matrix are more variable and range from 0.7 to 7.2×10^{-8} events yr^{-1} for intersection models and 6.3×10^{-10} events yr^{-1} to 1.1×10^{-8} events yr^{-1} for range intersection models. The *maximum* estimates for the probability of magmatic disruption of the repository are the largest calculated for the YMR. Careful examination of the data shows that they result from spatial and structural models that have a very low likelihood of intersecting the potential repository site. Judgment is required whether these models should be incorporated in probability estimates. A final set of estimations of the probability of magmatic disruption of the repository is evaluated for specific models of the probability of disruption, E2. This is required because some spatial and structural models exclude volcanic events. A probability matrix was assembled and E1 recalculated for individual spatial and structural models. The median estimate for all models using the revised estimates for E1 is $1.8 \pm 1.6 \times 10^{-8}$ events yr^{-1} (intersection models) and $2.7 \pm 2.1 \times 10^{-9}$ events yr^{-1} (range interior models) or smaller by 17% to a factor of 4 than the models without the revisions of E1. Two models are identified as worse cases in the probability matrix.

II. INTRODUCTION

Section VII of the Volcanism Status Report presents the status of volcanic risk assessment for the potential Yucca Mountain site current to the preparation of this report. The assessment builds on the data and methods for probability estimates from published studies (Crowe and Carr 1980; Crowe et al. 1982; 1983; Crowe 1986; Crowe et al. 1989; Crowe and Perry 1989; Smith et al. 1990; Ho et al. 1991; Wallmann et al. 1992; Crowe et al. 1992; Ho 1992; Connor and Hill 1993; Wallmann et al. 1993; Crowe et al. 1994), and adds the most recent results from site characterization studies. The terms *volcanic hazard* refer to the perception of a peril or jeopardy from future volcanic events. The term *risk* denotes the attempt to quantify the magnitude of a volcanic hazard. *Risk assessment* includes evaluation of the probability of event occurrence combined with the consequences of that event. Most volcanism studies for the potential Yucca Mountain site have focused on estimating the *occurrence probability* of magmatic disruption of a repository; only a few studies have combined the occurrence probability with assessments of the *consequences* of a volcanic event. We use the formal definitions of these terms throughout this section of the *Volcanism Status Report* to avoid confusion, and to discriminate between *probabilistic assessment* (occurrence probability) and *risk assessment* (occurrence probability combined with event consequences). The term *risk* is used when either the occurrence probability or consequences of a volcanic event have been determined; its usage does not require definition of both occurrence probability *and* consequences. Some authors use the term *hazard* to refer to the probability that a specific area will be affected by a volcanic eruption (Scandone et al. 1993). We prefer to use the term *volcanic hazard* less specifically, and use *probabilistic assessment* or *occurrence probability* to refer to probabilistic studies.

The primary emphasis of past volcanism studies was on evaluation of the potential disqualification of the Yucca Mountain site from the hazards of future volcanic activity (Crowe and Carr, 1980; Crowe et al. 1982), recognizing that the Department of Energy (DOE) has the formal responsibility to assess the potential disqualification of the Yucca Mountain site. One of the purposes of this report is to attempt to define the occurrence probability of volcanic events for given areas or regions as an aid to the DOE in their continuing assessment of the potential Yucca Mountain site. To accomplish this task, a conditional probability model is described for future volcanic events in the Yucca Mountain region (YMR). The logic of volcanism studies are presented. These studies are designed to test underlying assumptions, and meet the data requirements of the conditional probability model. The volcanic record of the YMR that is applied to the volcanic model is defined carefully to avoid confusion in probability estimations. Assumptions needed to apply the record to the probability model are described, and the basis for the assumptions are described from the perspective of the underlying volcanic processes in the YMR. Probability estimations are constructed for a range of alternative recurrence and structural models of basaltic volcanism. The uncertainty of the probability range is defined by calculating cumulative probability distributions through application of risk simulation. The cumulative probability distributions for E1 and E2 are integrated for the potential repository area, the controlled area, and the Yucca Mountain region (YMR). These probability distributions represent the best approximation, given current site data, of the occurrence of volcanic events using a scientific perspective. These numbers *may differ* from those used by the DOE in formal assessments of the suitability or unsuitability of the potential Yucca Mountain site from regulatory perspectives.

This section of the *Volcanism Status Report* focuses on the occurrence probability of magmatic disruption of a potential repository, the controlled area encompassing a repository, and the YMR. We use a slightly different perspective than past studies, including past studies by ourselves and other workers. Past volcanism studies attempted primarily to bound the occurrence probability of volcanic events. This was accomplished through identification of a range of *permissive* values that could be assigned to attributes of the probabilistic assessment. If there was uncertainty involving assignment of data values, conservative values or values that would *not* underestimate risk were used (Crowe and Carr 1980; Crowe et al. 1982; 1992). Many assessments emphasized worst case or maximum estimates of volcanic occurrence probabilities (Ho et al. 1991; Ho 1992; Connor and Hill 1993). In contrast, we initiate a new perspective of assessing attribute values for probabilistic risk assessment that includes *most likely*, *minimum*, and *maximum* values for a range of alternative models of the geologic record of basaltic volcanism in the YMR. The identification of most likely values (mid-point estimates) avoids the addition of non-systematic bias toward worst case calculations that are built unavoidably into calculations when only conservative attribute values are used. This bias results primarily from the absence of a standard definition of "conservatism" in the assignment of probability values. The choice of what constitutes "reasonable" levels of conservatism in assigning attribute values varies dramatically with the perspective of the assignee. This is especially true for an issue like assessing risk for a potential site for storage of high-level radioactive waste. The political and scientific sensitivities of the issue can lead to dramatic differences in probabilistic assessments for technical issues that could potentially disqualify the site. In contrast, assigning mean or most likely values for probability attributes are better defined. These values are chosen as the approximation of the central tendency of data distributions. They can be expressed as means, medians, or other appropriate univariate statistical descriptors. The uncertainty of estimates of the occurrence probability of volcanic events is assessed using simulation modeling incorporating the mid-point, minimum, and maximum estimates of probabilistic attributes (Crowe et al. 1994). Our primary goal in this work is to explore the range of probability estimates that can be supported scientifically from systematic examination of multiple alternative models of the volcanic record in the YMR.

The traditional and most common approach for defining volcanic hazards is to study the past record of volcanism at and around a site of interest. These studies employ standard geological methods (field mapping, geochronology, petrology, geochemistry and geophysics). Information from the conventional studies is used to make subjective judgments about the hazards of future volcanism. This generally involves identifying the eruptive styles of past volcanic events, the area affected by past volcanic activity, and the hazards represented by similar future events. A general but not universal assumption of these studies is that future volcanic activity will follow the same patterns as past volcanic activity. This approach has utility for historically active volcanoes. Recent growth in world population has led to occupation of land surrounding the flanks of many active volcanoes, and created the need, often in a crisis situation, to define volcanic hazards. However, that is a very different assessment than the probabilistic volcanic assessment conducted for the YMP. There is a higher degree of predictability for hazard assessment of historically active volcanoes. Generally, historically active polygenetic volcanoes are fed from a shallow magma chamber with an established magma feeder system. Alerts to impending eruptive activity or a volcanic crisis develop when there are changes in the volcano from changes in a magma chamber or parts of the magma feeder system. The continued existence of the chamber through periodic replenishment with new pulses of magma results in a high chance that future volcanic activity will occur at or near the same vent areas. Often eruptive patterns of new volcanic events are similar to past volcanic eruptions. The time perspective of volcanic hazard studies is months, to years, to decades, at most.

The conventional approaches to volcanic hazard studies are not easily applied to the issue of defining risk for the long-term isolation of high-level radioactive waste. Here the task of identifying the nature of a future volcanic hazard is obvious. It is the simple recognition that future volcanic activity could disrupt a buried repository, and spread radionuclides to the accessible environment. A more pertinent and difficult question is how can the risk of the perceived volcanic hazard be quantified? The risk in most cases is not from another eruption at an existing volcano, but from the birth of a new volcano that potentially could erupt through or near a repository. The added uncertainty is that the volcanic risk is more difficult to define with respect to the timing and location of a future volcanic event.

Past basaltic volcanic activity in the YMR was characterized by the intermittent formation of spatially isolated, small volume basalt centers of Pliocene and Quaternary age (Crowe 1986; Crowe and Perry 1989; Crowe 1990). The geochemistry of these lavas almost certainly is inconsistent with storage of magma in a shallow crustal magma chamber (see Section IV, this report). The basalts are aphyric to sparsely porphyritic, and probably ascended rapidly from a depth below the plagioclase stability field (Perry and Crowe 1992). Magma formed as spatially and temporally separate pulses, and followed unique pathways to the surface.

There are atypical problems in evaluating recurrence rates and predicting the spatial location of the future volcanic centers in the Yucca Mountain region (see Section III). First, there is a limited record of past volcanic events (7 Quaternary volcanic centers). The record of events is insufficient to describe using conventional statistical approaches or to test hypotheses using measures of goodness of fit. We can only approximate time-distribution models, and attempt to construct probability calculations that do not underestimate risk. Second, volcanic centers tend to occur within a narrow northwest-trending zone called the Crater Flat Volcanic zone (CVFZ; Crowe and Perry, 1989). The most likely location of future events is in this zone. During the last 4.8 Ma, there were 19 volcanic events in the zone, and only one event outside of the zone. The Pliocene basalt of Buckboard Mesa is located in the Timber Mountain caldera about 37 km northeast of the potential Yucca Mountain site; it is the only Plio-Quaternary center that

occurs outside of the CFVZ. This raises a small but finite possibility that events could occur *outside* the CFVZ and possibly within Yucca Mountain (see Smith et al. 1990). Third, within the CFVZ, the location of subsequent volcanic events bears no simple relation to the location of preceding volcanic events (Crowe et al. 1994). Sites of successive volcanic events jump to new locations with no systematics to their either their jump directions or jump lengths. The only observed pattern is a high likelihood for events to remain within the CFVZ. Fourth, new volcanic events occur as individual centers, or as clusters of centers (Crowe and Perry, 1989). The lengths of the clusters vary from 2 to 13 kilometers. The clusters tend to be aligned northeast, parallel to the maximum compressive-stress direction (Crowe et al. 1986; Crowe 1990). Locally, this direction is coparallel to faults in Yucca Mountain (Crowe and Carr, 1980; Smith et al. 1990). The spatial patterns of Pliocene and Quaternary volcanic activity in the YMR lack the spatial predictability of repeated volcanic eruptions of a stratavolcano fed from a shallow and long-lived magma chamber.

A preferred strategy for attempting to quantify aspects of the risk of future volcanic events is to use a probabilistic approach; it has several distinct advantages over standard volcanic hazard studies. First, a probabilistic approach attempts to quantify a problem, and provide a more easily defined basis for judging acceptable or unacceptable risks. In contrast, hazard studies identify zones where future volcanic events might occur. Second, a probabilistic approach brings a structured formalism to the problem. This allows a complex issue like predicting the risk of future volcanism to be subdivided into logical sections with set rules for combining the results of each section. Precise answers cannot always be given for each section of a probabilistic approach, but the coupled probabilities can generally be bounded. Decisions can be made whether the bounding data are acceptable or unacceptable. Third, an often unappreciated advantage of a probabilistic approach is flexibility. The importance of alternative models or different data interpretations can be assessed by examining how they change the probability distributions. Volcanic studies for the potential Yucca Mountain site require working with a small data set. The limitations of the data set make it likely, if not expected, that there will be different views of the nature and risk of future volcanic activity. Moreover, by virtue of the limited data, it is very difficult to conclusively prove or disprove alternative models. Instead, the different views become important only if they change the probability distributions. Fourth, probabilistic studies are iterative. Once formulated, they can be refined readily with the addition of new data from site characterization studies. The results of the assessment can be upgraded continuously as new data are gathered. In fact, the test for judging the importance of new site characterization data is a determination of whether the new data change the probability distribution. Finally, the most important advantage of a probabilistic approach is it allows the data to be compared with the regulatory requirements for licensing of a repository.

There are three parts to this section of the *Volcanism Status Report*. First, the probability models are described, and the logic is presented of how the probability models are used to assess the risk of volcanism for the Yucca Mountain site. Much of the confusion and differences in assessing the probability of magmatic disruption of the potential Yucca Mountain site result from a lack of consistency in applying a probabilistic approach, and stating clearly the assumptions used for that assessment. Second, the data set used for the probabilistic assessment is defined, the assumptions used in the data set are described, and the underlying physical models controlling interpretations of the record of basaltic magmatism are assessed. These data are applied to estimations of revised values of the probability of magmatic disruption of a potential repository located beneath the surface of Yucca Mountain. The mid-point, maximum, and minimum values of the distribution of probability attributes are estimated. Simulation modeling is conducted using these values to define the uncertainty of probability assessments. This section of the volcanism status report constitutes the formal initiation of the systematic process of probabilistic studies

described in Study Plan 8.3.1.8.1.1 Probability of Magmatic Disruption of the Repository. The purpose of presenting these numbers is, again, to provide a scientifically defensible basis for probabilistic assessment of future volcanic events. The actual application of the data presented in this report to formal assessments of the potential Yucca Mountain site will be undertaken by the DOE.

The probabilistic estimates presented in this report are not final. There is always the possibility of new discoveries through continuing site characterization studies that may change the results of the assessment of the risk of volcanism. However, the basic data and approach used for assessing the risk of volcanism (occurrence probability combined with consequences) for the potential Yucca Mountain site were described as early as 1980 (Crowe and Carr 1980) and formalized in 1982 (Crowe et al. 1982). Continuing reviews, evaluations, and questioning of these assessments have occurred over more than a decade. Reviews of the probability studies have focused on identifying differences in assumptions used to make probability calculations. In almost all cases, the different assumptions do not result in significantly changed probability distributions. There is and will continue to be a virtually unconstrained number of methods that can be used to construct volcanic probability calculations for the potential Yucca Mountain site. Because of the limited data set used for the calculations, there never will be complete agreement on the best or even the more appropriate method to use. Given this uncertainty, the only realistic test of the significance of alternative models is whether they lead to probability distributions that differ significantly from existing estimations.

III. PROBABILITY MODEL

The probability of magmatic disruption of a repository and release of radionuclides to the accessible environment (Pr_{dr}) is defined as a conditional probability:

$$Pr_{dr} = Pr(E3 \text{ given } E2, E1)Pr(E2 \text{ given } E1)Pr(E1), \quad (7.1)$$

where $E1$ denotes the recurrence rate of volcanic events in the YMR, $E2$ denotes the probability that the future magmatic event intersects a specified area, and $E3$ denotes the probability that magmatic disruption leads to rapid release of radionuclides to the accessible environment in quantities that exceed the regulatory requirements. This probability can be expressed mathematically as (Crowe et al. 1982):

$$Pr[\text{no eruptive event before time } t] = \exp(-\lambda t p r), \quad (7.2)$$

where λ is the recurrence rate of volcanic events, p is the probability that an event is disruptive, and r is the probability that the radionuclide releases to the accessible environment exceed the regulatory requirements for licensing a repository. The λ can be defined in a number of ways (see following discussion). For this report, it is defined as the rate of formation of new volcanic centers or magmatic intrusions. The p is defined as a/A where a is the area of concern (repository, controlled area or YMR), and A is the area of the established volcanic rate or λ .

A basic assumption used in the application of the probability model is a homogeneous or modified homogeneous Poisson distribution of the volcanic events in time and space (Crowe et al. 1982; Crowe 1986). A Poisson random variable with parameter $\lambda > 0$, has a probability density function (Devore, 1987; Tuckwell 1988)

$$f(x) = \frac{e^{-\lambda} \lambda^x}{x!} \quad (7.3)$$

The probability density function can be integrated over (x_1, x_2) to obtain the probability of X

$$\Pr\{x_1 < X < x_2\} = \int_{x_1}^{x_2} f(x) dx. \quad (7.4)$$

A Poisson random variable has mean $E(X) = \lambda$, variance = λ , and standard deviation = $\sqrt{\lambda}$ (Tuckwell, 1988). The Poisson distribution is a special case of the binomial distribution when n , the number of trials, becomes very large, and p , the event probability, becomes very small. The Poisson distribution is easier to calculate than the binomial distribution because $np = \lambda$, and λ is the rate of occurrence of events (Davis, 1986). Critical assumptions of the Poisson distribution are that the events occur independently, they are exponentially distributed through time t , and the probability of more than one event occurring at the same time is vanishingly small (Davis 1986; Devore 1987). The rate parameter or intensity (λ) of a homogeneous Poisson (HPP) is assumed to be independent of its interval or time; λ for a nonhomogeneous Poisson (NHPP) is assumed to be a function of t , denoted as $\lambda(t)$ (Tuckwell, 1988; Ho 1991). The versatility of application of the Poisson process is that individual non-Poisson processes often become Poisson when considered together (Tuckwell, 1988).

Crowe et al. (1992) reviewed recurrence models for volcanic events, and discussed the rationale for choosing a simple Poisson model. Briefly, the model is conceptually simple, assumptions using this model are well defined, and potential errors can be constrained. The simple Poisson model is widely used in many volcanism studies (De la Cruz-Reyna 1991; Scandone et al. 1993). The Poisson model is particularly appropriate and may be conservative for the case of the YMR where multiple lines of evidence indicate patterns of volcanism may be waning over the last 4.8 Ma (Vaniman and Crowe 1981; Crowe et al. 1982; Crowe et al. 1992, Perry and Crowe 1992). Finally, a homogeneous Poisson distribution is used because the data set (number of past volcanic events) is too limited to apply statistical tests to select or justify use of more elaborate distribution models. The limited data set means that application of other distribution models can neither be proved nor disproved. Basically, a homogeneous Poisson model is used because it requires the fewest assumptions and simplifies probabilistic calculations.

There has and continues to be debate in the geologic literature concerning the suitability or nonsuitability of the use of homogeneous Poisson distribution for modeling volcanic recurrence patterns. Clearly this debate will not be resolved using the limited data set of Pliocene and Quaternary volcanic events in the Yucca Mountain region. A far more important issue than a debate over a choice of a distribution models is whether probabilistic assessments can be structured using a homogeneous Poisson model (or any other model) so that they do not underestimate the risk of volcanism. The choice of homogeneous or non-homogeneous Poisson distribution models has received lengthy discussion (Ho et al. 1991; Ho 1991; 1992; Connor and Hill 1993). This discussion continues *despite* minor differences in the probability estimates of magmatic disruption of the potential repository for nonhomogeneous Poisson distribution models compared to homogeneous Poisson models. Again, this tangential debate cannot be resolved with the small data set of volcanic events in the YMR. It diverts attention from the more important topic: the interpretation of the meaning of the probability estimates. To attempt to end debate over the choice of distribution models, and to emphasize the more important issue of the interpretation of

probability estimates, we also present and discuss the application of nonhomogeneous Poisson models for the volcanic record of the YMR.

Several geologic assumptions are required to apply a probabilistic approach to the potential Yucca Mountain site. First, the past record of basaltic volcanic activity in the YMR is assumed to be the most reliable indicator of the rates, and nature of future volcanic events. This means that the record of basaltic volcanism in the YMR is used as the primary basis for estimating and bounding future recurrence rates of volcanic activity. This assumption is supported by the consistency of the record of volcanism in the region for the last 10 Ma. All post-late Miocene volcanic centers formed from the eruption of small volumes ($< 1 \text{ km}^3$) of basaltic magma (Crowe 1990), except the basalt of Thirsty Mesa (3 km^3). The small volume, volcanic activity formed spatially isolated centers comprising scoria and spatter cones, fissure systems, and associated lava flows. The primary emphasis of probabilistic assessment is on the last 4.8 Ma, the youngest cycle of Postcaldera basaltic volcanism (Crowe, 1990).

We examine the record of volcanism from the perspective of multiple alternative models to develop different ways to apply this record to probabilistic assessments. There is no best or most correct method for interpreting and applying the geologic record; there is an almost unlimited number of different approaches. The important distinction is not in the choice of different models, but whether different models lead to significantly different distributions for the estimates of the probability of magmatic disruption of a potential repository.

Second, we assume there has been a sufficiently detailed study of the YMR to identify all Quaternary volcanic centers. This assumption is based on several lines of evidence, and may be changed pending the results of further site characterization studies. Quaternary basaltic volcanic centers are conspicuous and relatively stable geomorphic landforms in arid regions of the southwest United States. They persist as prominent landforms for long periods of time. For example, Pliocene basalt centers in Crater Flat (3.7 Ma) are readily identified by the presence of scoria deposits with exposed feeder dikes (Vaniman and Crowe, 1981; Crowe et al. 1983). The Pliocene and Quaternary basalt centers in the YMR can be identified through visual inspection of aerial photographs, and even satellite photographs. Detailed geologic mapping has been completed of the areas near and surrounding the potential Yucca Mountain site. The presence and location of Quaternary volcanic centers in the region have long been recognized, and their identifications have remained unchanged for several decades. Third, detailed drupe aeromagnetic surveys were completed for the YMR (Kane and Bracken 1983; Langenheim et al. 1991). Basaltic volcanic rocks have high magnetic susceptibility, and are identified easily among the generally nonmagnetic Paleozoic rocks, and the alluvial fill of the basins around Yucca Mountain (Kane and Bracken, 1983). Surface Pliocene and Quaternary volcanic centers form prominent anomalies on aeromagnetic data (Crowe and Carr 1980; Kane and Bracken 1983; Crowe et al. 1986; Langenheim et al. 1991). The detection of buried basalt centers or basalt intrusions may be more difficult in volcanic bedrock, where the country rock has higher magnetic susceptibility. We are developing field and laboratory experiments to test the depth and size resolution for detecting basalt intrusions through application of magnetic and possibly electrical methods. These studies will be conducted as part of continuing site characterization studies. However, undetected basalt centers are not expected to be a major problem for two reasons. First, a basaltic event must ascend to depths at or near a repository to adversely affect the waste isolation system (300 m). Basalt magma at these depths typically exsolves volatiles, and the volatile exsolution provides a strong driving force, pushing the magma toward eruption (Wilson and Head, 1981). Second, we have examined basalt intrusions at all known sites of intrusions in the YMR (Crowe et al. 1986; Crowe, 1990; Valentine et al. 1992). Every *known* site where intrusions formed is associated with sites of surface volcanic rocks formed

from eruptions. The recognition of Pliocene and Quaternary volcanic activity when they are recorded in the geologic record by eruptions is not a difficult problem. Third, the presence of basalt intrusions that are undetected requires that they are either deep, small or a combination of both. As the depth below the surface increases and the size of an intrusion decreases, the likely effect of these bodies on a waste isolation system decreases.

The issue of undetected basalt centers or intrusions has been raised repeatedly by the Nuclear Regulatory Commission (NRC). The possibility of undetected features is an issue that obviously must be considered in site characterization studies. Moreover, it is an issue that is difficult to assess (by definition). Existing geophysical data provide partial control for this question. Six aeromagnetic anomalies have been identified in the YMR that could be buried basalt centers or intrusions (Crowe and Carr, 1980; Kane and Bracken, 1983; Crowe et al. 1986). Three of these sites have been drilled and shown not to be produced by Quaternary basaltic volcanic rocks (see Section II). Additional geophysical studies are planned to assess the presence of undetected features. New data will be incorporated, if required, in future revisions of volcanic probabilistic assessment. Probabilistic assessment of volcanism for the potential Yucca Mountain site follows an iterative approach. Each step of probability assessment of volcanism is evaluated on the basis of *existing information*. Conclusions at each step are as reliable as the current status of the site characterization studies. The conclusions, obviously apply only to those data used for the assessment. As new information is obtained, it is easy to reassess and evaluate the probabilistic estimates.

Finally, we assume that the observations and interpretations of the geologic record are reliable, an assumption that is difficult to quantify. Here there are three sources of uncertainty. First, and by far the largest area of uncertainty, is differences in opinion concerning interpretations of the geologic record. Experience has shown already that a range of differences exists in interpretation of existing site data for the record of basaltic volcanism. There is controversy concerning eruptive models for individual volcanic centers (Turrin et al. 1991). Different interpretations of the structural controls of sites of basaltic volcanism have been presented (Smith et al. 1990). There is even some disagreement over the definition of what constitutes a volcanic event (Ho et al. 1991; Ho 1992). The limited number of volcanic events in the YMR makes it difficult to resolve or discriminate conclusively different interpretations. Thus different interpretations of the geologic record have to be resolved by using multiple alternative models in probabilistic assessment. This will be a source of uncertainty in all stages of probabilistic evaluations. Second, the primary method for dating of Quaternary basaltic volcanic rocks is the K-Ar method. The method becomes increasingly less precise with decreasing age of the rocks. However, this problem can be mitigated partly by using multiple chronology methods. Additionally, we assign multiple models for the age of volcanic events where there is uncertainty in age determinations. Third, the reliability of interpreting the record of basaltic volcanism decreases with increasing age of the volcanic centers. This is because older centers are progressively more modified, and parts of the record of volcanic events are eroded or covered. To reduce this uncertainty, we have attempted to reconstruct original volumes, have drilled exploratory holes, and used aeromagnetic and ground magnetic data to estimate the areal extent of buried basalt units (Crowe et al. 1983). Additionally, we accommodate this uncertainty by varying the assumptions of the eruptive models, and the volume determinations for the probability calculations.

IV. STRATEGY FOR ASSESSING THE VOLCANISM ISSUE

There are two fundamental questions that must be answered to determine if volcanism is a significant issue with respect to a potential repository at Yucca Mountain. These are:

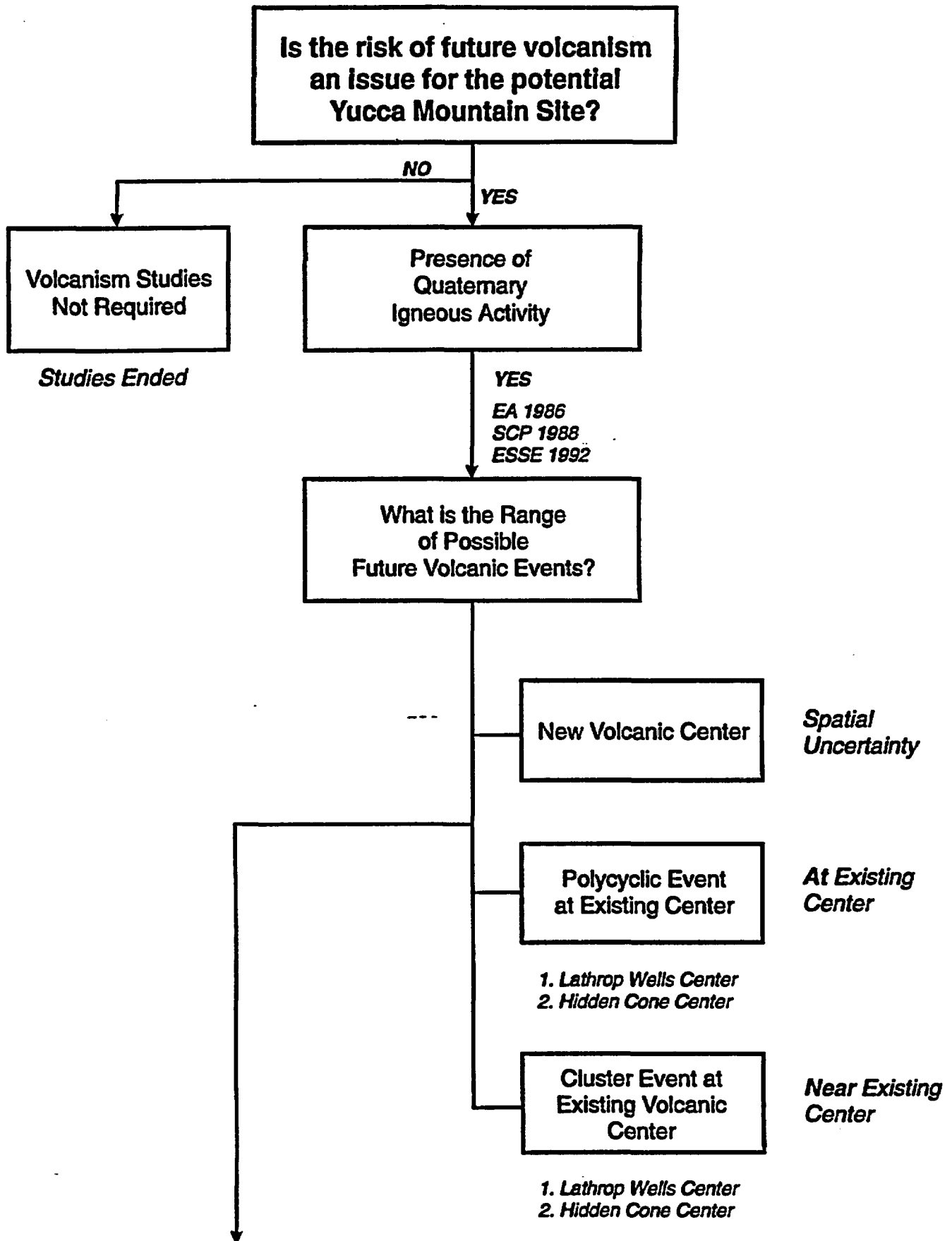
1. What are the probability and consequences of a range of future volcanic scenarios that could affect either the waste isolation system of a repository, or the repository itself?
2. Should the potential Yucca Mountain site be disqualified solely on the basis of the risk of future volcanism? (*Note: We use the term disqualification in reference to disruptive volcanic events that could, on the basis of their effects, eliminate the potential Yucca Mountain site from further consideration as a site for isolation of high-level radioactive waste. Volcanism data described in this report have been obtained primarily to aid the DOE in the responsibility of carrying out their decision whether the site should or should not be disqualified. The suitability of the site, a much broader issue, will be judged relative to the regulatory requirements.*)

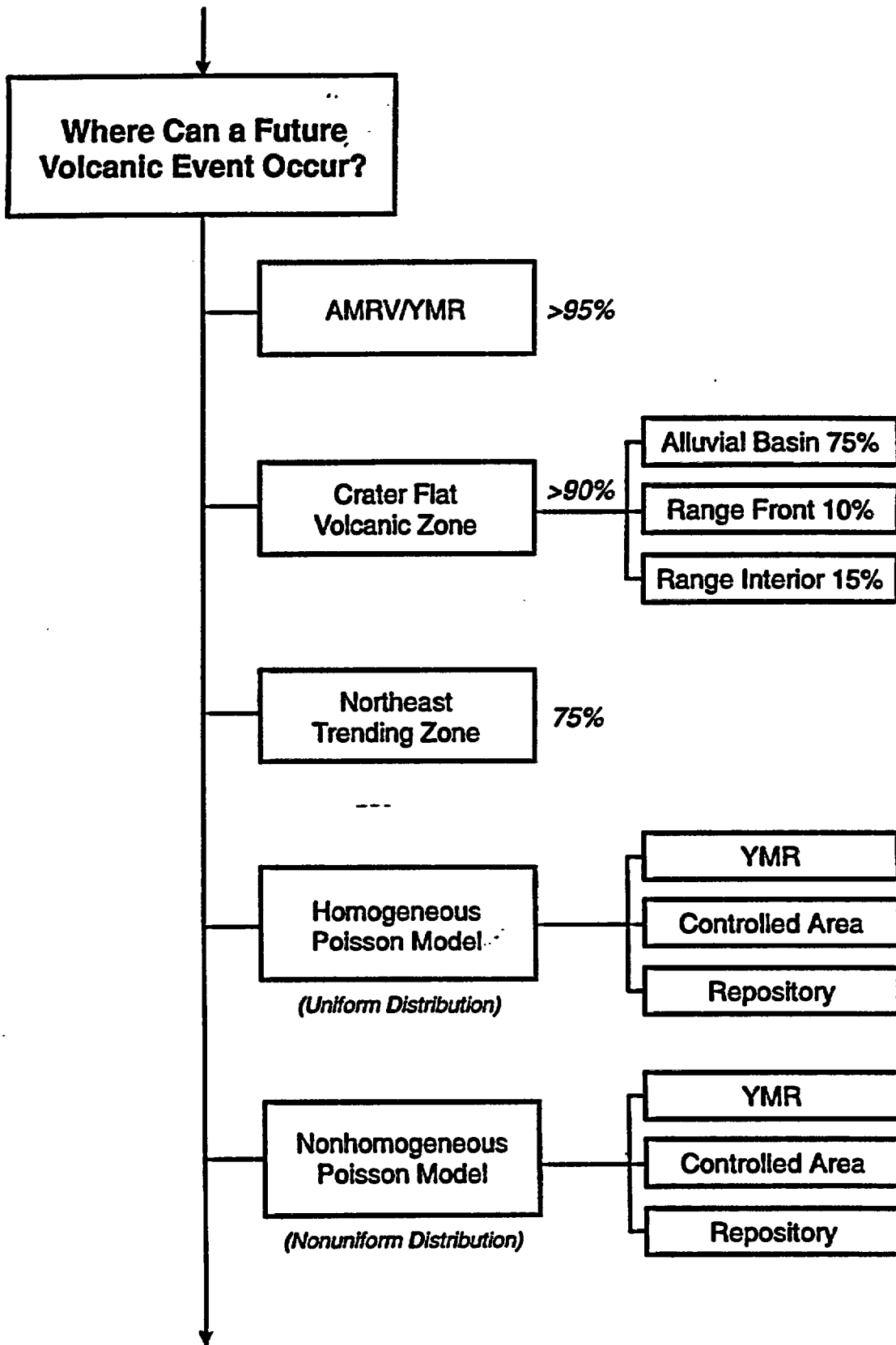
Assessment of both of these questions requires information from two classes of volcanic events. The first is what is referred to as the eruptive events. This is a category of volcanic activity that includes eruptive events. These events could lead to immediate releases of magma-transported radioactive waste at the surface. Eruptive processes are rapid, and represent a potentially catastrophic threat to the isolation system of a repository compared to the required 10,000 yr isolation period. The eruption event requires intersection or near intersection of the potential repository for ascending magma to incorporate radioactive waste prior to eruption. Establishing the occurrence probability of magmatic disruption of the repository and surrounding area the primary emphasis of this report.

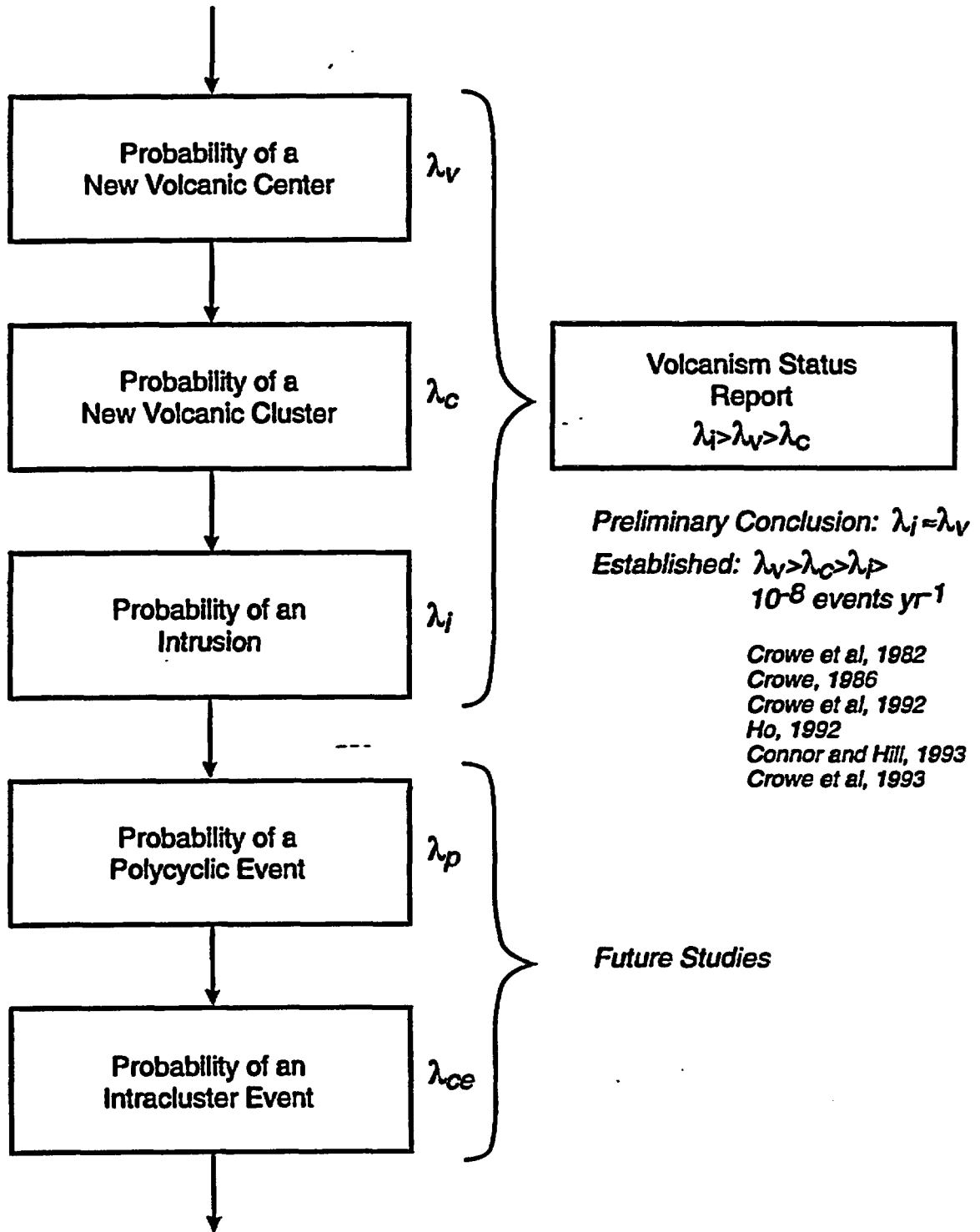
The second category of volcanism events is disruption or modification of the repository or isolation system from the effects of intrusions accompanied or not accompanied by an eruption. Here emplacement of magma into or through the controlled area or immediate vicinity of the repository could result in changes in the long term performance of the natural barriers of a waste isolation system. This is a more complicated problem than a determination of the occurrence probability of an eruptive event. It requires, first, identifying the occurrence probability of the event, then identifying a range of secondary or coupled processes caused by the intrusion of magma into or near a repository. The effects of these events must be projected over the required-isolation period of a repository. The probability of an intrusive event is defined somewhat differently than the eruptive event because of a potentially larger or more complicated subsurface geometry of an intrusive event. The significance of this second category will be evaluated through a combination of estimating their occurrence probabilities, and the consequences of their induced effects. Again, the emphasis of this report is only on the occurrence probabilities of eruptive events.

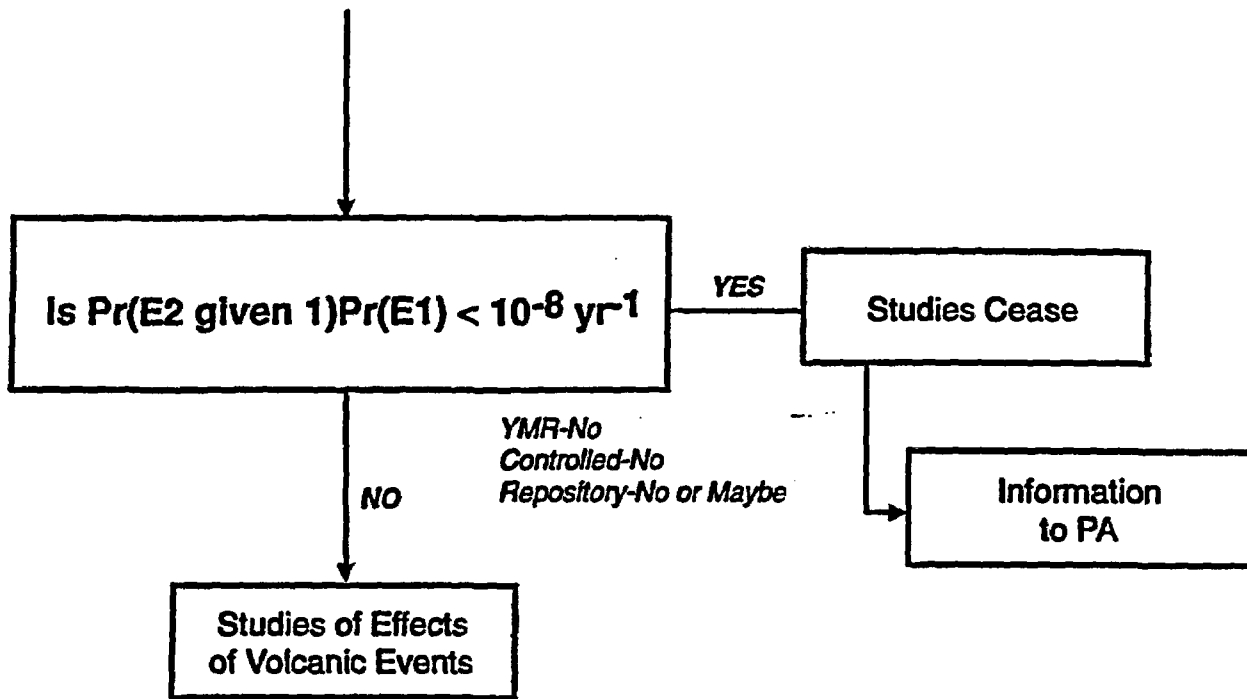
The logic of assessing the volcanism issue is illustrated on Fig. 7.1. Volcanism studies have sequential decision points that determine the priority of site characterization studies. The decision points determine whether the scenario categories need studies only of the occurrence probability, or whether the consequences or releases must also be assessed (Fig. 7.1). The primary basis for decisions is an assessment of whether the initiating volcanic events can or cannot be shown to have a probability of occurrence of less than 1 in 10,000 in 10,000 years (10^{-8} yr^{-1}). This criterion, which was part of Appendix B of 40 CFR191, is currently under review, and may or may not continue to apply. If this criterion is changed or removed, we will reassess the logic of volcanic studies on the basis of the revised regulations. At this phase of study, the 10^{-8} yr^{-1} criterion is used only to establish priorities in *volcanism studies*, not to judge against regulatory criteria for the suitability or unsuitability of a repository.

Fig. 7.1 Diagram of Logic Used to Study the Risk of Volcanism for the Yucca Mountain Region









If volcanism events have an occurrence probability of $< 10^{-8} \text{ yr}^{-1}$ they will be judged not to be an issue that could lead to disqualification of the potential Yucca Mountain site (*Note: the judgment of non-disqualification may or may not eliminate the events from consideration for their contribution to the cumulative releases from the waste isolation system (site suitability). This decision will be based on assessments of the overall performance of a waste isolation system.*)

If the events have an occurrence probability of $> 10^{-8} \text{ yr}^{-1}$, a two-step logic sequence will be used to assess the significance of the events. First, the occurrence probability will be evaluated that the event will occur, and will result in immediate releases to the accessible environment that exceed regulatory requirements. If the occurrence probability of exceeding allowable releases is $< 10^{-8} \text{ yr}^{-1}$, the event will be judged not to be an issue that could lead to disqualification of the potential Yucca Mountain site. If the occurrence probability of exceeding allowable releases is $> 10^{-8} \text{ yr}^{-1}$, studies will be undertaken to establish the contribution of volcanic-driven releases to the cumulative releases from the waste isolation system. Studies of the release component of magmatic-induced radiological releases are not the subject of this volcanism report. Volcanism studies for Study Plan 8.3.1.8.1.2, Physical Processes of Magmatism and Effects on the Potential Repository, provide the information needed to identify, and evaluate partly the secondary effects of magmatic activity on the waste isolation system. The calculation of the radiological releases from secondary or coupled effects of magmatic activity will also be undertaken as part of performance assessment studies.

There are several key questions that must be answered to assess the data needed for evaluating the risk of future volcanism. The first is whether igneous activity is a concern for the potential Yucca Mountain site (Fig. 7.1)? The DOE has established already that the presence of five Quaternary volcanic centers in the vicinity of Yucca Mountain is a potentially adverse condition, and requires assessment as a part of site characterization activities (DOE 1986; 1988). The affirmative answer to that question means that the probability of a future volcanic event in the Yucca Mountain region is $> 5 \times 10^{-7}$ events yr^{-1} or one igneous event in the Quaternary (Crowe et al. 1992; the calculation uses the definition of 2.0 Ma for the Quaternary period as recommended by the NRC).

The next questions are interlinked. First, what is the range of possible future volcanic events? Second, what is the probability of each type of volcanic event? The latter question must be answered first, because the recurrence probability may differ for different volcanic events. The λ is defined as the recurrence rate of volcanic events. It is divided into subsets, including: a) λ_v , the recurrence rate for formation of a new volcanic center, b) λ_c , the recurrence rate for the formation of clusters of volcanic centers, and c) λ_i , the recurrence rate for formation of magmatic intrusions. Defining the recurrence probability for these three subsets is a main goal of the *Volcanism Status Report*. Other subsets of λ that will require additional study include: a) λ_p , the probability of polycyclic events (Crowe et al. 1988; 1992a); λ_{ce} , the probability of formation of intra-cluster events, given the initiation of a future cluster event (λ_c).

Current site characterization information combined with simple logic require that $\lambda_i > \lambda_v > \lambda_c$. This follows from:

1. The number of volcanic clusters in the Pliocene and Quaternary in the YMR is $<$ the number of volcanic events (Crowe and Perry 1989; Crowe et al. 1994).

2. Magma rises through the crust along intrusive feeder dikes or more complex intrusive forms (Crowe et al. 1983b; Valentine et al. 1992). Therefore each volcanic event must be accompanied by at least one intrusive event.
3. The acceptance of (2) requires that λ_i must be $\geq \lambda_v$.

Interpretation of current site data (described above) leads to the conclusion that $\lambda_i \equiv \lambda_v$. However, this conclusion is regarded as a preliminary for two reasons. First, every known locality in the YMR where basaltic intrusive rocks of Cenozoic age have been identified is also a site where basaltic volcanic rocks were erupted at the surface. The cautionary note with that statement is that exposure of intrusive rocks requires considerable erosion (generally > 100 meters). Erosion of the Pliocene and Quaternary age volcanic centers is insufficient to assess whether there are extensive intrusive rocks (intrusions larger than simple feeder dikes) with these centers. Aeromagnetic data for Crater Flat and the Amargosa Valley show that basaltic intrusions are not present beyond the surface outcrops of Quaternary basalt centers (Kane and Bracken, 1983). However intrusions are possible directly beneath the centers where they aeromagnetic signature is masked by the surface volcanic rocks. Second, there are an insufficient number of sites where intrusions are present to assess the frequency of occurrence of extensive intrusive rocks (intrusions of more complex geometry than linear feeder dikes) formed below the Pliocene and Quaternary basalt centers of the YMR. There are six sites of Cenozoic basaltic volcanism in the southwest Nevada volcanic field (a notably larger area than the YMR) where at least part of the country rock beneath basalt centers are exposed. Basaltic intrusions more complicated than simple feeder dikes have been identified at two of those sites. These are the Paiute Ridge area of the Half Pint Range (Crowe et al. 1983; Valentine et al. 1993), and the southern center of the basalt of Nye Canyon. These conclusions will continue to be tested through ongoing field and geophysical studies. They are an important part of planned studies for Study Plan 8.3.1.8.1.2 Physical Processes of Magmatism and Effects on the Potential Repository. The conclusions will be changed if required by new data. *Because $\lambda_i \equiv \lambda_v$, the remaining discussion will only mention λ_v recognizing that the described assessments may or may not apply to both events.*

By definition (the presence of Quaternary igneous activity in the YMR):

$$\lambda_v \lambda_c \lambda_i > 10^{-8} \text{ events yr}^{-1} \quad (7.5)$$

The next important question is what type of volcanic activity can occur? This must be answered by examination of the volcanic record. Table 7.1 is a compilation of the predominant eruptive style of Pliocene and Quaternary basaltic volcanic centers in the YMR. Eruptive activity at basaltic volcanic centers in the YMR has been predominately mixed Hawaiian and Strombolian, with locally important hydrovolcanic eruptions. Further, there are some general patterns, in time and space, for the occurrence of different types of volcanic eruptions. Pliocene volcanic eruptions were mostly of Hawaiian type, with high eruption volumes (> 0.5 km³), and a low ratio of pyroclastic/lava compared to the total erupted volume (Crowe et al. 1983a). Quaternary eruptions were of mixed Hawaiian-Strombolian type, volumes were low (< 0.1 km³), the morphology of lava flows are consistent with low effusion rates, and the ratio of pyroclastic/lava for the eruptions was greater than the Pliocene eruptions. Hydrovolcanic eruptions occurred at one center (Lathrop Wells center), and are suspected at some of the Quaternary and Pliocene basalt centers of Crater Flat. The volume of hydrovolcanic deposits is minor at all centers (< 0.05 km³). The ground water table is relatively shallow at the Lathrop Wells volcanic center where hydrovolcanic eruptions occurred in three of the four eruptive episodes.

Table 7.1 Eruption Characteristics of Pliocene and Quaternary Volcanic Centers in the Yucca Mountain Region

Volcanic Center	Events	Lava Eruptions	Effusion Rate	Eruptions		Eruptions Hydrovolcanic
				Hawaiian	Pyroclastic Strombolian	
Basalt of Thirsty Mesa	1 to 3	Mesa or Shield	High	90%	10%	None
Pliocene basalt, SE Crater Flat	1 to 5	Aa lava sheets	Moderate	70%	30%	Minor?
Basalt of Buckboard Mesa	1	Mesa/Aa lava sheet	High	70%	30%	None
Quaternary Crater Flat	1 to 5	Blocky aa	Low	30%	70%	Minor?
Sleeping Butte	1 to 2	Blocky aa	Low	30%	70%	None
Lathrop Wells	1	Blocky aa	Low	20%	75%	5%

Table 7.2: Setting of Pliocene and Quaternary Volcanic Centers/Events in the Yucca Mountain region.

Geologic Unit	CFVZ	Other	NE Zone	Other	Alluvial Basin	Range Front	Range Interior
Thirsty Mesa #1	1			1			1
Thirsty Mesa #2	1	---		1			1
Thirsty Mesa #3	1			1			1
Amargosa Valley	1		1		1		
Undrilled Anomaly	1		1		1		
Undrilled Anomaly	1		1		1		
Anomaly CF	1		1		1		
Buckboard Mesa*		1	1		1		
Crater Flat 3.7#1	1		1		1		
Crater Flat 3.7#2	1		1		1		
Crater Flat 3.7#3	1		1		1		
Crater Flat 3.7#4	1		1		1		
Crater Flat 3.7#5	1		1		1		
Makani Cone	1		1		1		
Black Cone	1		1		1		
Red Cone	1		1		1		
Little Cones	1		1		1		
Little Black Peak	1			1	1		
Hidden Cone	1			1		1	
Lathrop Wells	1		1			1	
Totals	19	1	15	5	15	2	3
Group %	95%	5%	75%	25%	75%	10%	15%

* The basalt of Buckboard Mesa has been classified by some reviewers as occurring in a range interior setting. However the unit occurs in the moat zone of the Timber Mountain caldera, which is a basin-setting.

Future eruptions in the YMR would be expected to form small volumes of predominantly blocky aa lava, and the pyroclastic component would be expected to be predominately of mixed Hawaiian-Strombolian type. The occurrence frequency of hydrovolcanic eruptions is estimated to be < 10%, and may be even less for areas of deep ground water, like Yucca Mountain (<< 10%). Smith and Luedke (1984) estimated that hydrovolcanic eruptions occur in about 10% of volcanic eruptions in the western United States. Hasenaka and Carmichael (1985) noted that hydrovolcanic centers (tuff rings or tuff cones) form < 3 percent of the Michoacan-Guanajuato volcanic field of central Mexico (22 of 913 basaltic volcanic centers). distribution of future volcanic events will follow the distribution of past volcanic events.

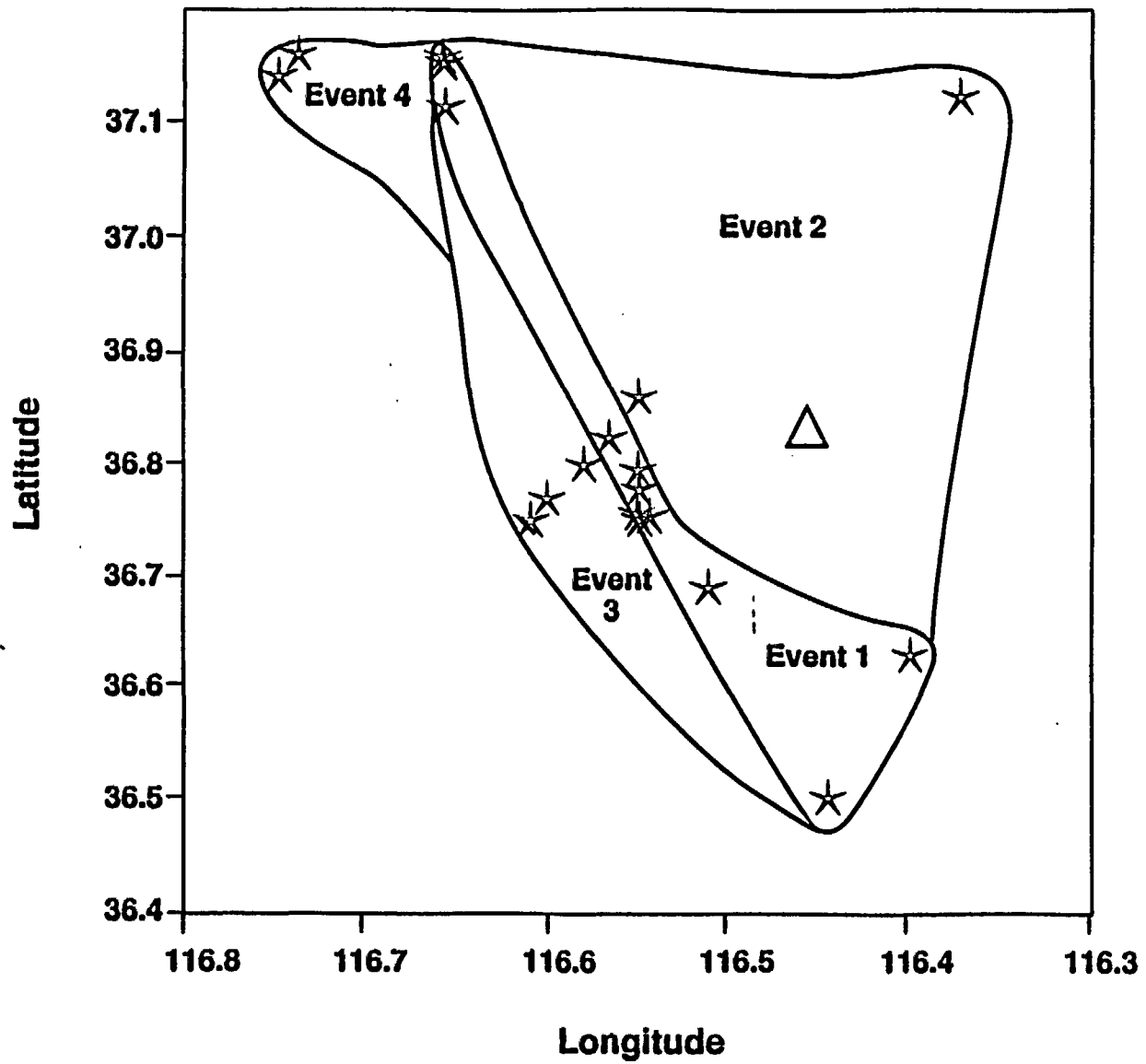
There is a relatively high probability (estimated to be > 95%; Table 7.2) that any future event will occur within the distribution area of past volcanic events. Fig. 7.2 illustrates the basis for this assumption. The sequence of Pliocene volcanic events in the YMR (4.8 to 2.9 Ma) outline an irregular polygon bounded on the northwest by the basalt of Thirsty Mesa, on the south and southeast by the aeromagnetic anomalies in the Amargosa Valley, and on the north and northeast by the basalt of Buckboard Mesa (Fig. 7.2). All subsequent volcanic events occurred near or within the bounds of that area (Fig. 7.2). The area encompassed by the distribution of Pliocene and Quaternary volcanic events on Fig. 7.2 is designated as the Yucca Mountain region (YMR). Second, based on the past record, there is > a 90% probability that a future volcanic event will occur within the CFVZ (Table 7.2; Fig. 7.2). There have been 19, possibly 20, volcanic events (see following section for a definition of a volcanic event) in the YMR during Pliocene and Quaternary. One volcanic event or 5% occurred *outside* the CFVZ. Third, if an event did occur outside the CFVZ, it would probably occur within a less-well defined, northeast-trending zone (Carr, 1990; Smith et al. 1990) Of the 20 Pliocene and Quaternary volcanic events in the YMR, 15 or 75% are in the northeast-trending zone, and 5 events or 25% are outside the northeast-trending zone; the CFVZ is a more consistent predictor of sites of volcanic activity than the northeast-trending zone (Table 7.2). Finally the distribution of past events suggests that a future event is about 6 times more likely to occur in an alluvial valley or range front than in a range interior (75% of the centers occur in alluvial basins, 10% along range fronts, and 15% occur in a range interior; Table 7.2).

A second approach to assessing recurrence rates and locations of future volcanic events is to use homogeneous and nonhomogeneous Poisson distribution models to describe the events. Multiple recurrence and structural models are used to assess the probability of a volcanic event in the YMR, the controlled area, and the potential repository block. We first examine the probability equations for a homogeneous Poisson distribution of events. The likelihood of the first option, a future volcanic or intrusive event in the YMR is:

$$Pr_o = 1 - \exp(-\lambda tp), \quad (7.6)$$

where Pr_o is the probability of intrusion or eruption in the YMR. The attributes λ and p are defined using homogeneous distribution models. Further, the attribute p is significant for the equation only for events close to the boundary of the controlled area. This attribute drops out of the equation as the area of the event occurrence (Yucca Mountain region) gets large because $a/\lambda \cong 1$ as a approaches λ . For this case the annual probability of a volcanic event occurring in the YMR approaches λ , the recurrence rate of volcanic events. We have already established that λ is $> 10^{-8} \text{ yr}^{-1}$. Therefore Pr_o is $> 10^{-8} \text{ yr}^{-1}$ for all cases of this option of the probability estimations. The significance of volcanic eruptions or magmatic intrusions in the YMR should be assessed through evaluation of secondary radiological releases. While this evaluation has not yet been completed, an obvious relationship is that the r_s , the probability of secondary releases exceeding the regulatory requirements associated with a volcanic event or intrusion in

Fig. 7.2: Distribution area of Pliocene and Quaternary volcanic events, including aeromagnetic anomalies, in the Yucca Mountain region (YMR). The first four Pliocene volcanic events (basalt of Thirsty Mesa, aeromagnetic anomalies of Amargosa Valley, basalt of southeast Crater Flat, and the basalt of Buckboard Mesa) defined the area of an irregular polygon that encloses the potential Yucca Mountain site. All subsequent volcanic events have been in or adjacent to that distribution area.



the YMR, decreases with increasing distance of the event from the repository. At some standoff-distance (d_s) from the repository, the likelihood of secondary effects resulting in secondary releases that exceed the regulatory requirements becomes very small, and approaches 0. For these cases, the conditional probability of an eruptive or intrusive event occurring outside the controlled area, and resulting in secondary releases that exceed the regulatory requirements are $\ll 10^{-8} \text{ yr.}^{-1}$. One of the goals of the studies of the secondary effects of magmatic processes on the waste isolation system is to identify the distances, and directions where this relationship is satisfied.

The second option using homogeneous Poisson models is the likelihood of a future volcanic event in the controlled area:

$$Pr_{ca} = 1 - \exp(-\lambda p), \quad (7.7)$$

where Pr_{ca} is the probability of intrusion or eruption through the controlled area, and p is the a/A where a is the controlled area. The controlled area is larger than the area of the repository by slightly greater than a factor of ten. Therefore, it is likely that $Pr_{ca} > 10^{-8} \text{ yr.}^{-1}$. This case should require an evaluation of the secondary effects of magmatic intrusion into or through the controlled area.

The third option is a future volcanic event penetrating the repository. The likelihood of a future volcanic event penetrating the repository is:

$$Pr_d = 1 - \exp(-\lambda p), \quad (7.8)$$

where Pr_d is the probability of intrusion or eruption through the repository, and p is a/A where a is equal to the area of the repository, and A is the area of the volcanic recurrence rate. The value of a is likely to be somewhat larger than the area of the repository for the general case of linear feeder dikes because some events could be centered outside of the repository, and have feeder dikes that extend into the repository (Crowe et al 1982; Connor and Hill 1993). Generally, this is a relatively small effect, and can be assessed easily by expanding the area of the repository. The dike effect is more important for assessing the consequences of volcanic events than their occurrence probabilities. For now, we treat a simply as the area of the repository.

Finally, nonhomogeneous Poisson models can be applied to the three areas (YMR, controlled area and the repository) using the same form of the above equations. However, λ is replaced in the equations with a function of t (λt), following the Weibull process models of Ho (1991; 1992). The distribution function of a Weibull process is (Tuckwell 1988)

$$F(t) = 1 - \exp(-\lambda t^\rho), \quad (7.9)$$

which by differentiation gives the Weibull density function

$$f(t) = (\lambda \rho) t^{\rho-1} \exp(-\lambda t^\rho), \quad (7.10)$$

where λ and ρ are distribution parameters and are ≥ 0 . Ho (1991; 1992) uses a slightly different form of the Weibull process where (λt)

$$\lambda(t) = \left(\frac{\beta}{\theta}\right)\left(\frac{t}{\theta}\right)^{\beta-1}, \quad (7.11)$$

and β and θ are parameters of the Weibull distribution (WEI(θ, β)).

The DOE has judged in previous documents that the site is not disqualified solely because of the occurrence probability of magmatic disruption of the repository (DOE 1986; 1988; Younker et al. 1992). A primary goal of this report is to continue to re-assess the basis for that judgment. This is accomplished by re-estimating the probability of magmatic disruption of the repository using the most current data from the volcanic record for the YMR.

If Pr_d is $< 10^{-8} \text{ yr}^{-1}$, the direct effects of repository disruption, and eruption are not an important issue. An important question for assessing this relationship is what constitutes an acceptable value of the probability of magmatic disruption of the repository. Is it the most likely value? Is it a confidence interval about the most likely value? Is it a determined percentage on a cumulative probability distribution? The median value of the probability of magmatic disruption of the repository is $\approx 10^{-8} \text{ yr}^{-1}$ (Crowe et al. 1994); the upper tail of the cumulative distribution extends to values $> 10^{-8} \text{ yr}^{-1}$.

If Pr_d is $> 10^{-8} \text{ yr}^{-1}$, assessments will be conducted of the probability of direct releases of radioactive waste to the assessable environment by a volcanic eruption. This relationship is modeled as:

$$Pr_d = 1 - \exp(-\lambda t p r), \quad (7.12)$$

where Pr_d is the probability of disqualification of the repository from future volcanic eruptions, and r is the probability that volcanic eruptions release radionuclides to the accessible environment in quantities that exceed the regulatory requirements. This relationship does not apply to the probability of volcanic intrusion because this event does not result in direct releases of radionuclides to the accessible environment (Note: An assessment of r for both extrusive and intrusive events is being conducted as part of Study Plan 8.3.1.8.1.2 Physical Processes of Magmatism and Effects on the Potential Repository. This work is not described in this report).

If $Pr_d > 10^{-8} \text{ yr}^{-1}$ we will determine if the potential for radiological releases from a volcanic event exceeds the regulatory requirements. The overview studies for that determination are described in Study Plan 8.3.1.8.1.2. Important parts of these studies are an evaluation of the abundance and depth of derivation of lithic fragments in basaltic volcanic deposits (Valentine et al. 1992; 1993). If these studies indicate that $Pr_d > 10^{-8} \text{ yr}^{-1}$ the recommendation will be made to the DOE that the radiological releases from volcanic events should be included as part of assessments of the cumulative releases from the waste isolation system over a 10,000 yr period. The logic of the choices of the studies required for assessment of Pr_d is critically dependent on r . If $r < 1$ and > 0.1 , identification, evaluation, and modeling of eruptive scenarios will probably be undertaken (see Study Plan 8.3.1.8.1.2; the logic is based on the assumption that the probability of repository disruption is $\approx 10^{-8} \text{ yr}^{-1}$ Crowe et al. 1980; Ho 1992; Connor and Hill 1993; Crowe et al. 1994). The information obtained from eruption modeling will be provided for

assessments of the performance of the waste isolation system. If r is < 0.1 , the releases associated with the eruptive scenarios may not require study because of a low occurrence probability. Volcanism studies are tasked with developing the logic of bounding possible values of r , using a probabilistic approach. The formal selection, application, and evaluation of estimated values for the conditional probability of the eruptive events will be developed by the DOE.

IV. REVISED PROBABILITY CALCULATIONS

A. Volcanic Record: Assumptions and Physical Models

This part of Section VII attempts to define the current understanding of the record of basaltic volcanism in the Yucca Mountain region so it can be applied consistently to the probabilistic assessment of the recurrence rate (E1), the disruption probability (E2), and the probability of magmatic disruption of the potential repository. The most current data from site characterization studies are used to make revised estimations of the probability of magmatic disruption of the potential Yucca Mountain site. Data on the distribution and chronology of Pliocene and Quaternary volcanic centers are taken from Crowe (1990), Wells et al. (1990), Smith et al. (1990); Turrin et al. (1991; 1992), Crowe et al. (1992; 1994), and from Sections II and III of this paper.

We accept without extended discussion that there is not a single accepted definition of the number of past volcanic events in the YMR. Multiple models of E1 are used including event cluster models, event center models, and a Quaternary accelerated model. Likewise, there is not a single, universally accepted model for the structural control of the location of basaltic volcanic events. The small number of past volcanic events makes it difficult to either prove or disprove recurrence or structural models of volcanism. Instead, we take the approach that it is more important to identify and evaluate a range of alternative models. The minimum, maximum, and most likely values of the conditional probability of magmatic disruption of the repository are evaluated. For E1, minimum values are defined as the smallest number of volcanic events required to produce the record of past volcanic events. Maximum values of E1 are defined as the largest number of volcanic events required to produce the observed volcanic record. The most likely values are defined as the number of volcanic events required to produce the volcanic record using *reasonable* constraints from multiple lines of geologic, geochemical, and geophysical evidence. The selection of these values is somewhat subjective, and requires judgment. However, by careful identification of the assumptions used to define the recurrence and structural models for the YMP, with *justification and documentation for the selections*, it is possible to narrow the range of alternative probability estimates. The systematic approach used for this assessment, and the description of alternate event models should help identify *why* specific probabilistic assessments are chosen, and why there are differences in probability estimates.

The best perspective for judging the results of probability assessments and ensuring they are neither underestimated or overestimated is through comparison with the geologic record. We use two criteria in assessing both the validity and applicability of probability estimates. First, they should include evaluations of a full range of recurrence (E1), and structural (E2) models. In many cases, estimates of the conditional probability of repository disruption are formulated only for the worst (sometimes *worse*) case (for example, Ho et al. 1991; Ho 1992; Connor and Hill 1994). This is not necessarily incorrect, but the calculations should be identified clearly as worse or worst case calculations. Second, events and models used in probability calculations should be physically plausible. In some cases, published probability estimates are correct mathematically, but physically implausible viewed from the perspective of volcanic processes (for example, the worst case estimations of Ho 1992).

Assessment of the suitability or unsuitability of probability estimates requires judgmental decisions. In assessing different probability models, we attempt to identify areas where judgment is required, and try to present a range of alternative options for those judgments. In almost all cases the range of alternative options is large, and as a result, there are many equally viable methods for assembling probability estimates. We attempt to constrain the variability in options of estimating probabilities by application of four approaches. First, the methods and approaches used for the calculations must be compatible with the record of volcanic activity in the YMR. Second, the assumptions used for probability

estimations must be consistent with and supported by the physical processes controlling volcanic activity. Third, we emphasize the resulting numerical range of probability estimates, not the different possible ways of making the calculations. Finally, Study Plan 8.3.1.8.1.1 calls for review, and refinement of probability estimations by an external group using formal methods of expert opinion. This purpose of external review is to provide an independent assessment of probability estimates while attempting to ensure a full range of alternative opinions are incorporated into the estimates.

1. Time Perspective of Probability Calculations: The first aspect of assembling probability calculations is selecting a time-perspective or interval for the probabilistic assessment. Regulatory guidelines by the NRC require an assessment of disruptive events during the Quaternary (1.6 Ma geologic definition; 2 Ma NRC definition). A more consistent perspective is to assess the record of volcanism for intervals corresponding to volcanic cycles (Crowe and Perry, 1989). Here the suggested interval for the examination of the volcanic record in the YMR is 4.8 Ma. This is the period corresponding to the Younger postcaldera basalt, the youngest and present volcanic cycle of basaltic volcanism in the southwest Nevada volcanic field (Crowe 1990). The YMR is defined for the probabilistic assessment as the area of distribution of Pliocene and Quaternary volcanic rocks, and aeromagnetic anomalies suspected or identified as buried volcanic or intrusive rocks (Fig. 7.2). It is similar to but slightly larger than the AMRV of Smith et al. (1990).

An area of misunderstanding or misinterpretation in past assessments of recurrence rates (E1) for the YMR is the use of an arbitrary or undocumented period of t , time, or the interval of the probability assessment. During the past 4.8 Ma, volcanic activity in the YMR has occurred episodically. There have been brief periods of volcanic activity separated by long periods of inactivity. Unrealistically short recurrence times result from narrowing the period of assessment to intervals closely bracketing the time or times of volcanic activity. Equally, vanishing small recurrence rates can be obtained by estimating recurrence rates during intervals of limited or no volcanic activity. Neither approach gives realistic recurrence rates. What is more important and a fundamental requirement for making probability estimations is to provide justification for selection of the time-perspective for probability calculations. Ideally the justification should be based on volcanic processes or the geologic record. In a following section, we illustrate why intervals defined on the basis of the volcanic record provide more realistic estimations of recurrence rates of volcanic events.

Crowe and Perry (1989) reviewed methods for assessing the time sensitivity of the record of volcanic events. They noted that plots of cumulative magma volume or magma volume versus time provide a means of evaluating the evolutionary stages of volcanic rates through time. The slope of the curve, or the magma output rate (Kuntz et al. 1986), is a sensitive indicator of changes in rates of magma production (Crowe and Perry, 1989). It is used frequently to assess the historic behavior of active volcanoes (Wadge 1987; Shaw, 1987). Crowe and Perry (1989) noted that the magma output rate shows characteristic changes through time in response to evolutionary patterns of basaltic volcanic fields (time scale of millions of years).

We use the last 4.8 Ma as the preferred time interval for estimating volcanic recurrence rates because this interval corresponds to an established volcanic cycle in the record of volcanism in the YMR. Additionally, the recurrence rates are calculated for the last 2 Ma and 1.6 Ma to correspond to the NRC regulations and the geologic definition of the Quaternary period. To bound maximum recurrence rates, we assess recurrence rates for the last 1.0 Ma, an interval of possible increased frequency of volcanic events (Vaniman and Crowe 1981; Connor and Hill 1994; Crowe et al. 1994).

2. Definition of Volcanic Events: The second aspect of assessing the volcanic record, and an additional source of confusion in published estimates of the probabilistic assessment of volcanism, is

defining and identifying a volcanic event. The definition of volcanic events used in the probability assessment conducted for this report includes λ_v , λ_c , and λ_i . Each of these events involves the birth of a new volcanic center or an episode of intrusion of basaltic magma in the shallow crust. These events have spatial variability in their locations, and therefore represent a finite risk of forming in or near the potential repository.

A volcanic event is defined from the perspective of its impact on a repository for underground storage of radioactive waste. The primary magmatic event of concern is the rise of a new pulse of magma through a repository. Figure 7.3 is a schematic block diagram of a typical dike-fed, eruptive event. The flow of magma moves upward initially along a near-vertical, sheetlike dike or dikes. As magma nears the surface and erupts, magma flow is concentrated in a near-circular conduit that becomes the predominant eruptive site or main vent. Multiple conduit sites can occur along the fissure (Fig. 7.3). Additionally, dikes can branch from the main dike at depth and form separate vents at the surface. From the perspective of the repository, the key variables in a consideration of a volcanic event are the depth of formation of branch dikes, and the depth of channeling of flow into conduits. Events occurring well above the depth of the repository will have a smaller effect on the repository with respect to the incorporation and surface dispersal of radioactivity. Events occurring below the repository could increase the geometric area of waste-magma contact, and potentially, the volume of dispersed radioactivity, either through eruptions or through secondary or coupled effects.

The rise and eruption of magma can lead to the formation of a single volcanic center such as the Lathrop Wells volcanic center, or a cluster of multiple centers like the basalt of Sleeping Butte (Crowe and Perry, 1991). A basaltic volcanic center is defined as a group of closely spaced vents that form a spatially distinct volcanic landform. Generally, a volcanic center consists of one main eruptive vent with a moderate-sized scoria cone and multiple satellite vents of smaller dimensions associated with the main cone (Crowe, 1986). Individual volcanic centers are formed by the rise and eruption of a pulse of magma from a single or multiple contemporaneous dikes. We use the term *volcanic center* to correspond to a *single* volcanic event. Multiple *vents* at a volcanic center are not necessarily counted as multiple volcanic events. Multiple *vents* can be formed by the rise of single pulse of magma. Multiple *vents* can also form as polycyclic episodes, a special subset of volcanic events that is not counted as a spatially unique volcanic event (Crowe et al. 1988; Wells et al. 1990; see following discussion).

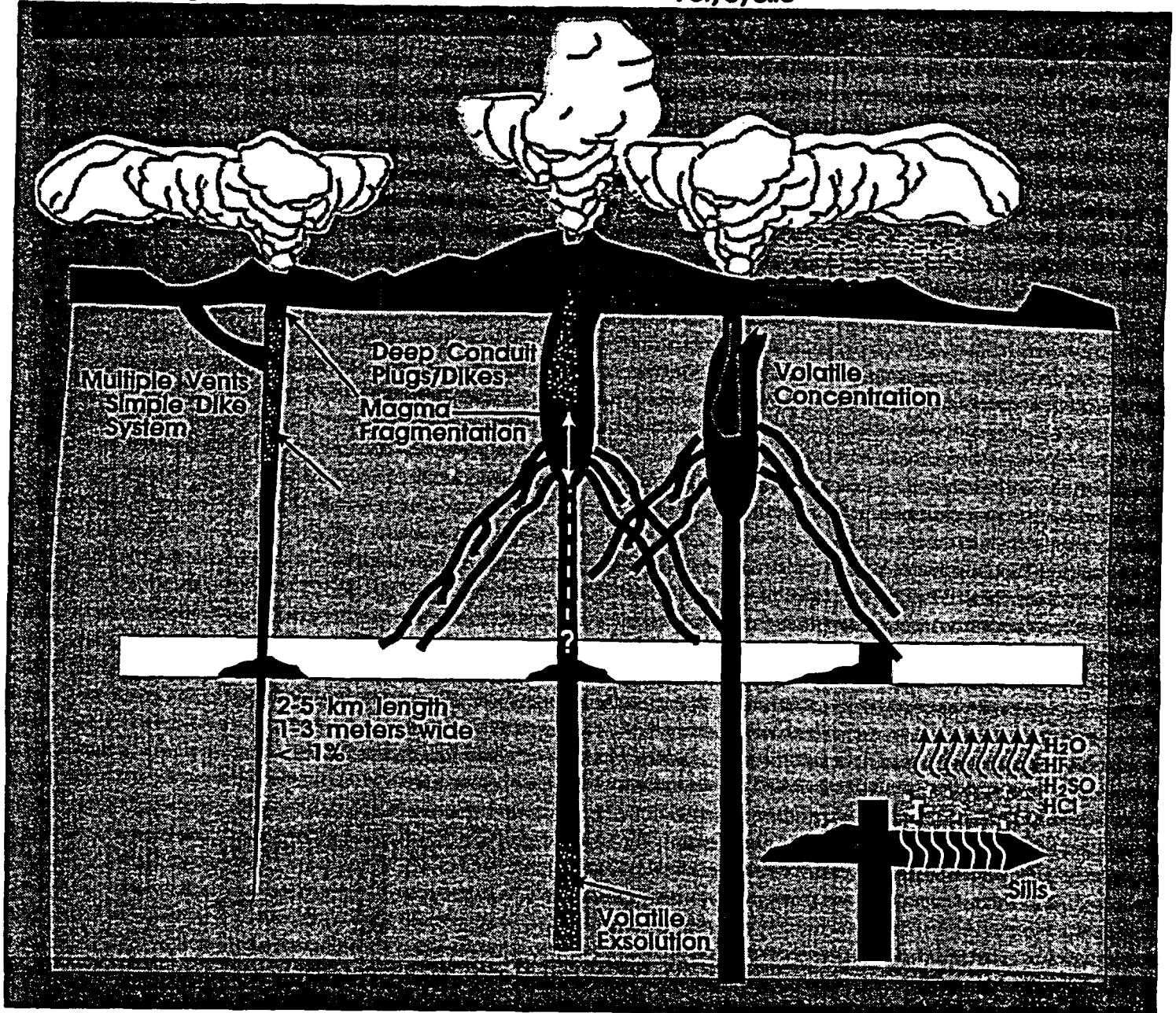
We assume a volcanic event (new volcanic center) consists of the rapid emplacement of 1 to 3 dikes that feed surface volcanic eruptions. More than one dike is probably required because the geometry of vent zones and fissures at volcanic centers cannot easily be satisfied by a single dike. This is illustrated by the distribution of fissure vents associated with the first chronostratigraphic unit of the Lathrop Wells volcanic center. The distribution of the vents defines three partly overlapping fissure systems (see Section II). The spacing of the fissures requires eruptions to have been fed from multiple dikes; a single feeder dike could not easily have produced the three fissures. Moreover, geochemical data suggest the fissures erupted magma of slightly different compositions (see Sections II and IV). One of the goals of Study Plan 8.3.1.8.1.2 is to evaluate whether basalt magma ascends as dike swarms, or whether a single feeder dike branches to form multiple feeder dikes.

The identification of volcanic events can be bounded approximately by the dimensions of feeder dikes. Dikes typically have aspect ratios ranging from 10^{-2} to 10^{-3} and widths of 1 to 5 meters (see Section V). Any volcanic vent or center spaced over 5 km distance (an arbitrary distance) from another center probably require a spatially separate feeder dike. They would be counted therefore, as separate

Fig. 7.3 Schematic Cross Section of Repository Penetrating Volcanic Event

Monogenetic

Polycyclic



volcanic *events*. Any vents spaced closer than 5 km are inferred to represent single *events* unless field or geochronology data indicate the vents formed from time-separate or geochemically distinct *events*. They could be classified as single or multiple volcanic *events*, or polycyclic episodes associated with a previous volcanic *event*. These definitions are generally useful but cannot always discriminate unambiguously the number of volcanic events. In ambiguous cases, multiple approaches are used to define volcanic events. For example, the Quaternary basalt of Crater Flat consists of four separate volcanic centers (see Section II). These could be identified as four distinct volcanic *events*, a single cluster *event*, or combinations of volcanic *events*, and cluster *events*. Because of the potential ambiguities, we attempt to carefully define the usage and assumptions in the definitions of volcanic events for all probability estimations.

3. Polycyclic Volcanism: Polycyclic volcanism (Crowe et al. 1989; Wells et al. 1990; Perry and Crowe 1992) represents a special subclass of volcanic events. A polycyclic episode is defined as an eruption at a preexisting volcanic center that is separated in time from the preceding *event* by an interval exceeding the resident time of basaltic magma in the shallow crust (decades). By definition, polycyclic episodes represent eruptions of discrete pulses of magma. Dike cooling times in the shallow crust, assuming dike widths of 5 meters or less, are no more than 10 years (Hubbert and Bruce 1990; Lister and Kerr 1991). Thus a polycyclic episode is regarded as the recurrence of an eruption at an existing center where there has been no activity for a minimum of several decades. The existence and significance of polycyclic eruptions are still under investigation, and have been controversial (Crowe et al. 1989; Wells et al. 1990; Whitney and Shroba 1991; Champion 1991; Turrin et al. 1991; 1992; Wells et al. 1992; Crowe et al. 1992). We regard the current field, geochemical, and geomorphic data for the Lathrop Wells center to be conclusive, with a high degree of confidence, that the center formed from multiple, time-distinct volcanic eruptions (Section II). Therefore the significance of polycyclic episodes are considered in probabilistic assessments.

The definition of a polycyclic episode and its distinction from a volcanic *event* affects probabilistic assessments. Ho et al. (1991) counted polycyclic episodes (and in some cases, individual vents) in estimation of E1 (Ho et al. 1991; p. 54). This is not consistent with the requirement of independence of the attributes of the conditional probability. The usage results in higher cone counts and a bias toward higher values for E1. Viewed probabilistically, the polycyclic model requires that there is an increased likelihood of another eruption at an existing volcanic center given a previous *event* that formed a new volcanic center (initiating event). Thus, there is spatial uncertainty in the location of a new volcanic center. Accordingly, there is a high probability that the first event will occur in the YMR and a finite probability that the event could disrupt the potential repository site. Because a polycyclic episode occurs at or near the same location as the first event, it does not have the same spatial uncertainty in location as an initiating volcanic event. If an initiating volcanic *event* passes through a repository, a subsequent polycyclic episode would also pass through the repository. If the initiating *event* did not pass through the repository, the subsequent polycyclic episode would not pass through the repository. The probability of a polycyclic *episode* is added as a probability branch to λ , the recurrence rate of volcanic events. Thus, the critically important concept for probabilistic assessment is the recognition that a polycyclic event is *dependent* on the occurrence of a preceding event.

We are still in the process of assessing the frequency of occurrence and recurrence rates of polycyclic episodes in the YMR. This will be of topic of continuing probabilistic studies (see Crowe et al. 1989). Accordingly, the following discussion is presented as a preliminary assessment of the logic and methods for assessing polycyclic volcanic eruptions.

Given a new volcanic event (formation of a new volcanic center) in the YMR, there appears to be an increased probability that subsequent events will occur at the same volcanic center. The duration

between polycyclic episodes is not well established. The results of ongoing geochronology studies at the Lathrop Wells volcanic center indicate that the time between eruptions may be on the order of 1 to 8×10^4 yrs (see section II). Similar intervals between eruptions appear to have occurred at the Black Tank center in the Cima volcanic field. A single polycyclic eruption at the Hidden Cone center may have occurred more than 200 ka after the initiating volcanic event (Crowe and Perry, 1991) but the identification of the polycyclic event still remains uncertain. Polycyclic activity is suspected at Black Cone (see Section IV). The time between polycyclic episodes at the center, if they exist, must be less than the analytical uncertainty of K-Ar and $^{40}\text{Ar}/^{39}\text{Ar}$ age determinations for the center (~ 100 ka).

A polycyclic eruption may be expressed as two possible forms. One form is illustrated by the Lathrop Wells and the Hidden cone volcanic centers. These centers comprise multiple, time-separate volcanic eruptions, all *at* a pre-existing volcanic center. A second possible form of polycyclic eruptions is multiple time-separate eruptions, where each separate eruption formed a distinct but spatially related volcanic center. This may be typified by the volcanic clusters of the basalt of Sleeping Butte, and the Quaternary basalt of Crater Flat. Each consists of a cluster of multiple volcanic centers. In this case, subsequent events, if they are polycyclic events, are confined not to an individual center, but to a *cluster*. The spatial variability in location of a polycyclic eruption in a cluster is controlled by the *dimensions* of cluster lengths of aligned volcanic centers (2.5 to 13 km). The existence of polycyclic clusters has not been proven at any of the volcanic clusters in the YMR; it is only possible. Current chronology data are insufficiently precise to test for polycyclic activity at either the Sleeping Butte or the Quaternary basalt of Crater Flat.

At some unknown length of time (probably several 100 ka), the likelihood of a polycyclic eruption must decrease. Future volcanic events would form a new volcanic center at an unconstrained location. The only data we currently have on the transition time between polycyclic events and the formation of a new volcanic center are the latter must be > 10 ka, and less than the typical recurrence time between successive volcanic events (200 ka to > 1 Ma; see the following section on volume-predictable volcanic events).

The most likely site of a future polycyclic volcanic eruption in the YMR is either the Lathrop Wells or the Hidden Cone volcanic centers. The last polycyclic episodes at both centers are probably < 50 ka; therefore the centers are inferred to be in a continuing stage of polycyclic events. The most likely event in the YMR in the next 10,000 yrs is, accordingly, the recurrence of a polycyclic eruption at either of the two centers. The recurrence rate of these type of eruptions is probably $< 10^{-4}$ and $\geq 10^{-5}$ yr^{-1} - - it is the highest probability of any identified future volcanic event in the YMR. However, the polycyclic episode would be expected to be either another small volume eruption at either center, or a related cluster event near either center. Because the Lathrop Wells center is 20 km south, and the Hidden Cone is 47 km northwest of the potential repository, the estimate of E2 for these events must be very small. Certainly, none of these events could intersect the repository. Equally, the probability of E3, or releases exceeding regulatory requirements, for these events should be negligible (Crowe et al. 1989). These conclusions are presented tentatively recognizing that studies of the effects of future volcanic events are in progress. Logically, a polycyclic episode is a relatively high probability event (E1) with a very low E2 and probably very low E3 (high probability event with a very low disruption ratio and probably extremely low consequences). We have focused volcanism studies on estimations of the highest risk event: the possibility of intersection or near intersection of the potential repository by a future volcanic event, where that event is the formation of a new volcanic center.

We will, in future studies, complete revised probabilistic assessments of polycyclic and *intracluster* events. This is the only discussion provided in the *Volcanism Status Report*. of our logic for

assessing polycyclic events Further studies of polycyclic and intracluster events are planned also for E3, the probability of releases of radioactive waste at the surface.

B. Volcanic Centers in the Yucca Mountain Region:

The following data set is used for the revised probability calculations. All data and interpretations used to generate the set are *not final*. They are regarded as the current best estimates of existing information from site characterization studies. The data set will be revised as site characterization studies continue. Quaternary volcanic centers in the YMR include (oldest to youngest):

1. 1.0 Ma Centers: Quaternary basalt of Crater Flat. These are defined as one cluster event or two to five center events. Each volcanic center is estimated to be 1.0 ± 0.1 Ma on the basis of existing chronology data (see Table 2.2, Section II). These data include the results of replicate conventional K-Ar age determinations from separate analytical laboratories. The resolution of chronology data are insufficient to establish whether each center of the Quaternary basalt of Crater Flat did or did not form as a result of polycyclic episodes. Moreover, the age of specific centers cannot be discriminated individually on the basis of existing data (see Section II). The close spacing and petrologic similarity of the Little Cone centers supports treating these cones as a single event. Alternatively, Ho (1992) and Connor and Hill (1993) treat the Little Cones center as two centers and as two volcanic events. The composite length of the arc of the four basalt centers of Crater Flat is probably too long for the complete cluster to have formed as one volcanic event. It could have been formed however, by a single dike branching from the mid-point of the volcanic cluster (see the following discussion of the dike-stress model). The volume of the Quaternary basalt of Crater Flat center is estimated to be 0.23 km^3 DRE. (*Note: We are in the process of completing revised volume calculations for the Pliocene and Quaternary basalt centers of the YMR. Descriptions of the methods of volume calculations, the uncertainty of the calculations, and the resulting data should be completed in late calendar year 1994.*)

Minimum Event Model: 1 event

Maximum Event Model: 5 events

Most Likely Event Model: 3 events

Polycyclic Episode: Unknown but suspected at Red Cone and Black Cone

2. 0.32 Ma Centers: Basalt of Sleeping Butte. These are treated as two individual centers formed either in one cluster event or as two center events at about 320 ka (Crowe and Perry 1991; Champion 1991; Turrin 1992, Minor et al. 1993). High precision $^{40}\text{Ar}/^{39}\text{Ar}$ age determinations have not been obtained for the basalt of Sleeping Butte under the approved Quality Assurance program. The mean age of existing age determinations for the center is 320 ± 50 ka. We arbitrarily assign a larger uncertainty of 150 ka to the age to reflect an incomplete data set. Existing soil and geomorphic data are consistent with an age of about 320 ka (Crowe and Perry 1991). A Pleistocene polycyclic episode may have occurred at the Hidden Cone center. The uncertainty of the age assignments for the center cannot be estimated from current data. The volume of the basalt of Sleeping Butte is estimated to be 0.06 km^3 DRE.

Minimum Event Model: 1 event

Maximum Event Model: 2 events

Most Likely Event Model: 1 event

Polycyclic Episodes: Hidden Cone: 2 temporally distinct eruptions

3. **0.1 Ma Center: Lathrop Wells center.** This is treated as a single-event, volcanic center formed by one initiating event followed by three polycyclic episodes. The initiating event (formation of a new volcanic center) is estimated at 120 to 130 ka. The first polycyclic episode followed at 80 to 100 ka, and a second polycyclic episode occurred at about 40 to 60 ka. The youngest polycyclic episode occurred at 4 to 9 ka. The uncertainty of the age of the events and episodes can be only bounded using existing data. The first initiating event and the first polycyclic episode are estimated to have an uncertainty of ± 35 ka; the second polycyclic episode is no younger than 25 ka, and probably no older than about 85 ka. The uncertainty of the youngest episode cannot be estimated with current data. The volume of the Lathrop Wells volcanic center is estimated to be 0.14 km^3 DRE.

Minimum Event Model: 1 event
Maximum Event Model: 1 event
Most Likely Event Model: 1 event
Polycyclic Events: Three polycyclic episodes

Pliocene volcanic events in the YMR include (oldest to youngest):

1. **4.8 Ma Centers: Basalt of the Thirsty Mesa.** This lava mesa formed from lava and scoria eruptions at three coalesced vents. It can be defined as one cluster event or as many as three center events, each with an age of 4.8 ± 0.13 (2σ) Ma. Unpublished $^{39}\text{Ar}/^{40}\text{Ar}$ ages by the US Geological Survey are consistent with this age (second laboratory verification). The volume of the basalt of Thirsty Mesa is estimated to be 3 km^3 DRE.

Minimum Event Model: 1 event
Maximum Event Model: 3 events
Most Likely Event Model: 1 event
Polycyclic Events: Unknown

2. **3.8 Ma Center: Basalt of the Amargosa Valley.** This volcanic event is represented by the aeromagnetic anomaly located a few kilometers south of the town of Amargosa Valley. The shape, size, and continuity of the anomaly suggest it should be treated as one volcanic event. The age of the volcanic event is 3.85 ± 0.05 Ma. There are insufficient data to estimate the uncertainty of the age of the center. The volume of the basalt of Amargosa Valley is estimated to be between 0.2 and 0.4 km^3 from the dimensions of the aeromagnetic anomaly, and comparison with surface basalt centers.

Minimum Event Model: 1 event
Maximum Event Model: 1 event
Most Likely Event Model: 1 event
Polycyclic Events: Unknown

3. **Undrilled Aeromagnetic Anomalies. Basalt of central Amargosa Valley.** These presumed Pliocene volcanic center(s) have not been explored by drilling. For this report, the two remaining aeromagnetic anomalies are included, and they are assumed to be the same age as the drilled Amargosa Valley anomaly (3.85 Ma). The anomalies define two circular bodies (Langenheim et al. 1991), and are presumed to represent one cluster or two center events. The cluster event includes the basalt of Amargosa Valley since the three centers are aligned on a northeast trend.

Minimum Event Model: 1 event

Maximum Event Model: 2 events
Most Likely Event Model: 1 event
Polycyclic Events: Unknown

4. **3.7 Ma Centers. Basalt of southeast Crater Flat.** This Pliocene unit consists of one cluster event and three to five center events (Vaniman and Crowe 1981; Crowe et al. 1983b; Champion 1991). The age of the centers is dated at 3.74 ± 0.10 (average of 2σ errors) Ma using replicate, high precision $^{39}\text{Ar}/^{40}\text{Ar}$ age determinations. This age has been verified with replicate conventional K-Ar ages at multiple analytical laboratories. The volume of the basalt of southeast Crater Flat, including reconstructed volumes of eroded or buried deposits is 0.68 km^3 .

Minimum Event Model: 1 event
Maximum Event Model: 5 events
Most Likely Event Model: 1 event
Polycyclic Events: Unknown

2.9 Ma Center. Basalt of Buckboard Mesa. This consists of one center erupted from a main scoria cone and associated fissure system. It is assumed to be a single cluster and single event center that formed a lava mesa in the moat zone of the Timber Mountain caldera (Crowe 1990). The age of the basalt of Buckboard Mesa is about 2.9 ± 0.13 Ma. The volume of the basalt of Buckboard Mesa is 0.92 km^3 .

Minimum Event Model: 1 event
Maximum Event Model: 1 event
Most Likely Event Model: 1 event
Polycyclic Events: Unknown

C. Revised Calculations of E1: The Recurrence Rate of Volcanic Events.

This section of the Volcanism Status Report initiates formal revisions of E1, the recurrence rate of volcanic events. We follow the logic of Study Plan 8.3.1.8.1.1, Probability of Magmatic Disruption of the Repository, and systematically examine values for E1 using three methods: time-series analysis, homogeneous Poisson and nonhomogeneous Poisson models using cumulative counts of volcanic events for specified periods of time, and modified homogeneous Poisson models using magma-output rate. The recurrence rates are estimated for minimum, maximum, and most likely values of E1.

Table 7.3 lists, with the referenced publication, published estimates of the recurrence rate (E1) for volcanic events in the YMR. The results are taken from publications from 1980 to 1993. There are 41 published estimations of E1. The estimates range from 1.3×10^{-5} to 6.0×10^{-7} events yr^{-1} . Distribution models for the estimations include homogeneous Poisson models based on event, cluster and stress-field dike counts, modified homogeneous Poisson models using magma-output rate, and Weibull (nonhomogeneous) models using event counts (but not cluster counts). The observation periods for the calculations vary from 1.0 to 12 Ma. Descriptive statistics for the published data set include (excluding the confidence interval calculations of Ho 1992): $n = 39$, mean 4.9×10^{-6} , median 4.0×10^{-6} , minimum 0.6×10^{-6} , maximum 28×10^{-6} , standard deviation 4.5×10^{-6} (all as events yr^{-1}), and skewness 3.6. The data are strongly skewed to higher values consistent with the bias introduced from attempts to identify upper bounds in probability estimates. Most of the recurrence rates are in the range of 1 to 6×10^{-6} events yr^{-1} . The significance of numbers in this range has been debated (Ho et al 1991; Ho, 1992;

Table 7.3. Published Estimates of the Recurrence Rate (E1) of Volcanic Events in the YMR

Publication	E1 (events yr ⁻¹ x 10 ^b)	Quaternary Events	Rate Model	Interval (Ma)
Crowe and Carr 1980	4.0	6.4	Poisson Cone Count	1.8 to 2.8
Crowe et al. 1982	0.6 to 11*	1.0 to 17.6	Volume predictable	1.8 to 3.7
	9.4	15.0	Poisson Cone Count	1.8
	6.4	10.2	Poisson Cone Count	2.8
	8.0	12.8	Poisson Cone Count	3.7
Crowe et al. 1989	28*	44.8	Volume predictable	3.7
	7.0	11.2	Volume predictable	3.7
	5.0	8.0	Volume predictable	1.8
	3.2	5.1	Volume predictable	1.8
Crowe and Perry 1989	1.9	3.0	Volume predictable	1.8
	1.6	2.6	Volume predictable	1.8
Ho 1991	2.3	3.7	Weibull Episode	12
	5.0	8.0	Weibull Cycle	3.7
	6.2	9.9	Cone Count	6.0
	5.5	8.8	Weibull Cone Count	1.6
Crowe et al 1992	3.9	6.2	Poisson Cone Count	1.8
	1.7	2.7	Poisson Cluster Count	1.8
	3.5	5.6	Poisson Cone Count	3.7
	1.3	2.1	Poisson Cluster Count	3.7
	3.2	5.1	Poisson Cone Count	5.0
	1.2	1.9	Poisson Cluster Count	5.0
Ho 1992	5.0	8.0	Weibull Episode	6.0
	5.5	8.8	Weibull Episode	1.6
	1.8**	2.9	Weibull 90% CI**	1.6
	13.0**	21	Weibull 90% CI**	1.6
Connor and Hill 1994	5.4	8.6	Weibull-Poisson	1.6
	1.5	2.4	Weibull-Poisson	1.6
	11.0*	17.6	Weibull-Poisson	1.6
	2.1	3.4	Weibull-Poisson	1.2
	4.8	7.7	Weibull-Poisson	1.2
	7.0	11.2	Weibull-Poisson	1.2
Crowe et al. 1994	1.5	2.4	Poisson Cluster Count	2.0
	4.0	6.4	Poisson Cone Count	2.0
	1.7	2.7	Poisson Cluster Count	4.7
	4.3	6.9	Poisson Cone Count	4.7
	3.4	5.4	Repose	2.0
	2.1	3.4	Volume predictable	2.0
	1.5	2.4	Accelerated Cluster	1.9
	4.1	6.6	Accelerated Cone	1.9
	3.0	4.8	Accelerated Cluster	1.0
	8.0	12.8	Accelerated Cone	1.0

* outlier values

** confidence intervals

Connors and Hill, 1993). They are not considered to be significantly different, however, given the small data base used for the calculations, and the underlying uncertainties of the event models (Crowe et al. 1992; 1993).

There are some important limitations of the data summarized in Table 7.3. First, as noted earlier, most of the calculations attempt to bound the recurrence probability to determine if the risk of volcanism could result in disqualification of the Yucca Mountain site. This perspective results in the introduction of non-systematic bias in the calculations toward higher recurrence rates (positive skewness). Assumptions used for most of the calculations were constructed to insure that the probabilities were not underestimated. Second, no attempt was made in the different calculations to structure the results so a representative distribution of recurrence rates could be determined. As a consequence, descriptive statistics derived from the calculations are difficult to interpret. Third, the recurrence rates were calculated with different levels of data for the ages, identification of eruptive centers, and identification of volcanic events. Generally, the more recent the calculations, the better the quality of data.

Recognizing these limitations, we nonetheless employed standard methods of exploratory data analysis of Table 7.3 (histogram, box, stem and leaf, probability plots). Three estimations of E_1 were rejected as outliers in successive iterations of the evaluation of the data distribution (2.8×10^{-5} events yr^{-1} of Crowe et al. 1989; 1.1×10^{-5} events yr^{-1} from Crowe et al. 1982; Connor and Hill 1994). Descriptive statistics for the edited data set include: $n = 36$, mean 3.9×10^{-6} , median 3.9×10^{-6} , minimum 0.6×10^{-6} , maximum 9.4×10^{-6} , standard deviation 2.2×10^{-6} (all as events yr^{-1}), and skewness 0.68.

a. Time-Series Analysis.

One standard method for assessing patterns of volcanic events in time is to apply techniques used for sequenced or time-series analysis (Davis 1986); this approach has been applied in the volcanological literature primarily for historic eruptions of active volcanoes. There is a diverse range of methods for analyzing time-series data. The primary problem with application of any of the methods is the limited number of volcanic events in the YMR. The standard advice for using limited data sets in textbooks describing techniques for application of time-series analysis is universal: obtain more data. Given that the volcanic events used in the YMR data set have been acquired (recorded in the geologic record) over the last 4.8 Ma, the prospects for obtaining more data in the immediate future are extremely limited. Accordingly, there is limited merit in applying time-series analysis. We proceed cautiously with only simple applications.

Table 7.4 lists the age, volume, cumulative volume, and the repose interval for volcanic events in the YMR. One problem noted immediately from simple examination of the data table is individual events can be identified on a center by center basis, but the ages of individual centers within clusters of centers cannot be discriminated. This is illustrated on Fig. 7.4, a plot of the cumulative events (events defined as cluster events) versus time. The slope of the line segments between points is the rate or number of events per unit time, and the plot readily shows changes in average event rates. The slopes are slightly steeper during the Pliocene and the last 1 Ma, and slightly lower during a middle period (1 to 2.9 Ma). One very steep slope segment results from plotting the event for the buried basalt of the Amargosa Valley. It is so close in age to the southeast basalt of Crater Flat, that it may be more appropriate to plot it with the latter unit. If center events for each cluster are added to the plot of events versus time, little additional insight is gained. (Fig. 7.5). This revised plot does underscore however, how volcanic events tend to occur in clusters, much like clustered seismic events.

Table 7.4. Age, Volume, Cumulative Volume and Repose Intervals for Pliocene and Quaternary Volcanic Events of the YMR.

Center	Age (Ma)	Volume (km ³)	Cumulative Volume (km ³)	Repose Interval (Ma)
Basalt of Thirsty Mesa	4.8	3.0	3.0	1.5
Amargosa Anomaly	3.8	0.3*	3.3	0.1**
Basalt of Southeast Crater Flat	3.7	0.68	3.98	1.1
Basalt of Buckboard Mesa	2.9	.92	4.90	.8
Quaternary Basalt of Crater Flat	1.0	.23	5.13	1.9
Basalt of Sleeping Butte	.32	.06	5.19	.7
Lathrop Wells Volcanic Center	.12	.14	5.33	.2
<i>mean</i>		0.84		1.0
<i>std deviation</i>		0.11		0.6
* volume of undrilled anomalies not included				
** not included in repose statistics				

An alternative plot can be constructed to partly discriminate clustering events by changing the y-axis to magma volume. However, the problem with this approach is the older basalt units are too modified by erosion to identify volume components from individual volcanic centers. This can be resolved partly by plotting the y-axis as the cumulative magma volume. Better event separation is obtained but the assignment of volumes for some clustered centers and the older basalt centers is arbitrary (Fig. 7.6). The data and slope segments can be divided visually into two groups: Pliocene volcanic events (higher magma-output rate), and Quaternary events (lower magma-output rate). This relationship is examined more carefully in a following section.

The event repose times vary from 200 ka to 1.9 Ma with a mean of 1000 ± 570 ka ($n = 6$; Table 7.4). The number of events is too limited to be statistically significant. However, some potentially important observations are noted from a plot of repose intervals (time between the initiation of volcanic events). First, three of the five repose periods are between 700 and 1100 ka, and the other three periods are approximately half, and double those values (Fig. 7.7). Second, the minimum repose period between events for the duration of the YPB (4.8 Ma) is 200 ka. If the minimum observed repose period is used as a worst case bound for predicting the next volcanic event (corrected for the time since the last eruption, the Lathrop Wells volcanic center, 9 ka) the predicted minimum time to the next event is 191 ka which is equivalent to a recurrence rate of 5.2×10^{-6} events yr.⁻¹ Third, the data can be fitted with a linear regression model (Fig. 7.7). There are an insufficient number of data points, and the data are too dispersed for the regression model to be significant, but the slope of the regression line is consistent with a slight decrease in repose intervals through time. The data can also be fitted with a distance weighted least squares model, an undulating curve fit that declines markedly in the Quaternary. Note that this curve fit intersects the y-axis at an age of 0. This would be equivalent to a 0 repose interval, a physically impossible value. Intuitively, the argument that future repose intervals cannot be less than the shortest observed repose interval appears compelling. During the last 4.8 Ma, there has never been a repose period of less than 200 ka. The long interval of the observed record makes it appear unlikely that this pattern would change over the next 10,000 years. However, from an opposite perspective, the shortest repose period preceded the youngest volcanic event in the region. Again, a consistent pattern emerges: the limited data make a range of interpretations permissive.

Fig. 7.4 Plot of Volcanic Events versus Age for the Pliocene and Quaternary Volcanic Record of the Yucca Mountain Region.

EVENT

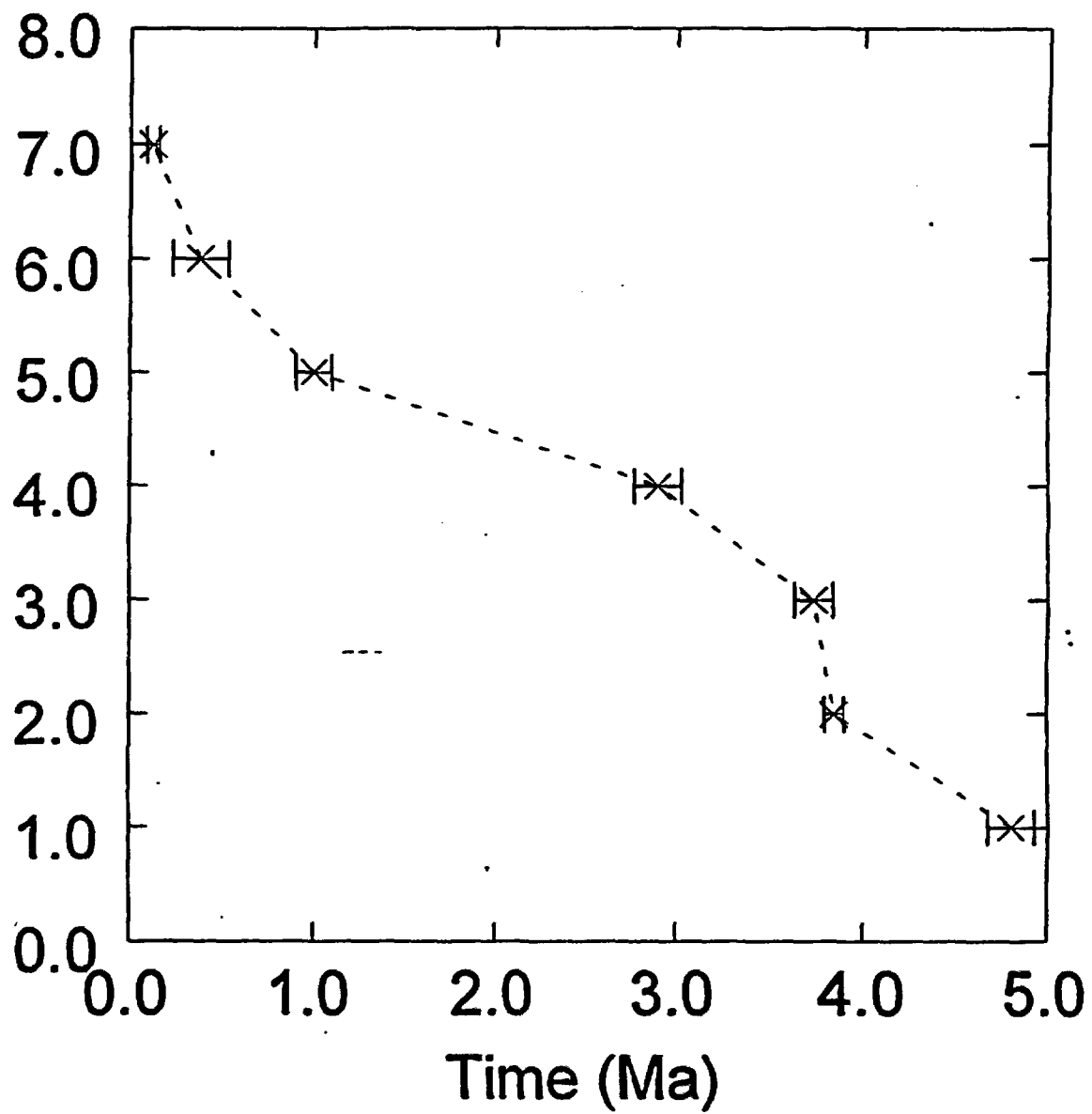


Fig. 7.5 Plot of Clustered Volcanic Events versus Age for the Pliocene and Quaternary Volcanic Record of the Yucca Mountain Region.

EVENT

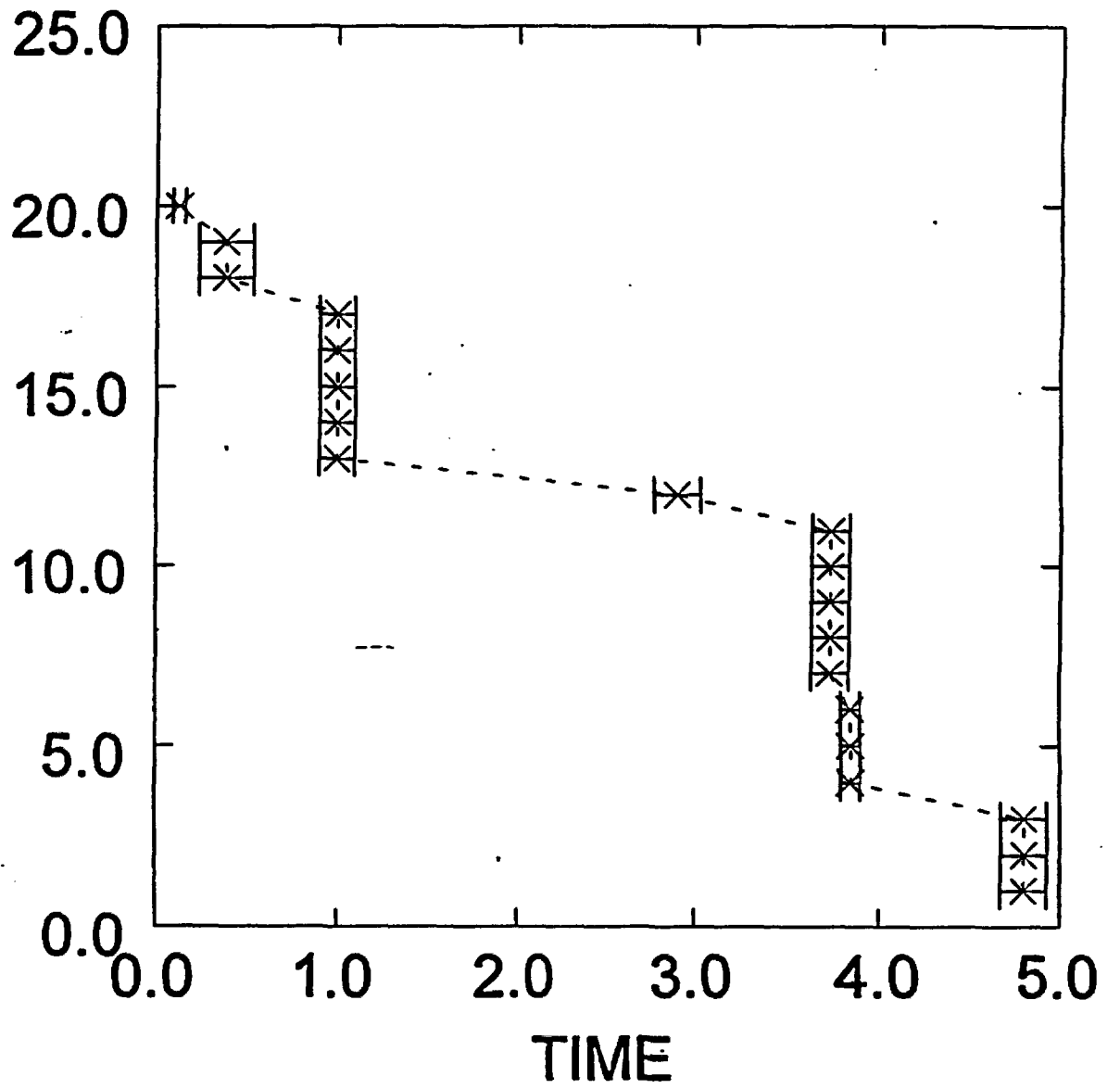
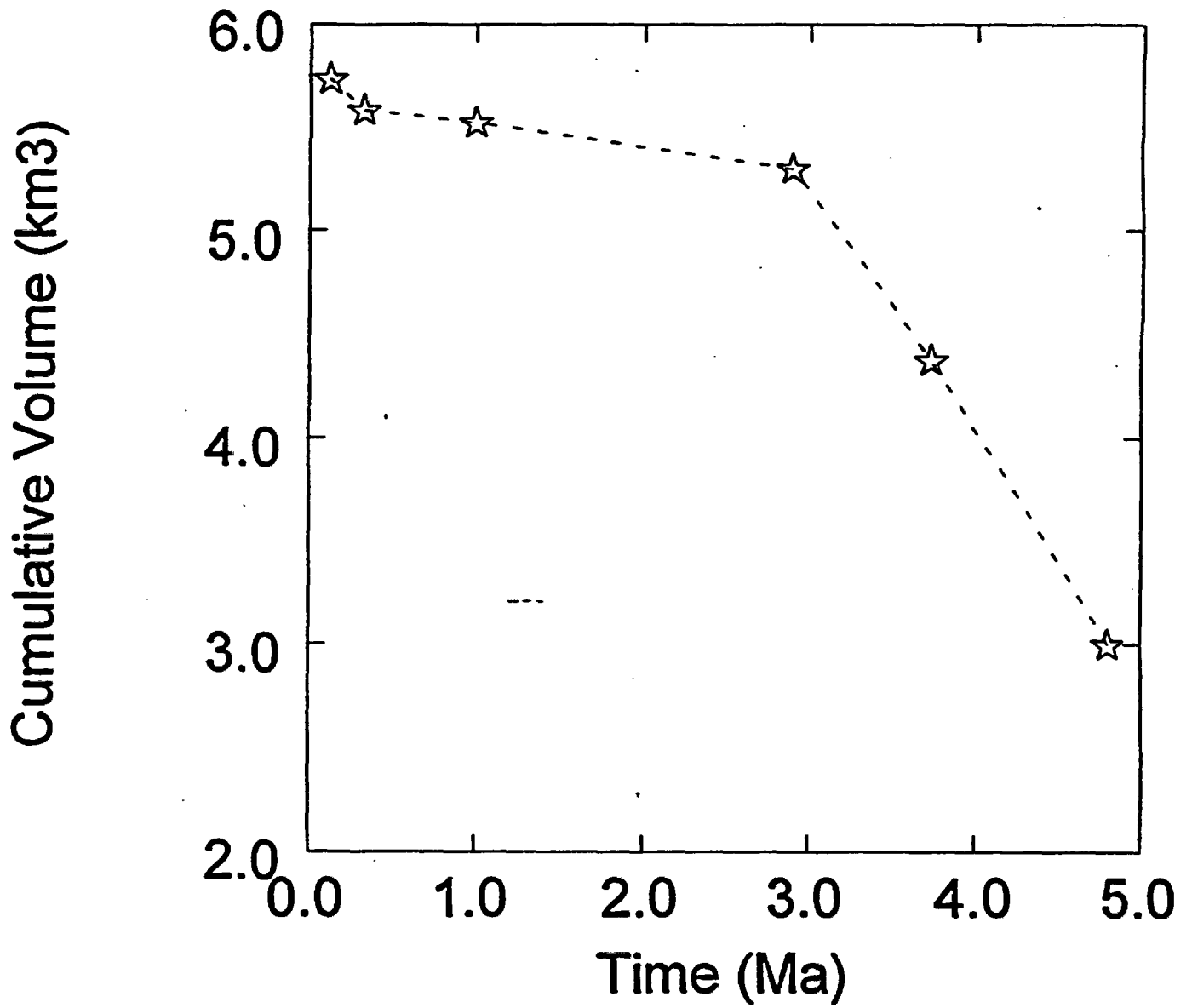


Fig. 7.6 Plot of Cumulative Volume versus Age for the Pliocene and Quaternary Volcanic Record of the Yucca Mountain Region.



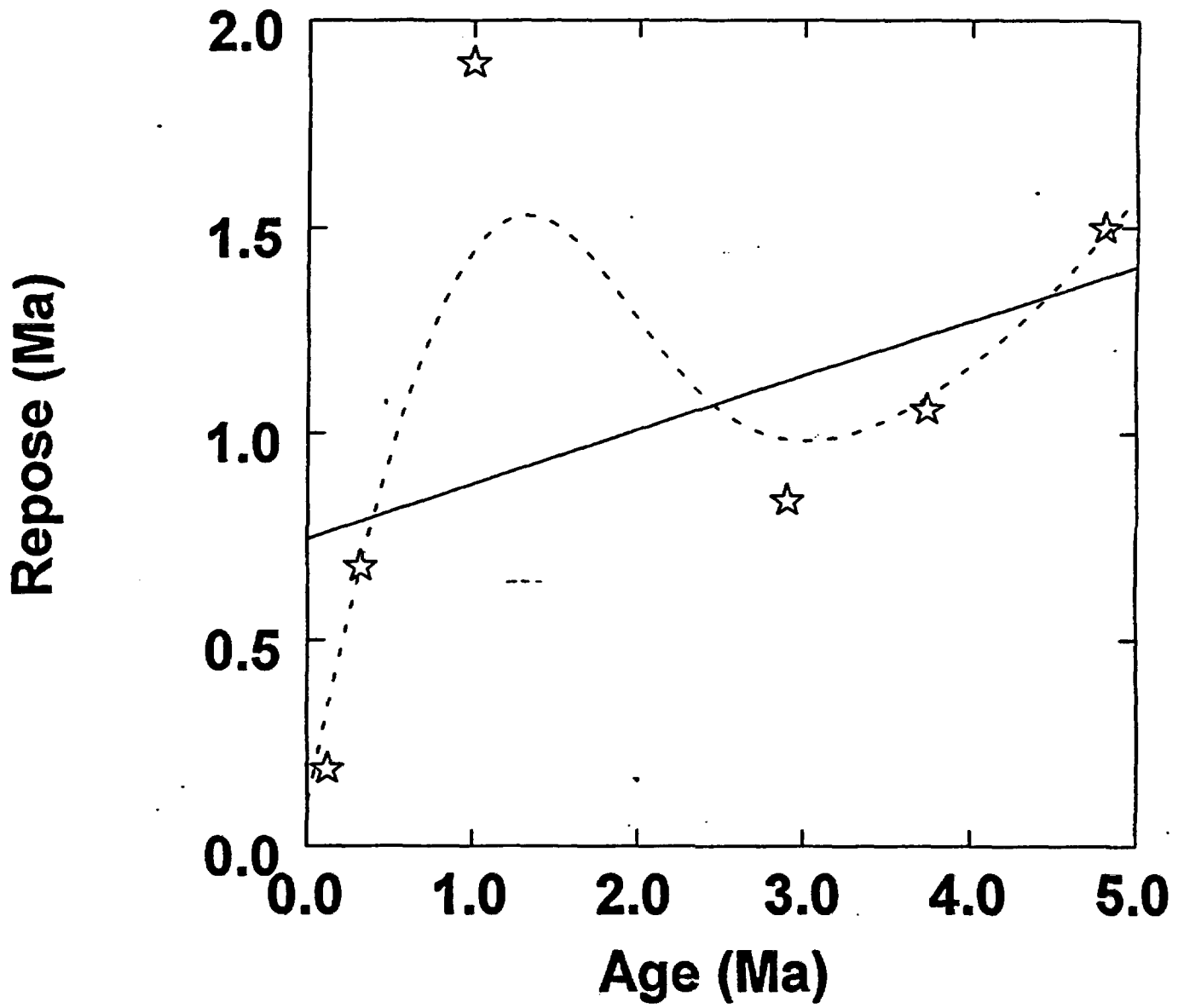


Fig. 7.7 Plot of Repose Interval versus Age for the Pliocene and Quaternary Volcanic Record of the Yucca Mountain Region.

b. Homogeneous Poisson Models (Event Counts). Table 7.5 is a compilation of revised calculations of the recurrence rate of volcanic events using a homogeneous Poisson model for the record of volcanic events in the YMR. We attempted, in this data compilation, to provide a representation of the distribution of values by identifying models that give the minimum, most likely and maximum values using geological reasonable combinations of event counts.

The event count models of Table 7.5 are divided into multiple cases, where the cases are identified under the column labeled "Model". The first category includes combinations of Quaternary (2 Ma) volcanic events. The second category is the last 4.8 Ma using the recognition of the basalt cycle of the Younger Postcaldera basalt (YPB; Crowe 1990). The third category examines data for the Quaternary using 1.6 Ma, the current geologic definition of the Quaternary. A fourth category examines data for an interval of decreased erupted volumes associated with an increase in the frequency of eruptive events. The actual interval of this increased frequency of volcanic events cannot be defined precisely (Crowe et al. 1994). It must have initiated somewhere between the age of the basalt of Buckboard Mesa (2.9 Ma), and the age of the Quaternary basalt of Crater Flat (1.0 Ma). We assume this interval initiates with the age of the Quaternary basalt of Crater Flat (1.0 Ma) so that it is equivalent to the definition of a volcanic cycle. Conceptually the interval may correspond with a time of decreased degree of partial melting resulting in a higher volatile content, and a greater tendency for the magma to erupt versus stagnate in the crust (Crowe et al. 1994).

The minimum event models of Table 7.5 for both the Quaternary and YPB event counts are based on the interpretations of the paleomagnetic data of Champion (1991). He argues that all geographically adjacent volcanic centers in individual clusters have closely spaced field magnetization directions, and therefore formed from a single magma pulse (monogenetic cluster model). This interpretation represents the *minimum* number of volcanic events (spatially and temporally distinctive magma pulses) that can be assigned to the volcanic centers of the YMR for both the Quaternary and the YPB categories.

The most likely volcanic models for Quaternary and YPB volcanic events are established through attempts to integrate all existing data for the volcanic centers. Insights provided by geologic, geochronologic, petrologic, and geophysical data are used to identify volcanic events. In some cases, the geochronologic, petrologic and paleomagnetic data are insufficiently precise to provide convincing proof of individual magmatic events. For example, the Quaternary basalt centers of Crater Flat can be divided into one to as many as four (possibly 5) events because the cluster length (12 km) exceeds the likely lengths of individual feeder dikes. Red Cone and Black Cone could be identified as one event, but the volume of each center, and their geochemical data (Vaniman and Crowe 1981; Perry and Crowe 1992) suggest the centers formed from separate (mostly separate; see Bradshaw and Smith 1993) magma batches. The Little Cones center is inferred to be a separate and single event because of the close spacing of the scoria cones, their small volumes, and their geochemical differences with the Red and Black Cone centers (Vaniman and Crowe 1981; Vaniman et al. 1982). The assignment of the Sleeping Butte centers is less clear. The close spacing of the centers (2.6 km; Crowe and Perry), and the paleomagnetic data (Champion 1991) are permissive with the centers representing a single volcanic event.

Table 7.5. Table of Homogeneous Poisson Models for Volcanic Events (E1) in the YMR.

Interval	Model	Interval (yrs)	Minimum events yr ⁻¹	Maximum events yr ⁻¹	Most Likely events yr ⁻¹
Quaternary		2.00E+06			
	Poisson Events		3	8	6
	Poisson Rates		1.5E-06	4.0E-06	3.0E-06
	Stress-Dike Events		3	8	5
	Stress-Dike Rates		1.5E-06	4.0E-06	2.5E-06
Volcanic Cycle*		4.70E+06			
	Poisson Events		8	19	12
	Poisson Rates		1.7E-06	4.0E-06	2.5E-06
	Stress-Dike Events		8	10	10
	Stress-Dike Rates		1.7E-06	2.1E-06	2.1E-06
Quaternary		1.60E+06			
	Poisson Events		3	8	6
	Poisson Rates		1.9E-06	5.0E-06	3.7E-06
	Stress-Dike Events		3	6	5
	Stress-Dike Events		1.9E-06	3.7E-06	3.1E-06
Quaternary Accelerated*		1.00E+06			
	Poisson Events		3	8	7
	Poisson Rates		3.0E-06	8.0E-06	6.0E-06
	Stress-Dike Events		3	6	5
	Stress-Dike Rate		3.0E-06	6.0E-06	5.0E-06
Summary Statistics (all Models)		<i>Mean</i>	2.0E-06	4.6E-06	3.5E-06
		<i>Median</i>	1.8E-06	4.0E-06	3.1E-06
		<i>Geomean</i>	1.9E-06	4.3E-06	3.3E-06
		<i>Std Deviation</i>	0.6E-06	1.7E-06	1.3E-06
Summary Statistics (Preferred Models)*		<i>Mean</i>	2.3E-06	5.0E-06	3.9E-06
		<i>Median</i>	2.3E-06	5.0E-06	3.8E-06
		<i>Geomean</i>	2.3E-06	4.5E-06	3.6E-06
		<i>Std Deviation</i>	0.75E-06	2.53E-06	1.8E-06

* Preferred models are models where the event counts span an interval that corresponds to cycles of volcanic activity (4.8 Ma to present; and 1.0 Ma to present).

The choice of events that correspond to the maximum estimates is established from the preceding definition of volcanic events (volcanic event = formation of a new volcanic center). This model corresponds generally to the worst case assignments of Ho (1991), Ho (1992) and Connor and Hill (1993). The only differences are that Ho et al (1991) include polycyclic episodes in their event counts. Additionally, both Ho (1992), and Connor and Hill (1993) separate the Little Cone center into two events. We regard this as an undocumented assignment, but count the center as two events in the maximum event counts to avoid controversy.

The stress-field dike model for the Quaternary and YPB categories is based on two observations described in Sections II, III, and V of the *Volcanism Status Report*. First, the clusters of basalt centers of the CFVZ are elongate north-northeast, parallel to the maximum compressive stress direction. This is the inferred direction of dike propagation in the shallow crust. Second, the clustered centers may have formed by upwelling of magma along a concealed northwest-trending structure. By inference, the magma diverted at shallow levels from the northwest-trending structure, and was emplaced by magma-generated

hydrofracture parallel to the maximum compressive stress direction. The site of upwelling is identified by the northwest alignment of basalt centers in the CFVZ which coincides also with the location of the surface of maximum erupted magma volumes (see Section III, Fig. 3.15). Magma upwelling has an equal probability of propagating either northeast or southwest to form clustered volcanic centers. On the basis of this model, for example, the 1 Ma basalt centers of Crater Flat can be inferred to have formed by two distinct or related dikes propagating in opposite directions: one to the northeast forming Black Cone and Makani cone centers, and one to the southwest forming Red Cone and the Little Cone centers. An appealing aspect of this model is that it is consistent with the volume relations of the Quaternary basalt centers of Crater Flat. The smallest volume centers (Makani and Little Cone centers) are located at the opposite ends of the cluster.

In most cases, there are sufficient data to make reasonable judgments about the event assignments for the model categories. These assignments will, of course, be tested and refined by acquisition of additional information from ongoing site characterization studies. There are limited data for selection of volcanic event models for the basalt of Amargosa Valley. The basalt of Amargosa Valley has been penetrated only in a single, exploratory drill hole (Harris et al. 1992). Information on the dimensions of the center are based on interpretations of aeromagnetic data (Kane and Bracken 1983; Crowe et al. 1986; Langenheim et al. 1991).

One major question concerning the listed calculations of Table 7.5 is what is a reasonable representation of the uncertainty of the homogeneous Poisson calculations? There is not a single and simple answer to that question. One method for defining the uncertainty is to examine the descriptive statistics using the data summarized in Table 7.5. Mean volcanic event rates using the combinations of homogeneous Poisson models listed in Table 7.5 are $2.0 \pm 0.6 \times 10^{-6}$ events yr^{-1} for the minimum model, $4.6 \pm 1.7 \times 10^{-6}$ events yr^{-1} for the maximum model, and $3.5 \pm 1.3 \times 10^{-6}$ events yr^{-1} for the most likely model. These ranges are equal to average recurrence intervals for volcanic events of 450 ka (minimum model), 220 ka (maximum model) and 290 ka for the most likely model. The minimum estimate of Table 7.5 is 1.5×10^{-6} events yr^{-1} (670 ka recurrence interval), and the maximum estimate is 8.0×10^{-6} events yr^{-1} (125 ka recurrence interval). A second method is to calculate univariate statistics for the most geologically reasonable sets of data from Table 7.5 (preferred models). These are the volcanic cycle (4.8 Ma) and the Quaternary accelerated (1 Ma) models. Mean recurrence rates combining the preferred models of Table 7.5 are $2.3 \pm 0.7 \times 10^{-6}$ events yr^{-1} (385 ka recurrence interval) for the minimum model, $5.0 \pm 2.5 \times 10^{-6}$ events yr^{-1} (200 ka recurrence interval) for the maximum model, and $3.9 \pm 1.9 \times 10^{-6}$ events yr^{-1} (260 ka recurrence interval) for the most likely model (data from Table 7.5). A third alternative method is to use the method of Ho (1992). He calculated a 90% confidence interval for the recurrence of Weibull-distributed volcanic events. The resulting values are 1.85×10^{-6} to 1.26×10^{-5} events yr^{-1} . Ho (1992) makes the valid argument that interval estimates are more informative than point estimates. However, he calculated confidence intervals for a worst case recurrence estimation, not a mid-point estimate. Moreover, the validity of calculations of confidence intervals is limited by the sparse data.

A third and preferred approach to calculating the uncertainty of the homogeneous Poisson models is to use simulation modeling (Crowe et al. 1994). We prefer this approach because of the paradox of the volcanic record of the YMR. That paradox is the following:

There are only a small number of volcanic events that have occurred in the YMR during the Quaternary. The small number of events means that volcanic recurrence rates are low, but the uncertainty of calculating the rate is large. Viewed conversely, if there were more volcanic events in the YMR during the Quaternary, there would be less uncertainty in calculating the recurrence rate. However, the risk of future events, by virtue of the larger number of events, would be higher. The trade-off between decreased risk and increased uncertainty seems logical. Accepting

the opposite view leads to two mutually illogical conclusions: 1) The best place to locate a repository would be in an active volcanic field because the recurrence rate could be calculated with decreased uncertainty or 2) The worst place to locate a repository would be in an area of no volcanic events because the uncertainty of calculating volcanic risk is unbounded.

The position taken in the *Volcanism Status Report* is the record of volcanic events in the YMR cannot be used to make robust calculations of the risk of volcanism. The recurrence rate of volcanic events is low ($< 10^{-5}$ events yr^{-1}), but the data sets are too limited to give meaningful statistical data. Therefore it is unrealistic to attempt to define the uncertainty of homogeneous Poisson models using a conventional statistical approach.

The problem can be solved through the application of risk analysis (Newendorp, 1974, Meggin 1984, Clemen 1991; Meyer and Booker 1991; Crowe et al. 1994). Elements of subjective judgment are used to translate uncertain data into probability distributions. We adopt this approach and combine the different approaches for estimating E1 with risk simulation to calculate the distribution of E1 in probability space. The results of simulation modeling for E1 are described at the end of the section on recurrence rates. Similar approaches are also used for E2 and $\text{Pr}(E2 \text{ given } E1)\text{Pr}(E1)$ in following sections.

c. Nonhomogeneous Poisson Models: We next examine the application of nonhomogeneous Poisson models (NHPP) to the record of volcanic events in the YMR. This approach suffers from the same limitations as the time-series analyses: the small data set. Under ideal conditions, the record of volcanic events in the YMR would be tested against different distribution models using statistical tests of the goodness of fit. There are three standard fitting methods for testing data distributions. The Chi-square test compares the data fit to a hypothesized probability density function (Tuckwell 1988). The Kolmogorov-Smirnov (K-S) test is similar to the Chi-square test but does not require grouping of data, and can be applied to small sample sizes (Davis, 1986). The Anderson-Darling test is similar to the K-S test but is designed to detect discrepancies in the tails of distributions (Walpole and Myers 1993).

The choice of NHPP models is large and many different approaches are possible. None of the standard statistical tests provide reasonable fits to the small data set for the time-distribution of volcanic events in the YMR. Lacking goodness of fit tests, the selection of distribution models must be based on non-statistical judgments. In fact, the sparse data set provides the primary justification for selection of simple or homogeneous Poisson distribution models, which require minimal data assumptions (Crowe et al. 1992). Ho (1991; 1992) reviewed NHPP recurrence models for the YMR, and applied a NHPP model with Weibull intensity for estimating the instantaneous recurrence rate. He used a HPP for predicting the time of future eruptive events. The density function of a Weibull process is described in equation (7.10); the form of the nonhomogeneous intensity function applied to the Yucca Mountain data set is shown in equation (7.11; after Ho 1992). The Weibull distribution is a versatile distribution that can be fitted to a wide range of data applications although with limited theoretical justification (Devore 1987). Equation 7.11 shows that the Weibull distribution includes the exponential distribution when $\beta = 1$. The modeling of the time distribution of volcanic events as a Weibull process avoids a major disadvantage of the Poisson process. The Poisson process assumes uniform or stationary values of the intensity parameter λ . For the application to the YMR, this means that the model is insensitive to the time-distribution of events, and the uncertainty in estimating the chronology of volcanic events. In contrast the form of the Weibull model is dependent on the time patterns of volcanic events (Ho 1991).

An important comparison between volcanic recurrence estimates using Weibull versus simple Poisson processes can be tested by examination of the values of β , a fitting parameter for the Weibull density function. The Weibull model is similar to the exponential distribution when $\beta \approx 1$, and therefore

includes the case of the Poisson or homogeneous Poisson model (Devore 1987; Tuckwell 1988). A "goodness-of-fit" test can be constructed, as noted by Ho (1991), to estimate whether β is \leq or \geq 1. Crowe et al (1992) argued that the simple Poisson model is appropriate for conditions of steady state or waning volcanism. This is equivalent in the Weibull model to $\beta \leq 1$. Therefore the Weibull model would be a more appropriate fit to the YMR data if $\beta > 1$.

Ho (1991) obtained a $\hat{\beta}$ of 1.09 for an analysis of Quaternary volcanic events and values of > 1 for analysis of three cases of Pliocene and Quaternary volcanic events. Careful examination of the latter calculations shows that the three cases of $\hat{\beta} > 1$ are a result of how the problems were structured because values of $\hat{\beta}$ are sensitive to the time-distribution of volcanic events. For one case of $\hat{\beta} > 1$, Ho (1991) used a t of 6 Ma, and assigned the youngest possible age to the Lathrop Wells event (10 ka). There were no volcanic events during the first 40% of the time interval of his calculations (6.0 to 3.7 Ma). This in combination with use of the youngest possible age of the Lathrop Wells center (polycyclic episodenot an initiating event) forces the value of $\hat{\beta}$ to be > 1 (see equation 7.11). For the second case of $\hat{\beta} > 1$, Ho (1991) used a t of 3.7 Ma. However, he discarded all the 3.7 Ma events because their recalculated cumulative times are zero. This forces all events into the late Pliocene and Quaternary and gives a $\hat{\beta}$ of > 1 . Clearly the limited data set of volcanic events in the YMR makes discarding of data an unacceptable approach. Finally, for the third case of $\hat{\beta} > 1$, Ho (1991) used a t of 1.6 Ma and assigned four events to the Lathrop Wells center, all at 10 ka. The assignment of four young events to the youngest volcanic center again forces $\hat{\beta}$ to be > 1 because the distribution of events is skewed toward recent events.

Connor and Hill (1993) reviewed existing calculations and made independent estimations of the probability of magmatic disruption of the potential Yucca Mountain site using nonhomogeneous approaches for estimating E1 and E2. They recognized the importance of t , the time interval of volcanic events, and β . Connor and Hill (1993) evaluated the sensitivity of β and θ , and calculated values for a range of assumptions, primarily by varying the estimated time of volcanic events. Their values of $\hat{\beta}$ are all < 1 except for one case. That case is where they assigned the youngest possible ages to all Quaternary volcanic events in the YMR ($\hat{\beta} = 2.2$; Connor and Hill 1994; their Table 2).

To independently assess the sensitivity of β , and to test the Weibull versus Poisson models, we calculated the fitting parameters (WEI β, θ) for the Weibull model using all combinations of cluster and event models listed in Table 7.6. A critical assumption of this calculation is again t , the time of volcanic events. We follow the same models and assumptions used to construct Table 7.5 with one important exception. If t of the interval $(0, t)$ is equal to the age of the oldest volcanic events, the cumulative times are 0 and the β is undefined. This is the reason Ho (1991) discarded the oldest volcanic events in his calculations. A more realistic approach is to assume the oldest events differ in age from t by the standard deviation of the replicate age determinations. For example, the assigned difference for the 4.8 Ma volcanic events is 0.13 ka. The importance of this data approach cannot be understated. Ho (1991) obtained a $\hat{\beta} = 2.55$ for a time interval of 3.7 Ma when the 3.7 Ma events were discarded. If the same calculations are repeated and the 3.7 Ma events are included, the $\hat{\beta} = 0.68$.

Table 7.6 is a compilation of $\hat{\beta}$ values and values of the recurrence rate using the form of the Weibull model of Ho (1992) for the minimum, most likely, and maximum values of cluster event, center event, and stress-field dike events for the different combinations of t (2.0 Ma, 4.8 Ma, 1.6 Ma, and 1.0 Ma). The $\hat{\beta}$ values fall into two groups. All values of $\hat{\beta}$ are ≤ 1 for the preferred Quaternary accelerated

and the volcanic cycle models (the $\hat{\beta}$ values range from 0.6 to 1.0). Thus for intervals where t is defined on the basis of the volcanic record, the Weibull model is less conservative than the homogeneous Poisson model. The values of $\hat{\beta}$ for all other data sets are > 1 . Examination of the data set provides the explanation for the values of $\hat{\beta}$ of > 1 . All of the calculations span intervals where the initial values of t coincide with a gap in the record of volcanic events (1.0 to 2.9 Ma; the interval between the Quaternary basalt of Crater Flat and the basalt of Buckboard Mesa). By the construction of the calculations, the distribution of volcanic events are skewed to younger ages, and therefore to higher values of $\hat{\beta}$. This illustrates an important perspective. Calculations of the recurrence rate using a Weibull model may not be appropriate when the interval $(0, t)$ initiates during a time of no volcanic activity. Structured in this manner, the fitting parameters for recurrence rate calculations using a Weibull distribution may overestimate λ . This perspective gives equal insight to the homogeneous Poisson calculations. The HPP calculations may underestimate λ when they are constructed across a significant interval of no volcanic activity. Accordingly, the most appropriate data sets for estimating the recurrence rate of volcanic events, from a geologic and calculation perspective, are the sets for the volcanic cycle (4.8 Ma to present) and the Quaternary accelerated model (1 Ma to present).

Mean values of the recurrence rate using estimations on the basis of a Weibull distribution model are $3.0 \pm 1.2 \times 10^{-6}$ events yr^{-1} , $5.5 \pm 2.4 \times 10^{-6}$ events yr^{-1} and $4.6 \pm 1.9 \times 10^{-6}$ events yr^{-1} for respectively, the minimum, maximum and most likely values of Table 7.6. The reciprocals of these mean estimations are 330 ka (minimum), 180 ka (maximum) and 220 (most likely), and represent estimations of the recurrence time between volcanic events. The minimum value of all the Weibull calculations is 1.4×10^{-6} events yr^{-1} (700 ka recurrence time), and the maximum is 8.4×10^{-6} events yr^{-1} (120 ka recurrence time). Collectively the recurrence estimations using a Weibull distribution tend to be slightly greater than estimations using a homogeneous Poisson distribution. However, if the sets are compared for the two preferred models (4.8 Ma volcanic cycle and 1.0 Ma accelerated interval), the mean values of the minimum, maximum, and most likely estimates using the HPP model exceed the NHPP estimations. The minimum, maximum, and most likely values of the preferred models using a NHPP model are respectively, $2.1 \pm 0.8 \times 10^{-6}$, $3.4 \pm 1.3 \times 10^{-6}$, and $2.9 \pm 1.0 \times 10^{-6}$ events yr^{-1} (compare summary statistics for the preferred models for Tables 7.5 and 7.6). The reason for this reversal in the recurrence estimations, is the $\hat{\beta}$ values for the preferred data sets are all < 1.0 , and are consistent with a waning volcanic system.

d. Volume-Predictable Recurrence Rates. Crowe et al. (1982) developed an alternative approach to estimating the recurrence rate of volcanic events. They examined magma-output rates from a plot of the erupted volume of magma versus time for basaltic volcanic events of the YMR. The slope of the curve on this plot is the magma-output rate. Crowe and Perry (1989) noted that there are several limitations of a homogeneous Poisson model based on event counts that can be overcome by application of volume-predictable recurrence rates. First, vent counts record only the recognition of a volcanic event. Its magnitude, commonly expressed as the volume of the event, is not accounted for through a vent count. A large volume eruption is given an equal weight in an event count as a small volume eruption. Second, the previous discussion of homogeneous and nonhomogeneous Poisson counts event counts show they can over-estimate or under-estimate recurrence rates, dependent on the observation period compared to the event distribution in the geologic record. This problem can be overcome by constructing vent counts over an interval that is tied to the geologic record. Crowe and Perry (1989) noted that an alternative approach,

Table 7.6 Nonhomogeneous Recurrence Models (E1) for the YMR

Interval	Model	Interval (yrs)	Minimum events yr ⁻¹	Maximum events yr ⁻¹	Most Likely events yr ⁻¹
Quaternary		2.00E+06			
	Events		3	8	6
	Beta		3.10	2.10	2.30
	Weibull Rate		4.6E-06	8.4E-06	6.9E-06
	Stress Dike		3	8	5
	Beta		3.1	2.10	2.10
Volcanic Cycle*		4.80E+06			
	Events		8	19	12
	Beta		0.84	0.72	1.00
	Weibull Rate		1.4E-06	2.9E-06	2.5E-06
	Stress Dike		8	10	10
	Beta		0.84	0.9	0.9
Quaternary Rate		1.60E+06			
	Events		3	8	6
	Beta		1.7	1.4	1.7
	Weibull Rate		3.2E-06	7.0E-06	6.4E-06
	Stress Dike		3	6	5
	Beta		1.7	1.7	1.8
Quaternary Accelerated*		1.00E+06			
	Events		3	8	6
	Beta		0.94	0.60	0.70
	Weibull Rate		2.8E-06	4.8E-06	4.2E-06
	Stress Dike		3	6	5
	Beta		0.94	0.70	0.60
Summary Statistics (all models)		<i>Mean</i>	3.0E-06	5.5E-06	4.6E-06
		<i>Median</i>	3.0E-06	5.6E-06	4.7E-06
		<i>Geomean</i>	2.8E-06	4.9E-06	4.0E-06
		<i>Std Deviation</i>	1.2E-06	2.4E-06	1.9E-06
Summary Statistics (Preferred Models)*		<i>Mean</i>	2.1E-06	3.4E-06	2.9E-06
		<i>Median</i>	2.1E-06	3.5E-06	2.7E-06
		<i>Geomean</i>	2.0E-06	3.2E-06	2.8E-06
		<i>Std Deviation</i>	8.08E-07	1.30E-06	9.76E-07

* Preferred models are models with event counts spanning intervals that correspond to cycles of volcanic activity (4.8 Ma to present; 1.0 Ma to present)

which is based on a process-based perspective of basaltic volcanism, is to construct time-volume curves of volcanic activity.

Estimations of recurrence rates for volcanic centers and fields using a time-volume relationship have been determined frequently in the geological literature. Bacon (1982) noted that time-volume behavior of basaltic and rhyolitic volcanism in the Coso volcanic field of eastern California exhibited time-predictable behavior. He discussed analogs between the volcanic events of the Coso volcanic field and slip-predictable behavior observed for some types of earthquake sequences. Kuntz et

al. (1986) described volume-predictable eruptions of the Great Rift in the Snake River plains of Idaho. They identified a change in magma-output rates on the basis of a change in slope of the curve of magma-volume versus time. Wadge (1982) described steady-state (volume-predictable) behavior of many polygenetic volcanoes. He used the slope of a time-volume curve to define the effusion rate of volcanoes, and speculated that the steady-state behavior was probably controlled by the magma-supply rates. Volume-predictable behavior was documented for historical eruptions of the volcanoes of Kilauea, Mauna Loa and Piton de la Fournaise (King 1989; Stieltjes and Moutou 1987). Theoretical support for a volume-predictable behavior of volcanoes controlled by magma supply rate was provided by Shaw (1980; 1987).

Estimation of magma-output rates for the basaltic volcanic record of the YMR has been established through examination of plots of magma volume through time (Crowe et al. 1982; 1989; Crowe and Perry, 1989). Published estimations range from 210 to 33 m³ yr.⁻¹ The variability in the estimated output rates is from different observation periods and different models of the age and volume of the volcanic centers. Crowe and Perry (1989) noted that the calculations of the magma-output rate for the YMP are especially sensitive to assumptions concerning the volume of the scoria-fall sheet associated with each volcanic center.

The major limitations in estimating magma-output rates in the YMP are the small number of Pliocene and Quaternary volcanic events (sparse data set), the difficulty of reconstructing eruption volumes for Pliocene volcanic events, and the variability and uncertainty of establishing the chronology of some volcanic events. We are still reassessing the eruption volumes of volcanic events. Moreover, the chronology of volcanic events has not been completed for all Quaternary and Pliocene volcanic events. Therefore, estimations of the magma-output rate through time remain preliminary. However, an important test of the models of Crowe et al. (1982; 1989) and Crowe and Perry (1989) is how the simple regression model of time (independent variable) versus magma volume (dependent variable) is affected by adding data not used in previous regression calculations. The important new data include the recognition of the Pliocene-age, basalt center of Thirsty Mesa (4.8 Ma; 3 km³), the drilling, dating, and volume estimates for the aeromagnetic anomalies of the Amargosa Valley (Section II), and changes in the estimated ages of individual volcanic centers using the most current geochronology data. Exploratory data analyses of the revised data set (Table 7.4) reveal several important features. First, the volume data are not randomly distributed. The large volume basalt center of Thirsty Mesa is an outlier, and skews the distribution of volume data toward larger values. Second, an influence diagram of volume-time data shows the correlation between volume and age is strongly influenced by the large volume of the basalt of Thirsty Mesa. Any regression analyses of the data set will be weighted heavily by this data point.

Fig. 7.8 is a plot of magma volume versus time and includes the most current data for volcanic events in the YMR. Visually, the fit to a linear model is not satisfactory. There is considerable dispersion from the regression curve, and the y-intercept occurs at negative values of magma volume (an unrealistic fit physically). The regression fit can be improved somewhat by modifying the data using geologic constraints. The aeromagnetic anomalies of the Amargosa Valley are close in age to the basalt of Crater Flat, and can be plotted as a single volume-age point. Fig. 7.9 is a revised plot with the two units combined. The fit of the linear regression curve (solid line) is improved but still remains unsatisfactory; the y-intercept is negative, and some of the points are still dispersed off the regression curve. Visually, the data distribution is curvilinear in the x,y plane and may be better fit with a transformed or nonlinear regression model. Two approaches are used to further test the data. First, the dashed line of Fig. 7.9 is the regression fit obtained using distance weighted least squares of volume-time data. Visually the fit is much improved, and the data distribution is consistent with an exponential decline in magma eruption rates through time. Second, to test for intrinsic linearity, the volume (y-axis data) were log transformed,

Fig. 7.8. Bivariate plot of magma volume (DRE) versus age for the Pliocene and Quaternary volcanic events of the YMR. The dashed line is the least squares, linear-regression fit to the data points. Symbols noted by stars represent volcanic events.

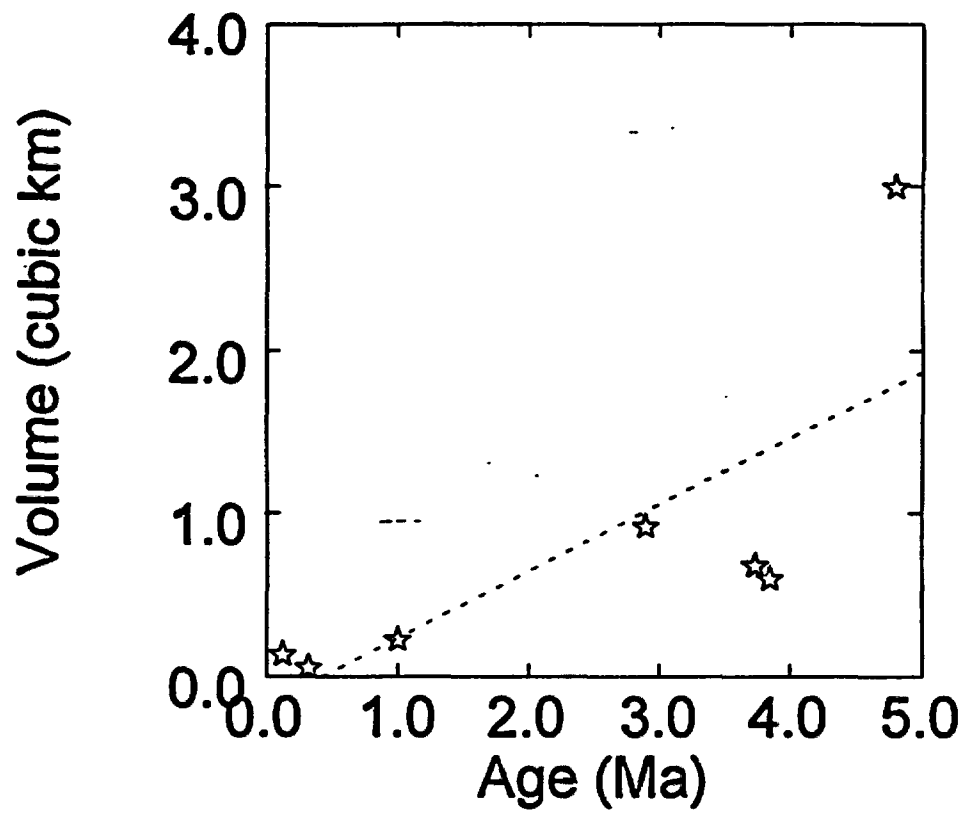


Fig. 7.9 Bivariate plot of magma volume (DRE) versus age for the Pliocene and Quaternary volcanic events of the YMR with the basalt of southeast Crater Flat combined with the aeromagnetic anomalies of the Amargosa Valley. The solid line is the linear-regression curve, the dashed line is fitted by distance weighted least squares..

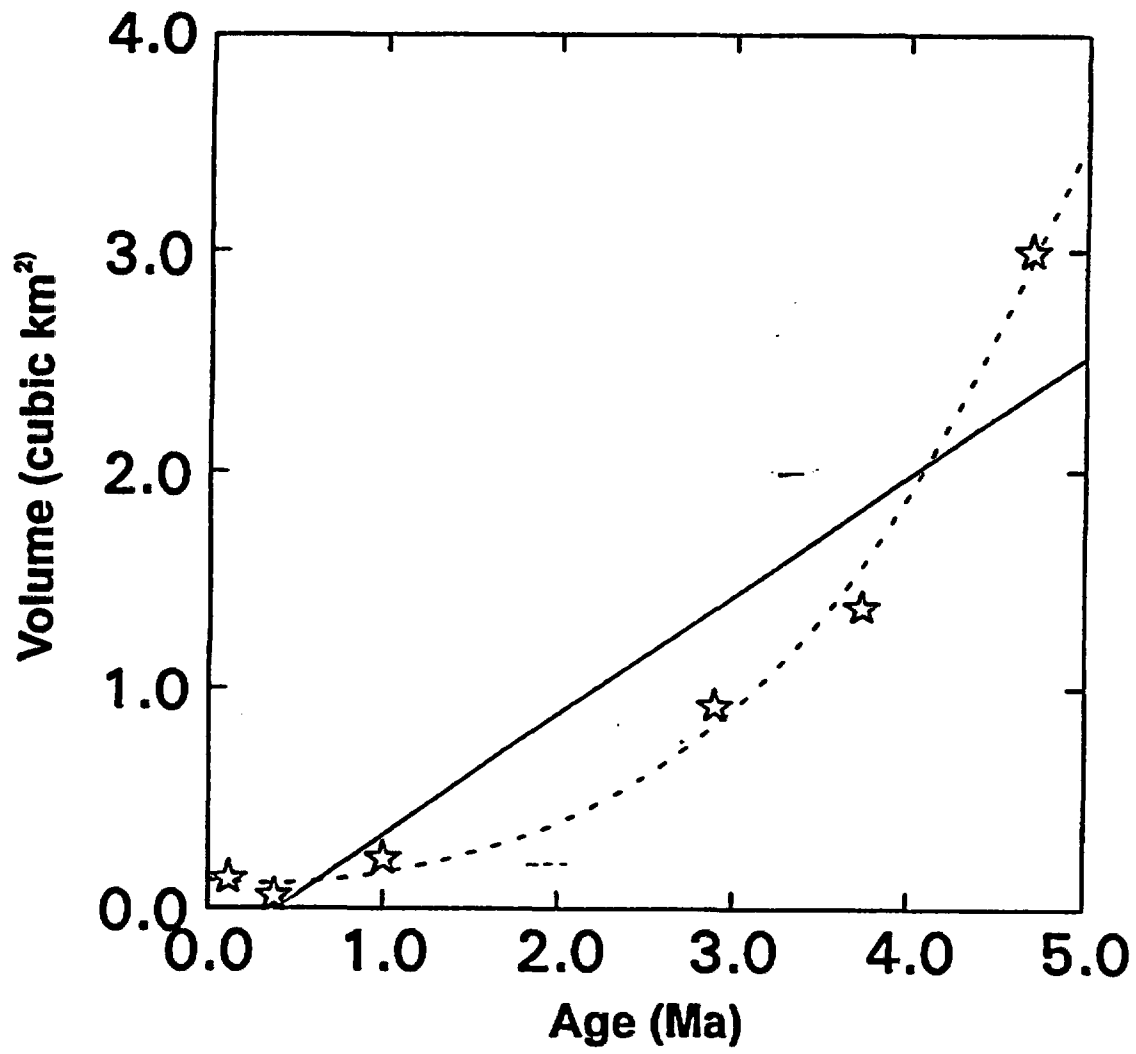
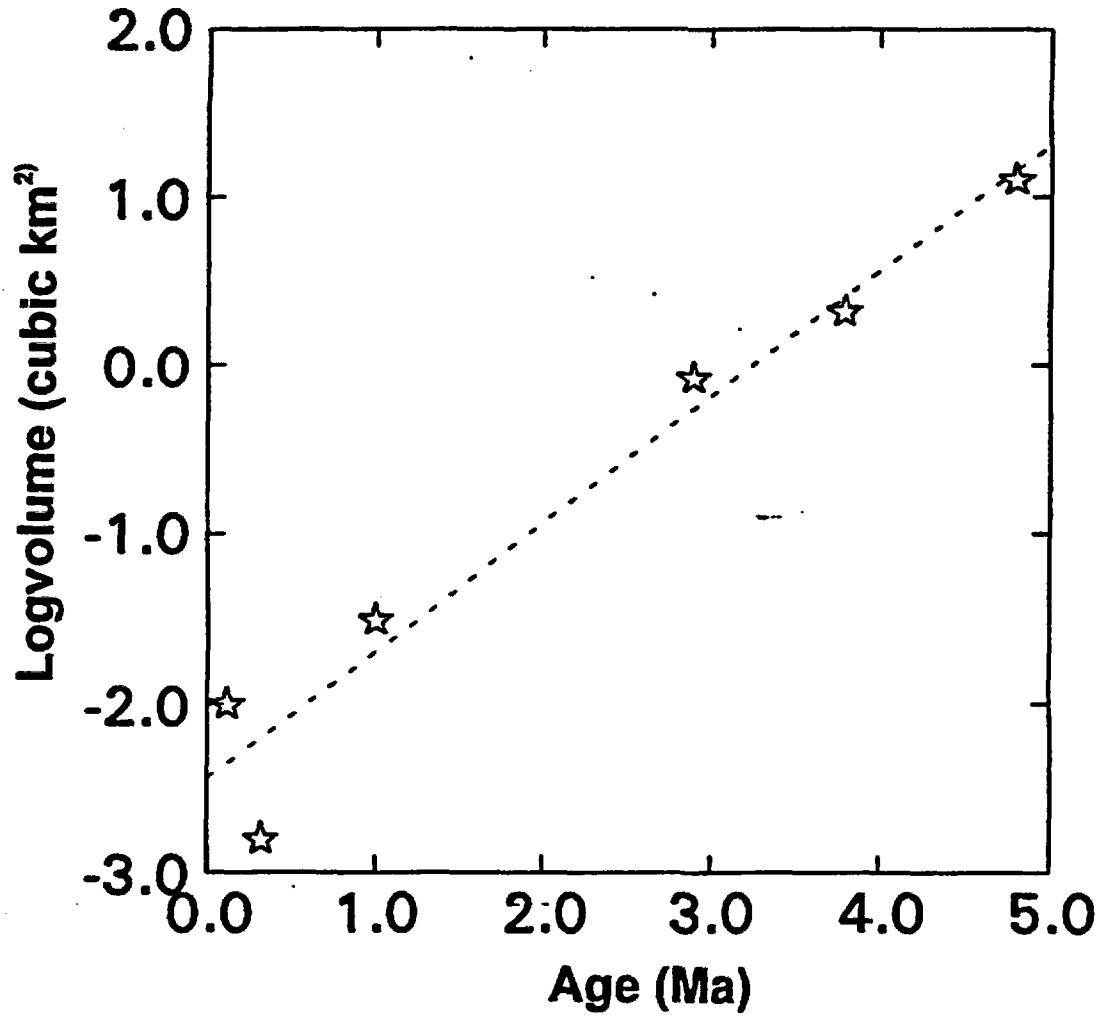


Fig. 7.10 Plot of log-transformed magma volume (DRE) versus age for the Pliocene and Quaternary volcanic events of the YMR with the basalt of southeast Crater Flat combined with the aeromagnetic anomalies of the Amargosa Valley. The solid line is the linear-regression curve of the volume-transformed data.



and fitted by regression using linear smoothing. Fig 7.10 is a plot of the linear regression fit obtained using a regression model of the form

$$E_v = a + b \ln(\text{age}) + \epsilon \quad (7.13)$$

where E_v is the volume a is a constant, b is the slope and ϵ is a random variable representing the regression prediction error. Visually the fit of the log-regression curve is much improved (Fig. 7.10). However, the linear fit is best for the Pliocene data points, and the data are more dispersed for the Quaternary data points. The fit is worse for the basalt of Sleeping Butte. We next examine the suitability of output coefficients and the residuals for a series of regression calculations.

Table 7.7 shows the regression results of a simple linear model using different combinations of the data set of Table 7.4. Table 7.8 is the regression residuals for each of the regression cases of Table 7.7. The regression coefficients (multiple R and squared multiple R) are > 0.86 for all regression cases except cases 1 and 6, and indicate a strong correlation between the volume of volcanic events and the event age. The most significant regression fits are for cases 3 and 4 (two tailed P). The slope or magma-output rate derived from all regression fits ranges from 140 to 750 $\text{m}^3 \text{yr}^{-1}$. These are higher estimates than previous calculations, and reflect the addition in the regression calculations of the large volume Pliocene volcanic events. Careful examination of the residuals shows that the regression fits are generally unsatisfactory (Table 7.8). The studentized residuals show that the data point for the basalt of Thirsty Mesa is an outlier for regression cases 1 and 2, the Lathrop Wells data point is an outlier for case 3, and the Sleeping Butte data point is an outlier for the log-normalized regression (case 7). Plots of residuals versus event age, and residuals versus estimated values show linearity and curvilinear structure. The patterns suggest the data distribution does not meet assumptions of the regression model (the distribution of the error variable ϵ is nonrandom). The patterns of the residuals suggest an added variable or quadratic term is needed in the regression model. The log normalized model improves the fit of the residuals, but also show linear and curvilinear patterns on plots of residuals versus the age (sequencing of residuals) of data points. The three point regression model of the Quaternary events gives a low value of multiple R (Table 7.7).

The difficulties with the regression calculations require caution in interpreting the results. Additional site characterization data will be obtained that may change the regression analysis. Revised volume estimations will be completed for all volcanic centers. Changes in estimated magma volumes may be important particularly for the log-transformed regression analyses that shows the basalt of Sleeping Butte as an outlier. We plan to reassess whether a previously mapped western lava lobe may be part of the Hidden Cone center (see Section II). Incremental addition of this lava volume may move the volume point for the basalt of Sleeping Butte closer to the log-transformed regression curve (Fig. 7.10). We will also examine whether better regression fits can be obtained using multiple regression models. There are strong bivariate correlations between magma volume and the location of basalt centers (see Section III). Moreover, there are systematic variations in magma chemistry with time that correlate with erupted volumes. It may be possible to examine these data as additional variables in multiple regression models.

Until further data are available, the only marginally significant regression results are for cases 3 and 4 of Table 7.7. The magma-output rate is used for these cases (270 and 300 $\text{m}^3 \text{yr}^{-1}$) for estimations of volume-predictable recurrence rates. Table 7.9 is a compilation of representative magma volumes of the volcanic events for the YMR. These values are divided by the magma-output rates to yield the predictor attribute, the generation time to produce a future volcanic event. The generation time is calculated as different combinations of the mean, median, and the geometric mean of the magma volumes of volcanic events during the Quaternary and the YPB. The event recurrence rate is the

Table 7.7 Results of simple regression models for seven combinations (cases) of Pliocene and Quaternary volcanic centers of the YMR.

Regression Model	N	Multiple R	Squared Multiple R	Variable	Coeff	Std Error	T	P (2 tail)
Case 1 All Events	7	0.78	0.61	Constant	-0.17	0.44	-0.39	0.716
				Volume	0.41	0.14	2.80	0.038
Case 2 Case 1 with SE CF and Aeromag Anomalies Combined	6	0.93	0.86	Constant	-0.19	0.30	-0.66	0.545
				Volume	0.53	0.10	4.97	0.008
Case 3 Case 2 without Thirsty Mesa	5	0.98	0.97	Constant	-0.02	0.07	-3.1	0.780
				Volume	0.34	0.03	10.57	0.002
Case 4 Case 3 Without Undrifted Aeromag Anomalies	5	0.98	0.96	Constant	0.03	0.07	0.44	0.940
				Volume	0.26	0.03	8.61	0.003
Case 5 Case 4 without SE Crater Flat	4	0.96	0.96	Constant	0.01	0.07	0.09	0.940
				Volume	.30	0.04	6.96	0.020
Case 6 Quaternary Volcanic Centers	3	0.76	0.58	Constant	0.08	0.07	1.04	0.487
				Volume	0.14	0.12	1.17	0.451
Case 7 All Events, Aeromag Combined Log-Transformed Volume	6	0.97	0.95	Constant	-2.43	0.28	-9.75	0.001
				Volume	0.75	0.10	8.45	0.001

Table 7.8 Regression residuals for the seven regression cases of Table 7.7.

Regression Model	Volcanic Events	Estimate	Residual	Leverage	Cook	Student	Seprad
Case 1	Thirsty Mesa	1.79	1.21	.41	1.67	8.33	.47
	Aeromag Anom	1.40	-.80	.24	.25	-1.37	.36
	SE Crater Flat	1.35	-.67	.23	.16	-1.07	.35
	Buckboard Mesa	1.01	-.09	.15	.00	-.12	.29
	Quat Crater Flat	.24	-.01	.23	.00	-.01	.35
	Sleeping Butte	-.04	.10	.34	.01	.15	.43
	Lathrop Wells	-.12	.26	.38	.07	.42	.45
Case 2	Thirsty Mesa	2.37	.63	.53	2.19	8.49	.34
	SE Crater Flat	1.83	-.45	.31	.30	-1.23	.26
	Buckboard Mesa	1.35	-.43	.20	.13	-1.03	.21
	Quat Crater Flat	.34	-.11	.24	.01	-.22	.23
	Sleeping Butte	-.03	.09	.34	.01	.20	.28
	Lathrop	-.13	.27	.38	.17	.69	.29
Case 3	SE Crater Flat	1.30	.08	.64	1.26	1.33	.10
	Buckboard Mesa	.99	-.07	.35	.17	-.73	.06
	Quat Crater Flat	.33	-.10	.24	.16	-1.04	.05
	Sleeping Butte	.09	-.03	.36	.03	-.28	.07
	Lathrop Wells	.02	.12	.41	.72	2.07	.07
Case 4	SE Crater Flat	1.04	-.06	.63	.92	-1.06	.08
	Buckboard Mesa	.81	.11	.36	.50	1.75	.06
	Quat Crater Flat	.30	-.07	.24	.10	-.74	.05
	Sleeping Butte	.11	-.05	.36	.13	-.61	.06
	Lathrop Wells	.06	.08	.41	.39	1.07	.06
Case 5	Buckboard Mesa	.90	.03	.93	9.55	1.43	.09
	Quat Crater Flat	.31	-.08	.25	.16	-.95	.05
	Sleeping Butte	.10	-.04	.37	.10	-.44	.06
	Lathrop Wells	.04	.10	.44	.71	2.88	.06
Case 6	Quat Crater Flat	.22	.01	.97	15.4	.	.08
	Sleeping Butte	.12	-.06	.39	.32	.	.05
	Lathrop Wells	.09	.05	.64	.88	.	.06
Case 7	Thirsty Mesa	1.16	-.06	.53	.03	-.19	.27
	SE Crater Flat	.40	-.09	.31	.02	-.24	.21
	Buckboard Mesa	-.27	.19	.20	.04	.51	.17
	Quat Crater Flat	-1.69	.19	.24	.05	.54	.18
	Sleeping Butte	-2.20	-.60	.34	1.00	-8.24	.22
	Lathrop Wells	-2.35	.35	.38	.45	1.30	.23

Table 7.9 Age, Cumulation Volume, Magma Output Rates, Generation Rates, and Event Rates for Pliocene and Quaternary Volcanic Centers of the YMR.

EVENT MODELS	AGE (Ma)	VOLUME	CUMVOL	MOR* (m ³ yr ⁻¹)			
Event: Case I							
Thirsty Mesa	4.8	3.0E+09	3.0E+09	305	GR** (mean)	GR (geomean)	GR (median)
Amargosa Valley	3.8	3.0E+08	3.3E+09	268	2.5E+06	1.2E+06	9.7E+05
CF3.7	3.7	6.8E+08	4.0E+09		2.8E+06	1.4E+06	1.1E+06
Buckboard	2.9	9.2E+08	4.9E+09		ER*** (mean)	ER (geomean)	GR (median)
CF1.0	1.0	2.3E+08	5.1E+09		4.0E-07	8.2E-07	1.0E-06
Sleeping Butte	.32	5.9E+07	5.2E+09		3.5E-07	7.2E-07	9.0E-07
Lathrop Wells	.12	1.4E+08	5.3E+09				
<i>Mean</i>	<i>7.6E+08</i>	<i>Median</i>	<i>3.0E+08</i>				
<i>Geomean</i>	<i>3.8E+08</i>	<i>Std Deviation</i>	<i>1.0E+09</i>				
Event: Case II							
CF1.0	1.0	2.3E+08	2.3E+08	305	GR (mean)	GR (geomean)	GR (median)
Sleeping Butte	.32	5.9E+07	2.9E+08	268	4.6E+05	4.0E+05	4.5E+05
Lathrop Wells	.12	1.4E+08	4.3E+08		5.2E+05	4.5E+05	5.1E+05
<i>Mean</i>	<i>1.4E+08</i>	<i>Median</i>	<i>1.4E+08</i>		ER (mean)	ER (geomean)	ER (median)
<i>Geomean</i>	<i>1.2E+08</i>	<i>Std Deviation</i>	<i>8.5E+07</i>		2.2E-06	2.5E-06	2.2E-06
					1.9E-06	2.2E-06	1.9E-06
Event: Case III							
CF-North	1.0	1.7E+08	1.7E+08	305	GR (mean)	GR (geomean)	GR (median)
CF-South	1.0	6.0E+07	2.3E+08	268	2.7E+05	2.1E+05	1.9E+05
Hidden	.32	3.5E+07	2.6E+08		3.1E+05	2.3E+05	2.1E+05
Black Peak	.32	2.4E+07	2.9E+08		ER (mean)	ER (geomean)	ER (median)
Lathrop	.12	1.4E+08	4.3E+08		3.7E-06	4.9E-06	5.3E-06
<i>Mean</i>	<i>8.6E+07</i>	<i>Median</i>	<i>6.0E+07</i>		3.2E-06	4.2E-06	4.6E-06
<i>Geomean</i>	<i>6.5E+07</i>	<i>Std Deviation</i>	<i>6.5E+07</i>				
*MOR : Magma Output Rate					<i>Preferred Models</i>	<i>Generation Rate</i>	<i>Event Rate</i>
**GR= Generation Rate					<i>Preferred mean</i>	2.9E+05	3.4E-06
***ER = Event Rate					<i>Preferred median</i>	2.0E+05	5.0E-06
					<i>Preferred geomean</i>	2.2E+05	4.5E-06

reciprocal of generation time. The calculation for the recurrence time to the next volcanic event using the magma-output rate is given by:

$$N_e = (R_v/O_p) - L_t \quad (7.14)$$

where N_e is the predicted time to the next volcanic event, R_v is the representative volume of a volcanic event, O_p is the magma output rate and L_t is the time since the last volcanic event (Crowe et al. 1982). The time of the last event is the age of the youngest volcanic event at the Lathrop Wells volcanic center and is estimated to be 9 ka (see Section II).

A difficult attribute to characterize for the magma-volume calculations is the representative volume of a future volcanic event. Table 7.9 compiles magma volumes, the magma-output rates from regression analyses, and generation-time and event-time estimations for three sets of data. These include the YPB volcanic events (4.8 Ma and younger), volcanic events ≤ 1 Ma, and the smallest volume events (event = volcanic center) of the Quaternary volcanic record (≤ 1 Ma). Examination of the predicted generation times of representative events for the YPB data set shows that all values exceed 1 Ma, a physically unrealistic value (Table 7.9). Figure 7.9, the plot of magma volume versus time for all volcanic events of the YPB provides an explanation for the long predicted magma-generation times. The volume of erupted magma has decreased exponentially through time. The volume of erupted magma for a representative volcanic event has decreased by more than a factor of 30 since the Pliocene. Averaging the volume of volcanic events for the Pliocene and Quaternary give mean values that are unrealistically large compared to the volume of volcanic events of the late Quaternary.

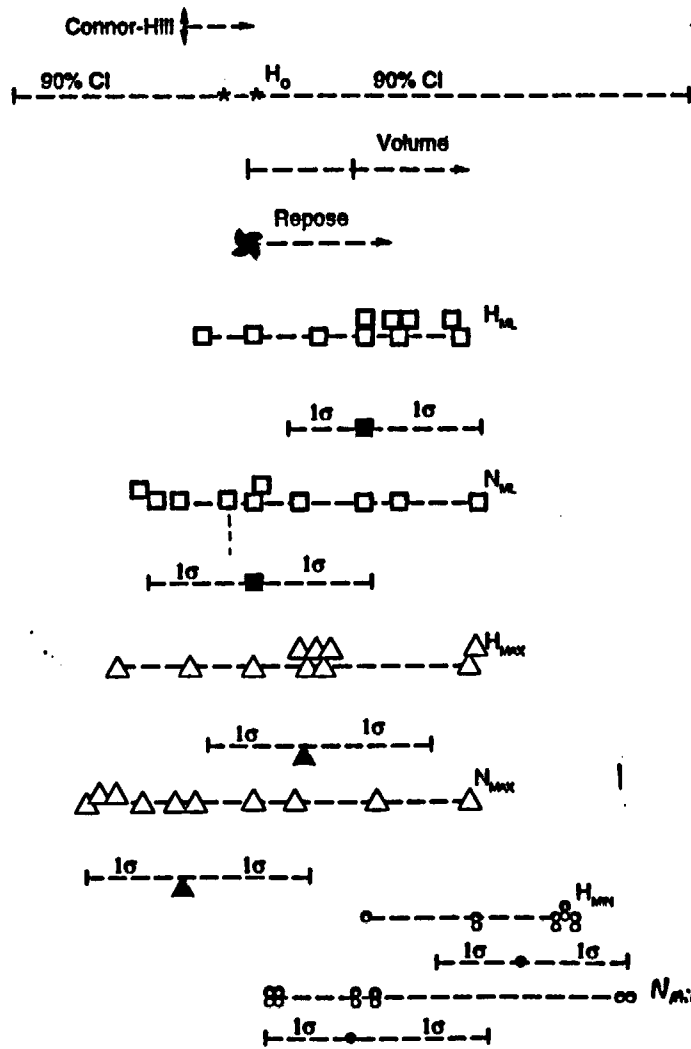
A second approach to estimating recurrence times using magma-volume plots is to use the volume of Quaternary eruptive events to establish the representative eruptive volume. This results in decreased estimated magma-generation times but the intervals are still consistently greater than 4×10^6 yrs. These generation times give estimated event rates of $\leq 2.5 \times 10^{-6}$ events yr⁻¹. These estimates are equal to the minimum homogeneous and nonhomogeneous Poisson rates derived from counts of volcanic events (Tables 7.5 and 7.6). Projection of these rates for the Quaternary and YPB intervals gives low predicted numbers of volcanic events compared to the observed geologic record.

A third approach is to use representative volumes of the smallest Quaternary volcanic events (data set III of Table 7.9). Here event rates are equal to and slightly greater (3.2 to 5.3×10^{-6} events yr⁻¹) than the homogeneous and nonhomogeneous Poisson event count rates of Tables 7.5 and 7.6.

e. Simulation Modeling: E1 the Recurrence Rate. This part of Section VII uses risk simulation to define and assess the distribution of E1 in probability space. Representative estimates for E1 are selected from the data tables for E1 (Table 7.5 and 7.6). These estimates are used systematically in simulation modeling to generate cumulative probability distributions curves. There are nearly an infinite number of approaches that can be used in risk modeling. No single approach is likely to gain complete acceptance. We attempt to bound the problem by producing a range of probability distribution curves using mid-point estimates for the range of models of the recurrence rate. We also explore the sensitivity of the risk modeling by systematically varying the bounding assumptions used to describe the distributions.

An upper bound for E1 is established from the regulatory guidelines of 10 CFR60 (Fig. 7.11). An adverse condition is defined as the presence of igneous activity in the Quaternary or 2 Ma using the regulatory definition. Formulated probabilistically, the risk of volcanism becomes a concern for siting a potential repository when there is at least one volcanic event in the Quaternary ($1 \text{ event}/2 \times 10^6 \text{ yrs}$ or $\approx 5 \times 10^{-7}$ events yr⁻¹) (regulatory perspective of Fig. 7.11). An upper bound to rates of volcanic events can be defined by event rates in large volume, very active basaltic volcanic fields of the basin-range province,

Fig. 7.11. Distribution of estimates of E1 in probability space. The x-axis is a log scale. The y-axis has no scale and is used only to distribute the overlapping estimates of E1.



\leftarrow Issue Non-Issue \rightarrow

Regulatory Perspective

Quaternary
Field Limits



E1 (Events yr⁻¹)

selecting fields in analogous tectonic settings as the YMR. The fields used for the rate bounds are the Lunar Crater volcanic field in central Nevada (Scott and Trask, 1971; Crowe et al. 1992; 1993) and the Cima volcanic field (Dohrenwend et al 1986; Wilshire, 1991; Crowe et al. 1992; 1993). The potential Yucca Mountain site is not located in a major volcanic field. Therefore, logically, the recurrence rates in the YMR must be less than rates in major basaltic volcanic fields. The Lunar Crater has a maximum of 82 vents occurring in 28 clusters of probable Quaternary age (Crowe et al. 1992). A cluster is defined as a closely aligned group of volcanic vents that could be fed from a single dike system. They are identified primarily from structural alignments and proximity of individual vents. The Cima volcanic field has 29 vents in 22 clusters, all of inferred Quaternary age. Translating these vent and cluster counts into event counts gives Quaternary recurrence rates of 4.5×10^{-5} to 1.1×10^{-5} events yr^{-1} (we assume a homogeneous Poisson model for the fields because the chronology of the events is too poorly constrained to test other distribution models). These rates are shown in the box labeled volcanic field limits on Fig. 7.11.

Table 7.10 is matrix of E1 values assembled for simulation modeling. The matrix is divided into columns representing five simulation conditions; the rows represent eight different approaches used to estimate E1. Crowe et al. (1993) showed that the median (50% estimates) from cumulative probability distributions for E1 are sensitive to the selection of probability bounds, and are somewhat insensitive to mid-point estimates. The five simulation models of Table 7.10 assign different values for the upper and lower bounds of assumed distributions for E1. There is insufficient information (limited number of volcanic events in the geologic record) to define precisely the shape of the probability distribution curve between the upper and lower bounds of Fig. 7.11. The most logical choice for a distribution form for E1 is the triangular distribution (boundary values constrained, midpoints estimated). Because the distribution bounds for E1 can be described (their values are > zero on a probability distribution curve), the triangular distribution is not appropriate (Newendorp 1974). We use a trigen distribution model for most of the modeling simulations. This is a modified form of the triangular distribution and allows input of upper, lower, and mid-point estimates. The midpoint estimate is the most likely value, and the upper and lower estimates are chosen from values that are > 0 and bracket the midpoint estimate (lower bound < midpoint < upper bound).

Simulation one of Table 7.10 uses midpoint estimates of E1 from the summary statistics and estimates of Tables 7.5, 7.6, and 7.9; the 25 and 75 percentiles of the distribution curve are assigned from the minimum and maximum values of the probability tables. Simulations two through four use the same midpoint estimates as simulation two but the upper and lower estimates of the distribution are used from the probability bounds of Fig. 7.11 (lower bound = regulatory perspective; upper bound = volcanic field limits). The lower estimate of 5×10^{-7} events yr^{-1} is assigned a fixed value of 10% in all the simulations. An upper bound of 1.1×10^{-5} events yr^{-1} is assigned a 1, 5, and 10 percentile value respectively, for simulations two through four. Simulation 5 uses a normal distribution, and values for the mean and standard deviation are taken from Tables 7.5, 7.6, and 7.9. The across column variation in the simulation matrix reflects differences in the distribution assumptions (trigen and normal), and boundary assumptions for the distributions.

The eight rows of the E1 simulation matrix vary only in the assignment of mid-point estimates for the trigen distribution. Row one uses mean values from the summary statistics for the most likely estimates of E1 for all homogeneous Poisson models from Table 7.5. Row two uses most likely estimates for homogeneous Poisson models from the summary statistics of the preferred models (corresponding to volcanic cycles of the 4.8 and 1.0 Ma intervals). Row three is identical to row one but assigns the most likely estimates from summary statistics for all nonhomogeneous Poisson models (Table 7.6). Row four is identical to Row two but derives the most likely estimates from the summary statistics of the preferred models of the nonhomogeneous distribution. Row five assigns the midpoint estimates for E1 from repose

Table 7.10 Simulation Matrix , expected values and matrix statistics for E1, the recurrence rate.

Model	Min	Most Likely	Max	Min(all)	Max(all)				
Homogeneous: All	2.1E-06	3.6E+00	4.8E-06	1.5E-06	8.0E-06				
Homogeneous: Pref	2.3E-06	4.1E-06	5.0E-06	1.7E-06	8.0E-06				
Nonhomogeneous: All	3.0E-06	4.4E-06	5.5E-06	1.4E-06	8.4E-06				
Nonhomogeneous: Pref	2.1E-06	2.9E-06	3.4E-06	1.4E-06	4.8E-06				
Repose			5.3E-06						
Volume-Predict	1.0E-06	3.2E-06	5.3E-06						
<i>Distribution Boundaries</i>	quartiles	10%/1% limits	10%/5% limits	10%/10% limits	Normal (1 σ)				
Risk Simulations	Sim1	Sim2	Sim3	Sim4	Sim5	<i>Mean</i>	<i>Median</i>	<i>Geomean</i>	<i>Std Dev</i>
Homogeneous: All	4.8E-06	4.4E-06	4.9E-06	5.4E-06	3.6E-06	4.6E-06	4.8E-06	4.6E-06	6.8E-07
Homogeneous: Pref	4.8E-06	4.1E-06	5.0E-06	5.5E-06	4.1E-06	4.8E-06	4.8E-06	4.8E-06	5.2E-07
Nonhomogeneous: All	4.8E-06	4.6E-06	5.1E-06	5.6E-06	4.5E-06	4.9E-06	4.8E-06	4.9E-06	4.4E-07
Nonhomogeneous: Pref	4.8E-06	4.3E-06	4.8E-06	5.4E-06	2.9E-06	4.4E-06	4.8E-06	4.3E-06	9.3E-07
Repose		4.7E-06	5.2E-06	5.7E-06		5.2E-06	5.2E-06	5.2E-06	4.7E-07
Volume	2.8E-06	4.4E-06	4.9E-06	5.4E-06	3.4E-06	4.5E-06	4.6E-06	4.5E-06	1.1E-06
Minimum		4.0E-06	4.6E-06	5.2E-06	2.2E-06	4.0E-06	4.3E-06	3.8E-06	1.3E-06
Maximum		5.3E-06	5.7E-06	6.1E-06	4.5E-06	5.4E-06	5.5E-06	5.5E-06	6.7E-07
Ho (1992)	7.0E-06								
<i>Mean</i>	4.4E-06	4.5E-06	5.0E-06	5.5E-06	3.6E-06				
<i>Median</i>	4.8E-06	4.5E-06	5.0E-06	5.5E-06	3.6E-06				
<i>Geomean</i>	4.3E-06	4.5E-06	5.0E-06	5.5E-06	3.5E-06				
<i>Std Deviation</i>	8.8E-07	3.8E-07	3.1E-07	2.5E-07	8.4E-07				

Simulations 1 - 4: Trigen distribution. Simulation 1: min- max from Tables 7.5 and 7.6. Simulations 2-4: min-max from Fig. 7.11
 Simulations 5: Normal distribution. Median and standard deviation from Tables 7.5 and 7.6.

Table 7.11. Results of simulation modeling using the simulation matrix of Table 7.10.

Homogeneous Poisson: All Models						Homogeneous Poisson: Pref Models					
Cell:	Sim1	Sim2	Sim3	Sim4	Sim5	Sim1	Sim2	Sim3	Sim4	Sim5	
<i>Minimum</i>	-5.5E-06	-2.4E-06	-2.7E-06	-2.9E-06	-8.8E-07	<i>Minimum</i>	-5.9E-06	-2.6E-06	-2.9E-06	-3.1E-06	-6.9E-06
<i>10Perc</i>	-1.1E-06	4.99E-07	4.99E-07	4.99E-07	2.08E-06	<i>10Perc</i>	-1.3E-06	4.99E-07	4.99E-07	4.99E-07	9.45E-07
<i>Mean</i>	4.79E-06	4.41E-06	4.93E-06	5.45E-06	3.62E-06	<i>Mean</i>	4.77E-06	4.52E-06	5.02E-06	5.52E-06	4.15E-06
<i>90Perc</i>	1.11E-05	8.59E-06	9.78E-06	1.1E-05	5.16E-06	<i>90Perc</i>	1.1E-05	8.66E-06	9.82E-06	1.1E-05	7.35E-06
<i>Maximum</i>	1.62E-05	1.21E-05	1.39E-05	1.57E-05	8.37E-06	<i>Maximum</i>	1.6E-05	1.2E-05	1.38E-05	1.56E-05	1.37E-05
Nonhomogeneous : Poisson All Models						Nonhomogeneous Poisson: Pref Models					
Cell:	Sim1	Sim2	Sim3	Sim4	Sim5	Sim1	Sim2	Sim3	Sim4	Sim5	
<i>Minimum</i>	-8.1E-06	-2.7E-06	-3E-06	-3.3E-06	-4.1E-06	<i>Minimum</i>	-5E-06	-2.2E-06	-2.4E-06	-2.7E-06	-9E-07
<i>10Perc</i>	-1.3E-06	4.99E-07	5E-07	4.99E-07	1.65E-06	<i>10Perc</i>	-9.2E-07	4.99E-07	4.99E-07	5E-07	1.64E-06
<i>Mean</i>	4.76E-06	4.58E-06	5.07E-06	5.57E-06	4.48E-06	<i>Mean</i>	4.82E-06	4.28E-06	4.82E-06	5.36E-06	2.9E-06
<i>90Perc</i>	1.09E-05	8.7E-06	9.84E-06	1.1E-05	7.27E-06	<i>90Perc</i>	1.12E-05	8.51E-06	9.74E-06	1.1E-05	4.16E-06
<i>Maximum</i>	1.59E-05	1.2E-05	1.37E-05	1.55E-05	1.48E-05	<i>Maximum</i>	1.66E-05	1.21E-05	1.39E-05	1.59E-05	6.77E-06
Repose Models						Volume Models					
	Sim1	Sim2	Sim3	Sim4	Sim5	Sim1	Sim2	Sim3	Sim4	Sim5	
<i>Minimum</i>		-2.9E-06	-3.3E-06	-3.5E-06		<i>Minimum</i>	-5.9E-06	-2.4E-06	-2.6E-06	-2.9E-06	4.51E-07
<i>10Perc</i>		4.99E-07	4.99E-07	4.99E-07		<i>10Perc</i>	-2E-06	5E-07	4.99E-07	4.99E-07	2.42E-06
<i>Mean</i>		4.73E-06	5.19E-06	5.67E-06		<i>Mean</i>	2.82E-06	4.38E-06	4.9E-06	5.43E-06	3.43E-06
<i>90Perc</i>		8.81E-06	9.89E-06	1.1E-05		<i>90Perc</i>	7.41E-06	8.57E-06	9.77E-06	1.1E-05	4.44E-06
<i>Maximum</i>		1.19E-05	1.36E-05	1.53E-05		<i>Maximum</i>	1.09E-05	1.21E-05	1.39E-05	1.57E-05	6.36E-06
Minimum Models						Maximum Models					
	Sim1	Sim2	Sim3	Sim4	Sim5	Sim1	Sim2	Sim3	Sim4	Sim5	
<i>Minimum</i>		-1.4E-06	-1.7E-06	-1.9E-06	1.96E-06	<i>Minimum</i>		-3.7E-06	-3.9E-06	-4.2E-06	-2.6E-06
<i>10Perc</i>		5E-07	5E-07	4.99E-07	2.15E-06	<i>10Perc</i>		5E-07	4.99E-07	4.99E-07	2.06E-06
<i>Mean</i>		4.04E-06	4.62E-06	5.2E-06	2.25E-06	<i>Mean</i>		5.33E-06	5.68E-06	6.06E-06	4.5E-06
<i>90Perc</i>		8.37E-06	9.66E-06	1.1E-05	2.35E-06	<i>90Perc</i>		9.35E-06	1.01E-05	1.1E-05	6.93E-06
<i>Maximum</i>		1.22E-05	1.41E-05	1.6E-05	2.56E-06	<i>Maximum</i>		1.17E-05	1.3E-05	1.44E-05	1.17E-05

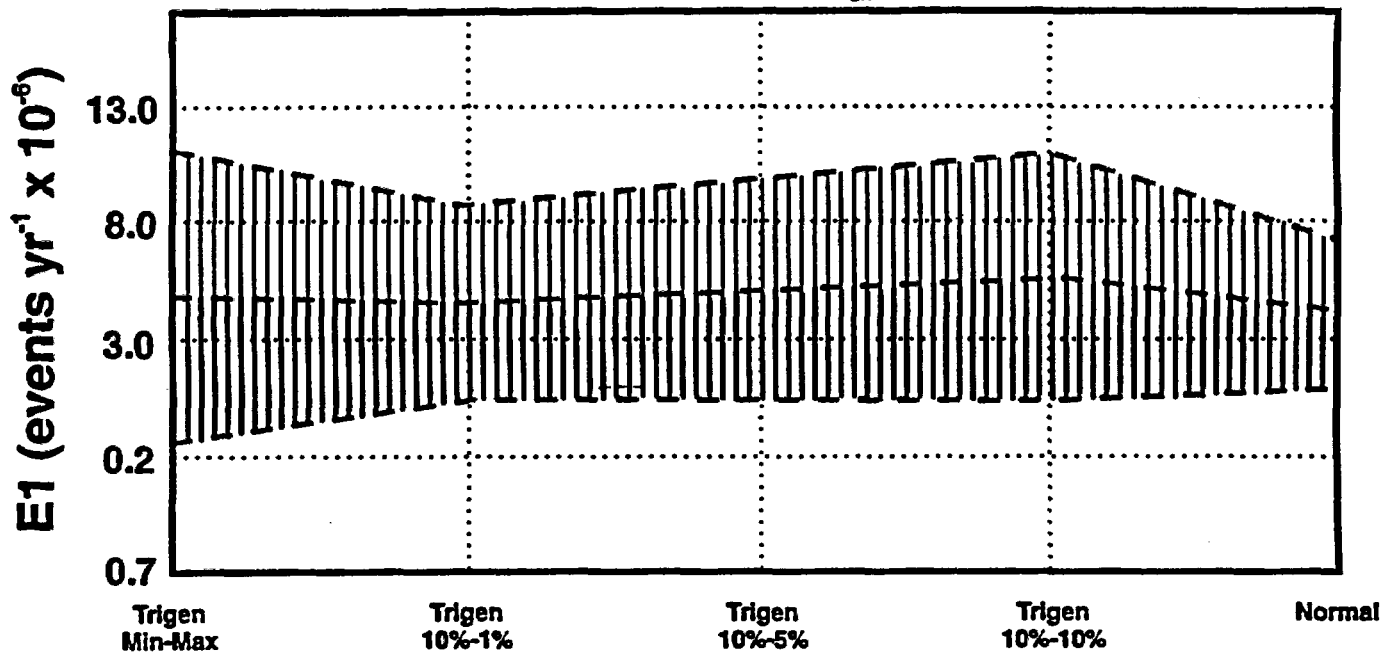
calculations. However, because only the minimum repose interval was used in the calculations, row five estimates are biased toward higher or maximum recurrence rates. The most likely estimates of rows six and seven were obtained from the summary statistics for the minimum and maximum recurrence rate estimates using all homogeneous and nonhomogeneous Poisson models. Finally, row nine uses the midpoint estimates, and the 90% confidence intervals from the most recent calculations of Ho (1992). These midpoint estimates and confidence limits are biased toward higher probabilities for E1 because they were derived from a *worse case estimate*, and the confidence intervals are centered about that estimate (instead of a mid-point estimate). The distributions are shown primarily for comparison, and the distribution assumptions are not varied across the simulation matrix.

Table 7.11 lists summary statistics for the risk simulations using the simulation matrix of Table 7.10. The simulations were run with 10,000 iterations using the Latin Hypercube sampling method. The across row simulations of the preferred model using a homogeneous Poisson distribution (Table 7.11) show only minor variations in the uncertainty (mean, 10 and 90 percentile estimates) for the risk simulations (Fig. 7.12). Simulation one shows the widest distribution because of the assignment of 25% values for the upper and lower bounds. The cumulative distribution curves for simulations two through four are shifted systematically toward higher probability values reflecting the progressive skewing of the distribution toward the upper probability bounds (1, 5 and 10% lower bound). The distribution curve for simulation five has the smallest uncertainty because the data were modeled as a normal distribution (Fig. 7.12). Fig. 7.13 is the same plot as Fig. 7.12 but is for the preferred model using a nonhomogeneous Poisson distribution. The uncertainty again is smallest for simulation five because it is modeled as a normal distribution. Also, simulation five has the smallest mean estimate because β is < 1 for the nonhomogeneous Poisson distribution (Fig. 7.13). The range of the mean estimates (Table 7.11) for the across row simulations are 2.2×10^{-6} (minimum model) to 6.1×10^{-6} events (maximum model). The range of mean estimates for the preferred data sets using homogeneous and nonhomogeneous recurrence models is 2.9×10^{-6} (nonhomogeneous Poisson) to 5.5×10^{-6} events yr^{-1} (homogeneous Poisson).

Additional insight into the cumulative probability distribution curves for E1 is provided by examining simulation summaries for individual columns of the simulation matrix. Fig. 7.14 shows the mean estimates and the 10 and 90 percentile estimates for simulation 3 for eight recurrence models (homogeneous and nonhomogeneous preferred, repose, volume, minimum, and maximum). For comparison, the mean estimate and confidence limits from the worst case estimate of Ho (1992) is also shown. The mean estimates and the uncertainty bands are almost uniform except for the estimate of Ho (1992). The similarity in model variation is illustrated also by Fig. 7.15, which is identical to Fig. 14 except it shows the results of risk simulations as cumulative distribution curves. The curves are tightly clustered and there is little difference between all recurrence models except for the minimum and maximum models (Fig. 7.15). The median estimates (50 percentile values) range from 3.3×10^{-6} (volume model) to 7.0×10^{-6} events yr^{-1} (Ho (1992) model). The cumulative probability distribution curve for the estimates of Ho (1992) is separated from the other curves because it is for a maximum estimation, and the confidence are calculated for a maximum estimate not a mid-point or most likely estimate. Overall, the simulation modeling shows that there is limited variation in cumulative probability curves for a range of recurrence models of E1.

Fig. 7.12. Results of simulation modeling of the across row variation of the simulation matrix of Table 7.10 for the homogeneous Poisson distribution model.. The figure shows the variations in the recurrence rate on the y-axis plotted against the mean, and 90 and 10 percentile estimates. This figure examines the variability of the simulation results that are controlled by the distribution assumptions and assumptions of maximum and minimum values for the distributions.

Risk Simulation: Homogeneous Poisson



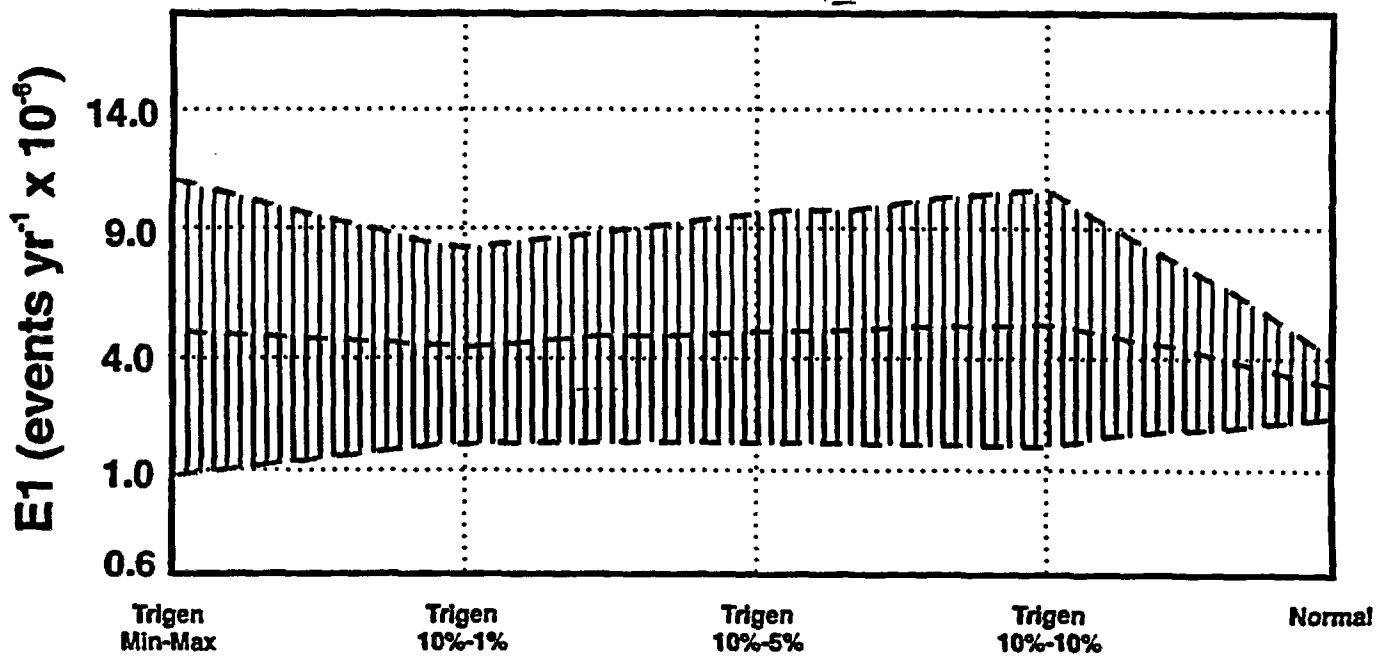
Top - - - - 90 per %

Center - - - - 50 Per %

Bottom - - - - 10 per %

Fig. 7.13. Results of simulation modeling of the across row variation of the simulation matrix of Table 7.10 for the preferred nonhomogeneous Poisson distribution model.

Risk Simulation: Nonhomogeneous Poisson



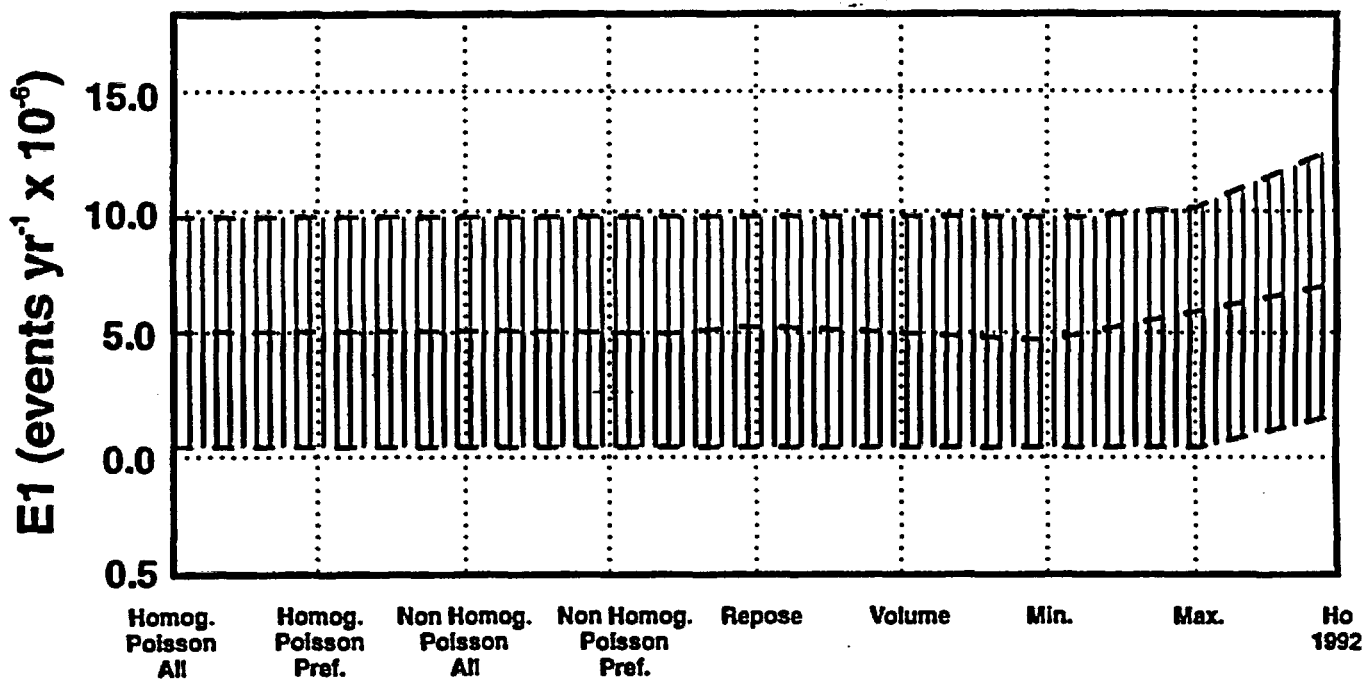
Top - - - - 90 per %

Center - - - - Mean

Bottom - - - - 10 per %

Fig. 7.14. Results of simulation modeling showing the column variation in the simulation matrix of Table 7.10 for simulation three (trigen distribution, upper bound is 10%, lower bound is 5%). This figure examines the variability of the simulation results that are controlled by different models of the recurrence rate.

Risk Simulation: All Models



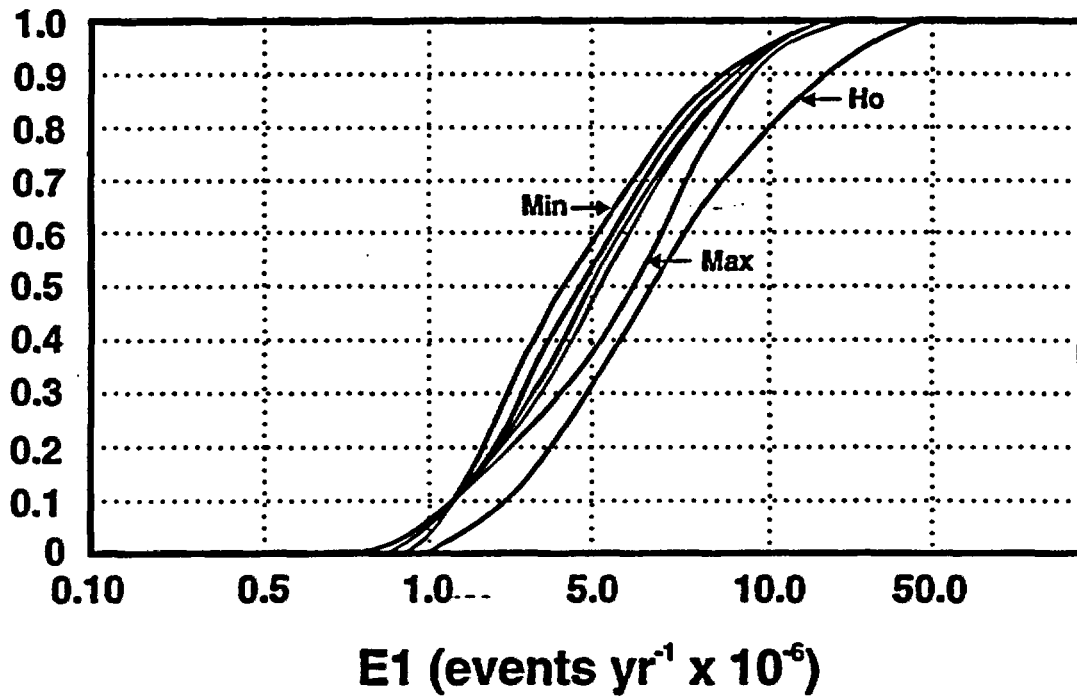
Top - - - - 90 per %

Center - - - - Mean

Bottom - - - - 10 per %

Fig. 7.15. Results of simulation modeling showing the column variation in the simulation matrix of Table 7.10 for simulation three (trigen distribution, upper bound is 10%, lower bound is 5%). This figure is the same as Fig. 7.14 but presents the simulation results as cumulative probability distribution curves.

Simulated Results: E1



Expected Values:

Homogeneous $5.0E^6$
Nonhomogeneous $4.8E^6$
Repose $5.2E^6$
Volume $4.9E^6$
Minimum $4.6E^6$
Maximum $5.7E^6$
Ho(1992) $7.0E^6$

D. Revised Calculations of E2, the Disruption Probability

The second attribute of the conditional probability of magmatic disruption of the potential repository is E2, the probability of magmatic disruption or penetration of a specified area. The primary area of concern is the potential repository, or exploratory block. However, additional attention is given to the controlled area and the YMR in order to assess the occurrence probability of magmatic penetration of the waste isolation system of a geologic repository. The disruption probability, like E1 the recurrence rate, is difficult to quantify because of the small number of volcanic centers in the region. The small number of widely distributed events means that there is considerable uncertainty in calculating E2, and as a result an unconstrained number of models that can be proposed for the spatial distribution of volcanic activity. Further, by virtue of the small number of events, it is difficult to prove or disprove convincingly alternative structural models. Crowe and Carr (1980), and Crowe et al. (1982) attempted to bound the disruption probability using spatial fitting models established from the distribution of volcanic events. Smith et al. (1990) presented alternative models of E2, assuming the distribution of volcanic vents in Crater Flat and vicinity are controlled by local northeast-trending faults. Sheridan (1992) used Monte Carlo simulation to model the distribution of volcanic dikes in the YMR using the geometry of the volcanic field, the dike geometry (aspect ratio, orientation), and structural controls as constraints for the modeling. Wallmann et al. (1993; 1994) also used stochastic models of dike dimensions, and orientation for sets of structural models to establish probabilistic estimates of repository disruption. Connor and Hill (1994) used cluster models (near-neighbor linking) to examine controls on the distribution of volcanic events in the YMR.

There is considerable variability in the structural and topographic setting of Pliocene and Quaternary volcanic centers in the YMR (see Section III). Some centers are located on ring-fracture zones of known and inferred caldera complexes; others occur along existing faults or at the intersection of fault systems. Alternatively, the local stress field may control the location and distribution of clusters of volcanic centers of similar age. The frequency of occurrence of basalt centers is higher in topographic basins compared to range fronts or range interiors (Table 7.2). Volcanic events tend to occur in age-correlated structural clusters (Crowe and Perry 1989). The patterns of the sequenced distribution of the *location* of volcanic events in the YMR are variable and difficult to generalize. There is a tendency for the events to occur in the CFVZ, and possibly secondarily in the NESZ. As a consequence, it is more difficult to limit or bound constraints on the disruption probability (E2) than the recurrence rate of volcanic events (E1).

The approach followed in this section of the *Volcanism Status Report* is to place priority on integrating observational data obtained from the detailed field, chronology and structural studies of volcanic centers. These data provide the primary constraints for development of multiple alternative distribution models. Inferences gathered from statistical analyses of the time-space distribution of volcanic events are given secondary priority for two reasons. First, the small data set is insufficient to test most statistical hypothesis. Second, the variation in the possible controls of the location of volcanic events makes the assumptions required for application of statistical methods difficult. Statistical methods can lead to inferences or identification of patterns in event distribution that are not consistent with the geologic record. Estimating or bounding the disruption probability for the YMR is a difficult and somewhat subjective problem. The only logical approach with the limited data set is to attempt to develop systematically a range of alternative models primarily from geological intuition, and to apply methods of risk analyses. Data from alternative models is assessed and combined through risk simulation to establish cumulative probability distributions for E2. The important comparisons are the similarities or differences in the cumulative probability distributions, not the strengths or weaknesses of individual models. The alternative models for E2 are grouped into three cases. These include models developed

from the spatial distribution of volcanic centers, models involving structural control of the location of volcanic centers, and comparison with analog basaltic volcanic fields of the basin and range province.

a. Published Estimates of E2. Table 7.12 is a compilation of existing estimations of the disruption ratio obtained from published studies of the probability of magmatic disruption of a potential repository at Yucca Mountain. The descriptive statistics for the unedited data from Table 7.12 are: $n = 34$, maximum = 1.7×10^{-2} , minimum = 1.3×10^{-3} , mean = 4.5×10^{-3} , median = 3.7×10^{-4} , standard deviation = 3.1×10^{-3} , skewness = 2.2. The data are strongly skewed to higher or worse case values consistent with bias in the calculations introduced from attempts to bound the distribution of estimates for E2 (similar to published estimates of E1). Exploratory data analyses show that the Lathrop chain model (Smith et al. 1990) is identified as a far outside outlier, and the caldera model (Carr, 1990), the Crater Flat field model (Crowe et al. 1994), and one set of the stochastic dike models (Sheridan 1992) are identified as outlier values. Elimination of these models from the data set of Table 7.12 gives the following summary statistics: $n = 30$, maximum = 7.0×10^{-3} , minimum = 1.3×10^{-3} , mean = 3.6×10^{-3} , median = 3.0×10^{-3} , standard deviation = 1.5×10^{-3} , and skewness = 0.7. The edited data remain skewed toward positive values, and the median is a better statistical descriptor than the mean. However, the edited data distribution is much improved and approaches a normal distribution. A median estimate of $3.0 \pm 1.5 \times 10^{-3}$ represents the best approximation of published estimates for E2.

b. Spatial Distribution Models. Spatial distribution models were used by Crowe et al. (1982) to attempt to bound the disruption ratio, E2. They defined the area of the ratio from the distribution of basalt centers used to calculate a correlated value for E1. The area was established using a spatial-fitting program to calculate minimum area circles and minimum area ellipses enclosing the volcanic centers used to calculate E1 and the potential repository. The circles and ellipses were varied using different combinations of volcanic centers and the resulting areas were compiled into a matrix of disruption ratios. Maximum and minimum estimates were identified from the data matrix and used to establish bounds for the disruption ratio. These spatial distribution models are described generally as random models and that has led to some confusion (Connor and Hill 1994). The spatial zones are not established through assuming a homogeneous spatial distribution of volcanic events in space. Instead the areal dimensions of individual models are established from the spatial distribution of volcanic events using different combinations of the age and location of volcanic events. The assumption is made that there is a random distribution of volcanic events within the area defined by the distribution of combinations of volcanic events. These models presume the large scale structural controls of the distribution of volcanic events (nonrandom spatial events) are reflected in the distribution of volcanic centers. They do not account for local structural control of individual centers (Crowe et al. 1982; Crowe 1986; Smith et al. 1990).

Davis (1986) and more recently Cressie (1991) have summarized some of the many different approaches to statistical analyses of spatial point patterns. The problem is complicated by time, for the case of basaltic volcanism in the YMR. Volcanic events must be examined not only for their spatial distribution but additionally for their space-time distribution (space-time point patterns; Cressie 1991). Further, the recurrence rate for volcanic intrusions (λ_v) may vary with depth in the crust. There may be higher recurrence rates at given cross-sectional depths compared to surface rates. This problem is probably not severe because we are concerned mostly with surface penetrating volcanic events (< 2 km). For these events λ_v is probably $\approx \lambda_i$ (see earlier section). Finally, volcanic events exhibit spatial and temporal variability in the location, the age, the type of eruptions (hawaiian, strombolian, hydrovolcanic), and possibly magma composition (see Section IV). This requires analyses of multivariate spatial point processes in addition to space-time point processes (Cressie 1991). Given the complex options of data analyses and the sparse data set of volcanic events, we do not attempt to apply formal methods of statistical

Table 7.12. Published Values of E2, the Disruption Ratio.

Structural Model	Publication	Area (km ²)	E2 Ratio	Comments
Fixed Circle- 25 km	Crowe and Carr 1980	1963	3.0E-03	Circle fixed at YM
Fixed Circle- 50 km	Crowe and Carr 1980	7845	1.3E-03	Circle fixed at YM
Random Circle	Crowe et al. 1982	2437	2.5E-03	Quaternary Centers
Random Ellipse	Crowe et al. 1982	4419	1.4E-03	Quaternary Centers
Random Circle	Crowe et al. 1982	2470	2.4E-03	Quaternary + Buckboard Centers
Random Ellipse	Crowe et al. 1982	1953	3.0E-03	Quaternary + Buckboard Centers
Strike Slip Quaternary	Swchweickert, 1989	1310	4.6E-03	Quaternary Centers
Strike Slip Plio-Quaternary	Swchweickert, 1989	1450	4.1E-03	Subset Plio-Quaternary Centers
CFVZ	Crowe and Perry 1989	1310	4.6E-03	Quaternary Centers
CFVZ	Crowe and Perry 1989	1450	4.1E-03	Plio-Quaternary Centers
YMR or YPB	Crowe 1990	2180	2.8E-03	Slightly Larger than AMRV; all volcanic centers
AMRV	Smith et al. 1990	1955	3.1E-03	Similar but Slightly Smaller than YMR
NE Chain Model	Smith et al. 1990	390	7.8E-04	Subset Plio-Quaternary Centers
Lathrop Chain Model	Smith et al. 1990	360	1.7E-02	One Quaternary Center
Caldera Model	Carr 1990	400	1.5E-02	Subset Plio-Quaternary Centers
NE Structural Zone	Carr 1990, Smith et al 1990	2250	2.7E-03	Subset Plio-Quaternary
Pull-apart Basin	Fridrich and Price 1992	690	8.7E-03	Subset Plio-Quaternary Centers
Stochastic Dike/NW-NE	Sheridan 1992		6.0E-03	Subset Plio-Quaternary
Stochastic Dike/NE-NE	Sheridan 1992		1.0E-02	Subset Plio-Quaternary
Lathrop Wells Dike	Sheridan 1992		5.1E-03	One Quaternary Center

Structural Model	Publication	Area (km ²)	E2 Ratio	Comments
Stochastic Dike	Wallman et al. 1993		2.0E-03	Bounds for Three Structural Models
Stochastic Dike	Wallman et al. 1993		5.0E-03	Bounds for Three Structural Models
Nonhomogeneous Poisson:	Connor and Hill 1994		2.0E-03	Cluster, 6-7 neighbors fitting model
Nonhomogeneous Poisson	Connor and Hill 1994		2.4E-03	Cluster, 6-7 neighbors fitting model
Nonhomogeneous Poisson	Connor and Hill 1994		2.8E-03	Cluster, 10-13 neighbors fitting model
Nonhomogeneous Poisson	Connor and Hill 1994		3.4E-03	Cluster, 10-13 neighbors fitting model
Nonhomogeneous Poisson	Connor and Hill 1994		2.7E-03	Cluster, $\lambda = 4 \times 10^{-6}$
Nonhomogeneous Poisson	Connor and Hill 1994		2.7E-03	Cluster, $\lambda = 1 \times 10^{-6}$
Nonhomogeneous Poisson	Connor and Hill 1994		3.1E-03	Cluster, $\lambda = 1.1 \times 10^{-6}$
Stress Field Dike-Q	Crowe et al. 1994	1310	4.6E-03	Quaternary Centers
Stress Field Dike-P	Crowe et al. 1994	1450	4.1E-03	Subset Plio-Quaternary Centers
Crater Flat/Buckboard	Crowe et al. 1994	1700	3.5E-03	Subset Plio-Quaternary
Crater Flat Field	Crowe et al. 1994	400	1.5E-02	Subset Plio-Quaternary Centers
Disruption Simulation	Crowe et al. 1994		4.0E-03	Integration of 24 Structural Models

analyses of the spatial data. Instead we attempt to systematically combine ranges of alternative spatial models of the distribution of volcanic events.

Fig. 7.16 is a plot of the locations (latitude and longitude converted to Mercator projections) of the Pliocene and Quaternary volcanic centers of the YMR. Simple visual examination of Fig. 7.16 shows that the centers are not randomly distributed in space. Connor and Hill (1994) used a combination of a Clark-Evans test and a Hopkins F-test to reject the null hypothesis that basaltic volcanic centers in the YMR are randomly distributed, an unsurprising conclusion. Fig. 7.16 shows that basaltic volcanic centers are concentrated primarily in a northwest-trending zone extending across the middle of the YMR; one isolated center occurs outside this zone, the basalt of Buckboard Mesa. This northwest-trending zone has been named the Crater Flat Volcanic Zone (CFVZ of Fig. 7.16 Crowe and Perry 1989). Secondary or small-scale distribution trends are defined by clusters of volcanic centers, and are oriented approximately perpendicular to the 60 to 75 km-long, northwest-trending CFVZ. The secondary event clusters are defined by closely spaced volcanic centers (1 to 13 km) of coeval age that follow systematic trends defined by the structure of vents and vent alignments. The identified secondary distribution trends include clusters of north-trending centers (Fig. 7.16 basalt of Thirsty Mesa; basalt of southeast Crater Flat), and clusters of north-northeast-trending basalt centers (Amargosa valley aeromagnetic anomalies; basalt of Sleeping Butte, Quaternary basalt of Crater Flat). The secondary distribution trends probably were controlled by emplacement of feeder dikes parallel to the maximum compressive stress direction (see Sections III and V). Alternative views of the structural controls of the distribution of volcanic centers in the YMR are presented by Smith et al. (1990). They argue that the primary trends of volcanic centers of the YMR follow north-northeast patterns that parallel local normal faults cutting bedrock in Yucca Mountain (NESZ of Fig. 7.16).

Fig. 7.17 shows bivariate plots of the distribution of volcanic events in the YMR and the distribution centroids (95% confidence) drawn for different combinations of volcanic centers. The distribution centroids are centered on the means of the Mercator transformed locations (latitude and longitude). Their major axes are determined by the standard deviations of the variables, and their orientations are determined by the covariance of the variables. All distribution centroids are located in the vicinity of Crater Flat. Fig. 7.17a shows the distribution centroid for all Pliocene and Quaternary volcanic centers of the YMR. Fig. 7.17b shows the distribution centroid for all centers *excluding* the basalt of Buckboard Mesa (CFVZ model). Fig. 7.17c includes all centers *except* the basalt of Thirsty Mesa and the basalt of Sleeping Butte (NESZ model). Exclusion of the basalt of Buckboard Mesa elongates the distribution centroid parallel to the CFVZ. Exclusion of the basalt of Thirsty Mesa and Sleeping Butte results in a near-spherical centroid "pulled" or offset toward the location of the basalt of Buckboard Mesa.

The distribution centroids are used as starting points to divide visually the volcanic centers into clusters (Fig. 7.18). Visual methods are used because they are effective for identifying patterns on bivariate data plots, and the data are too sparse to obtain meaningful results using statistical methods of cluster analyses. The first event cluster consists of basalt centers in and adjacent to Crater Flat (cluster 1; basalt of SE Crater Flat, Quaternary basalt of Crater Flat, and the Lathrop Wells volcanic centers; Fig. 7.18a). A spatially separate cluster in the Amargosa Valley is defined by the distribution of aeromagnetic anomalies (cluster 2; Fig. 7.18a). Cluster 3 is defined by the volcanic vents of the basalt of Thirsty Mesa. It is separated from the basalt of Sleeping Butte (cluster 4) because of the large age difference between the centers (4.8 and .32 Ma, respectively). Cluster 5 is defined by a single basalt center, the basalt of Buckboard Mesa (Fig. 7.18a). The five clusters are joined into a smaller number of larger clusters by merging adjacent clusters. The first iteration of the joining reduces the event clusters to three (Fig. 7.18b). Cluster 1a is formed by joining the Crater Flat cluster with the aeromagnetic anomalies of the Amargosa Valley. Cluster 2a is formed by joining the basalt of Thirsty Mesa with the basalt of Sleeping Butte. The third cluster (Cluster 3a) remains as a single center, the basalt of Buckboard Mesa. The third iteration joins cluster 1a with cluster 2a to form the CFVZ, cluster 3a with cluster 1a to form the NESZ,

Fig. 7.16. Distribution of Pliocene and Quaternary volcanic centers in the YMR. The latitude and longitude coordinates have been converted to Mercator coordinates.

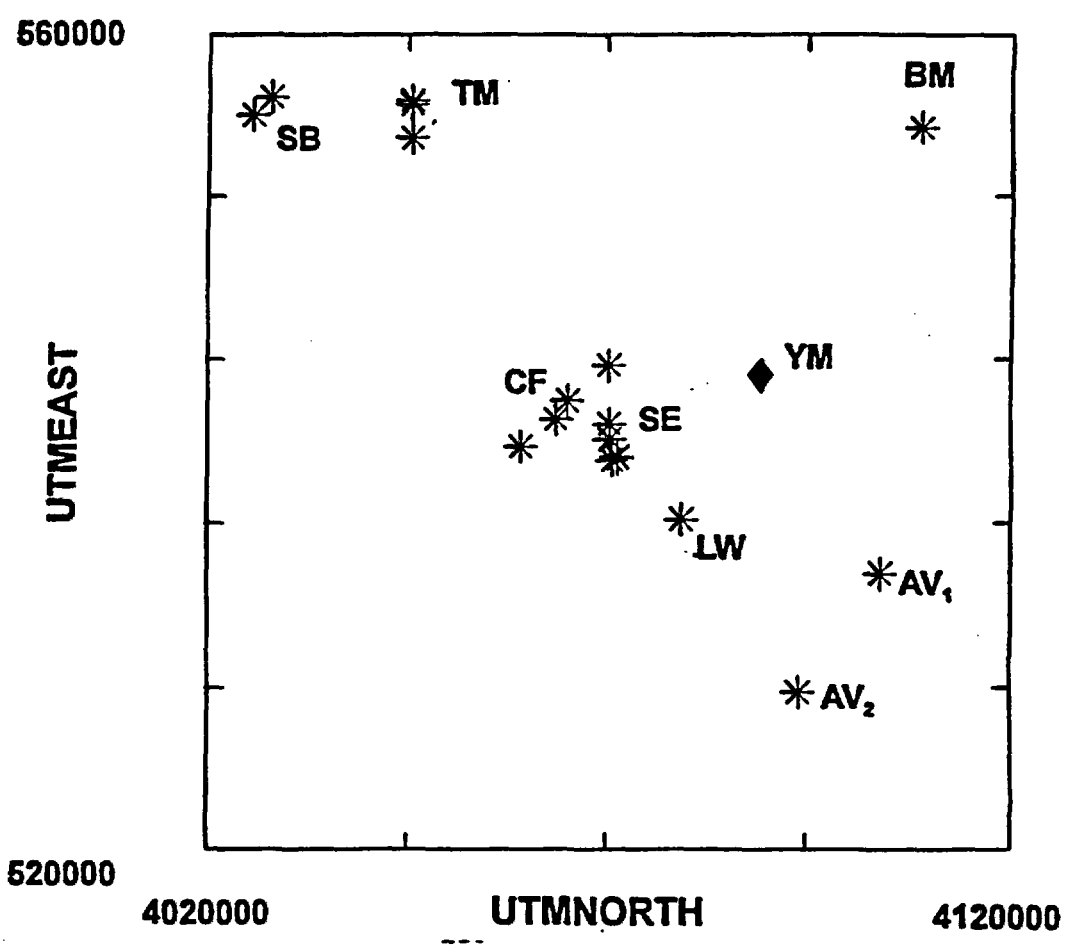
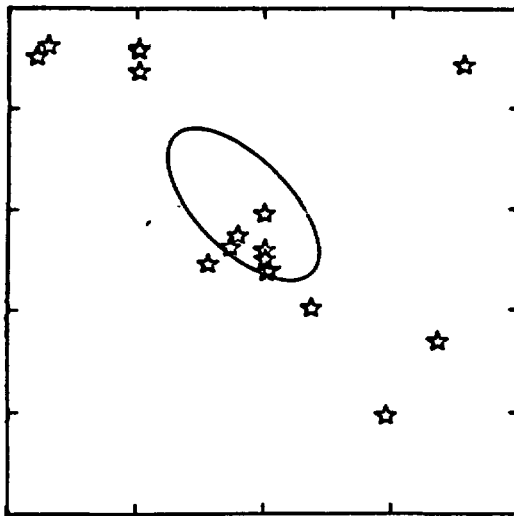


Fig. 7.17. Distribution centroids (95% confidence interval) for combinations of Pliocene and Quaternary volcanic centers in the YMR. The top figure is the centroid using all Pliocene and Quaternary volcanic centers. The middle figure *excludes* the basalt of Buckboard Mesa. The bottom figure *excludes* the basalt of Thirsty Mesa and the basalt of Sleeping Butte.

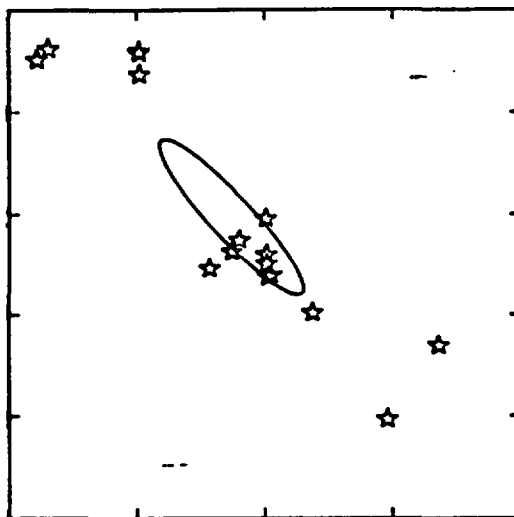
UTMEAST

560000



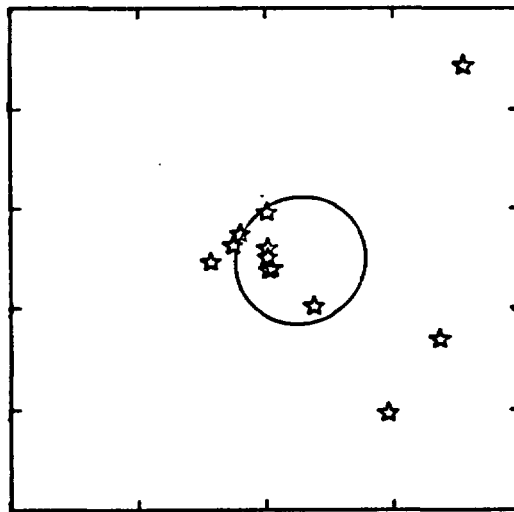
520000

560000



520000

560000



520000

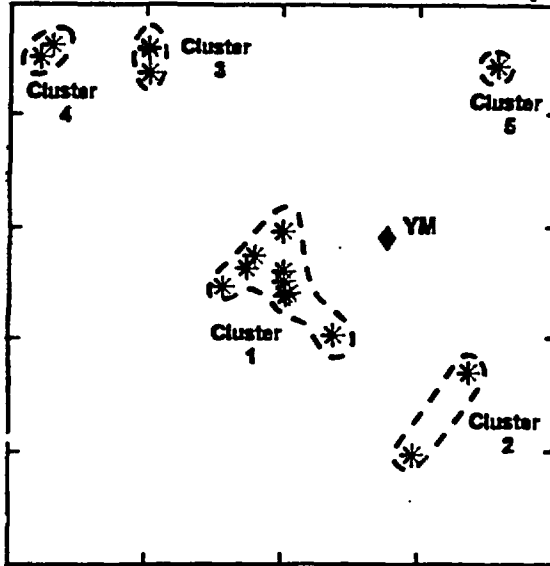
4020000

4120000

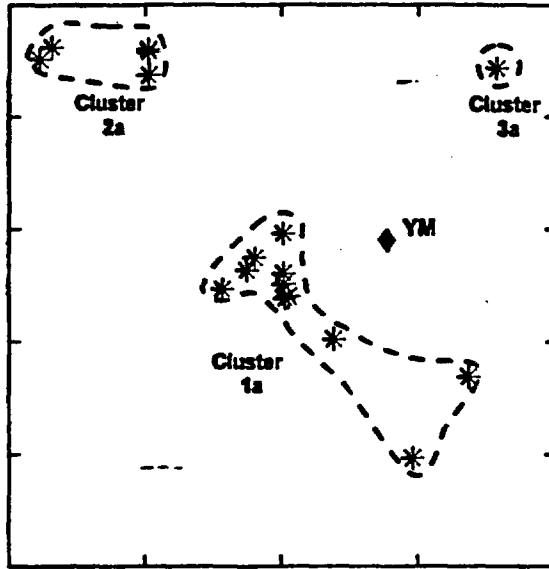
UTMNORTH

Fig. 7.18. Visual clustering of different combinations of Pliocene and Quaternary volcanic centers in the YMR. The top figure joins the adjacent closely adjacent centers. The middle figure joins the adjacent clusters of the top figure. The bottom figure joins the clusters of the middle figure and results in the CFVZ, the NESZ, and an East-West zone.

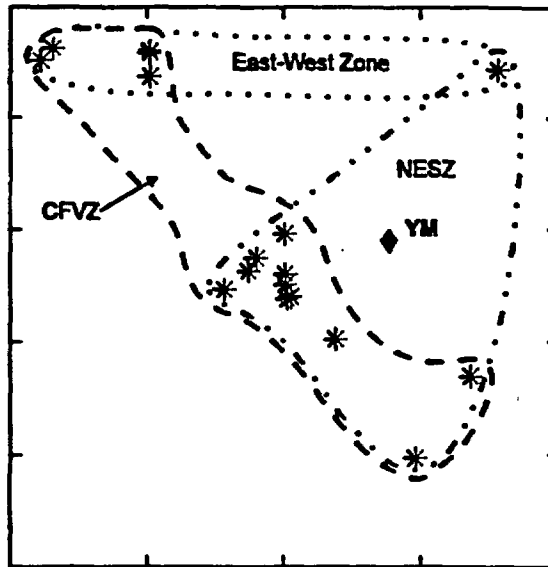
560000



520000
560000



520000
560000



520000

402000

UTMNORTH

412000

↑
Add

UTMEAST

and cluster 2a with cluster 3a to form an east-west trending zone (Fig. 7.18c). This same method of visual clustering is repeated using bivariate plots to assess the distribution of Quaternary volcanic centers in the YMR (Fig. 7.19). The Quaternary centroid, and three iterations of cluster definitions are shown on Fig 7.19a-c. In this case, the cluster joining ends with the definition of the Quaternary CFVZ (Fig. 7.19c).

The cluster models of Figs. 7.18 and 7.19 are used to define disruption zones for E2 by simply expanding each cluster to form an irregular polygon that encloses the potential Yucca Mountain site. The clusters are expanded while attempting to maintain their geometric dimensions -- they are not just expanded toward the potential Yucca Mountain site. The expansion presumes the fields could broaden in a northeast and southeast direction (stress-field controlled), not just toward the potential Yucca Mountain site. The area of each repository-enclosing zone is listed on Table 7.13. E2 is estimated using three sets of models and assuming a 6 km² area of a potential repository. The first model assumes a random distribution of volcanic events in the disruption zone. The second and third models assume the distribution of volcanic events follows the spatial patterns of Table 7.2: 75% of future volcanic events would occur in alluvial basins, 10% occur in range fronts, and 15% occur in range interiors. The areas of the structural zones listed on Table 7.13 were measured from topographic maps of the YMR (1:250,000). These areas will be recalculated more precisely using a geographic information system (GIS) when the computer programs used for the GIS are certified for the Yucca Mountain Project.

Disruption probabilities (E2) are not calculated for all clusters defined on Figs. 7.18 and 7.19. Cluster zones located more than 30 km from the potential repository block are assumed not to be capable of disrupting the potential repository; their areas and disruption ratios are not listed. Additionally, the cluster 2 of the Quaternary cluster models (the Lathrop Wells center) is identified as a case where intersection is not possible. We have highlighted this *excluded* case in Table 7.13 because it may be regarded as controversial by some workers (Smith et al. 1990). There are two explanations for the exclusion of the Lathrop Wells cluster. First, projection of the cluster along a north-northeast trend (stress field control) does not result in intersection of the potential repository site; the cluster extends east of the exploratory block. Second, the length of the projection of the cluster (20 km) exceeds substantially the 1/2 length of the longest observed cluster in the YMR (6.5 km), and the 1/2 length of expected dike dimensions.

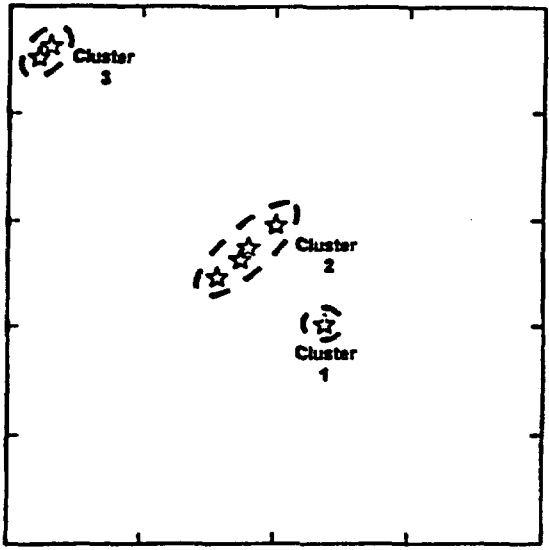
Finally, three cases from Table 7.13 are judged to be possible but unlikely of intersecting the potential Yucca Mountain site. This basis for this judgment is twofold. First, the required 1/2 length of projected north-northeast trending dikes (stress-field control) required to intersect the potential repository exceeds slightly the expected maximum dike dimensions. Second, assuming projection of north-northeast trending dikes, intersection of the potential repository site is possible for only a part of the area of the cluster zone. Thus, we regard the assumptions required to expand these spatial models to include the potential repository site to be marginal geologically. These spatial models are noted with asterisks on Table 7.13. We *included* those models in the first group of summary statistics for E2, and *excluded* them from the second group of summary statistics. The primary effects of *excluding* the identified cases are to decrease significantly the mean, standard deviation and skewness and slightly decrease the median (Table 7.13). The data of Table 7.13 *including* the three marginal cases are strongly skewed toward larger values. Because of the degree of skewness, the median is a more robust indicator of the central tendency of the data. Median estimates for models of intersection, range interior models, and range front plus range interior models are respectively, $3.1 \pm 4.5 \times 10^{-3} \times 10^{-3}$, $4.6 \pm 6.8 \times 10^{-4} \times 10^{-3}$ and $7.6 \pm 11.3 \times 10^{-4} \times 10^{-3}$ (Table 7.13).

A different method for estimating E2 was developed by Connor and Hill (1994), and their approach is a variant of the spatial distribution model. They related the recurrence rate (E1) per unit area in the YMR to cluster models using near-neighbor clustering routines for both the age and location of volcanic centers. An important observation resulting from this approach is that both the recurrence rate

Fig. 7.19. Visual clustering of Quaternary volcanic centers in the YMR following the same steps as Fig. 7.18. The clustering ends with the definition of the CRFZ.

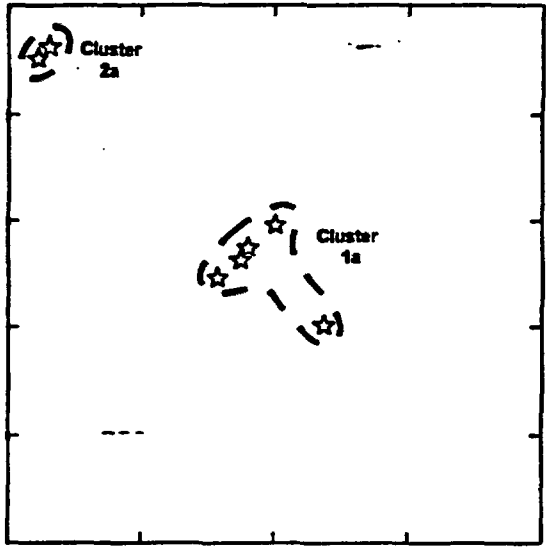
UTMEAST

560000



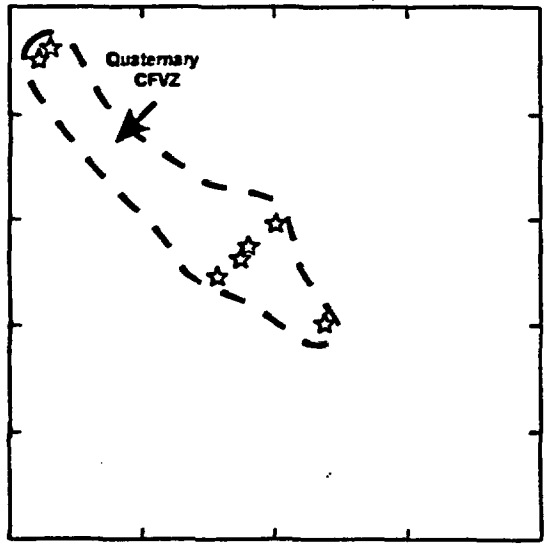
520000

560000



520000

560000



520000

4020000

4120000

UTMNORTH

(E1) and probability of repository disruption ($\Pr(E2 \text{ given } E1)\Pr(E1)$) are dependent on the number of near neighbor volcanic centers used in nonhomogeneous Poisson models. Connor and Hill (1994) presented bivariate plots showing families of curves for the recurrence rate and the probability of repository disruption established using near-neighbor models. They also showed contour maps of the probability of magmatic disruption of the potential repository, and argued that the probabilities vary in the YMR because of the tendency for volcanic centers to cluster. Connor and Hill (1994) did not explicitly calculate values for E2 but E2 can be approximated through rearranging their equations and substituting values for estimates of E1 and for the probability of magmatic disruption of the repository.

The positive merits of identifying the spatial distribution models for constraining E2 are several. First, the estimations used for E2 tend to be less arbitrary than other calculational methods. The disruption probability is established by the area of irregular zones encompassing the distribution of combinations of Pliocene and Quaternary volcanic centers and the potential Yucca Mountain site. Second, the shapes of the distribution zones are irregular, and it is therefore relatively easy to extend the zones to include the

Table 7.13. Spatial Distribution Models for E2. Model 1 = Random, Model 2 = Range Interior, Model 3 = Range Interior + Range Front

Spatial Model	Time (Ma)	Area (km ²)	Model 1	Model 2	Model 3	Comments
Quat Centers (circle)	1.00	2400	2.5E-03	3.7E-04	6.2E-04	Crowe et al. 1982
Quat Centers (ellipse)	1.00	4400	1.4E-03	2.0E-04	3.4E-04	Crowe et al. 1982
Quat + BB (circle)	3.75	2500	2.4E-03	3.6E-04	6.0E-04	Crowe et al. 1982
Quat + BB (ellipse)	3.75	2000	3.0E-03	4.5E-04	7.5E-04	Crowe et al. 1982
Cluster 1*	3.75	400	1.5E-02	2.2E-03	3.7E-03	Crater Flat Volcanic Field*
Cluster 2	3.85					Intersection not possible
Cluster 3	4.80					Intersection not possible
Cluster 4	4.80					Intersection not possible
Cluster 5	2.90					Intersection not possible
Cluster 1a*	3.75	750	8.0E-03	1.2E-03	2.0E-03	Crater Flat + Amargosa*
Cluster 2a	4.80					Intersection not possible
Cluster 3a	2.90					Intersection not possible
CFVZ	4.80	1450	4.1E-03	6.2E-04	1.0E-03	Crater Flat Volcanic zone
NESZ	3.85	1200	5.0E-03	7.5E-04	1.2E-03	Northeast Structural Zone
East-west zone	4.80					Intersection not possible
Cluster 1	1.00					Intersection not possible
Cluster 2	1.00	110				Lathrop Wells cluster
Cluster 3	1.00					Intersection not possible
Cluster 1a*	1.00	400	1.E-02	2.2E-03	3.7E-03	Quaternary CF + Lathrop*
Cluster 2a	1.00					Intersection not possible
CFVZ	1.00	1310	4.6E-03	6.9E-04	1.1E-03	Crater Flat Volcanic Zone
NHPP Cluster	3.75		2.0E-03	3.0E-04	5.0E-04	Connor and Hill
NHPP Cluster	3.75		2.4E-03	3.6E-04	6.0E-04	Connor and Hill
NHPP Cluster	1.00		2.7E-03	4.0E-04	6.7E-04	Connor and Hill
NHPP Cluster	1.00		3.1E-03	4.6E-04	7.7E-04	Connor and Hill
	Summary Statistics	Mean	6.1E-03	7.6E-04	7.6E-04	
		Median	3.1E-03	4.6E-04	7.6E-04	
		Std Dev	4.5E-03	6.8E-03	1.1E-03	
		Skew	1.8	1.8	1.8	
	(unlikely cases excluded)	Mean	3.0E-03	4.5E-04	7.5E-04	
		Median	2.6E-03	3.9E-04	6.5E-04	
		Std Dev	1.2E-03	1.8E-04	2.9E-04	
		Skew	0.6	0.6	0.6	

* Spatial models noted by the asterisk are included in the first group of summary statistics but repository intersection is judged to be unlikely from geometrical constraints on the propagation of dikes from the cluster areas, and the long $1/2$ length of projected dike dimensions required to achieve intersection.

potential Yucca Mountain site. Third, the number of models is determined by the number of different combinations of volcanic centers. It is relatively easy to include all possible event combinations, and be systematic in establishing alternative disruption models.

There are several areas of weaknesses or limitations in the spatial distribution models. First, the assumptions required to expand each distribution zone must be assessed for validity. If it is not logical to include the potential Yucca Mountain site in the distribution zone, the disruption model may overestimate the disruption ratio. These disruption ratios are worse cases because the ratio must be less than the estimated disruption ratio. Second, the weighting percentages used for the range interior and range front models were established for the YMR. They may be different for individual distribution models. Third, the spatial models of Connor and Hill (1994) employ multivariate cluster analyses of the location of volcanic events for the Postcaldera basalt (Older postcaldera basalt and Younger postcaldera basalt). The number of data points used in the analyses makes the application of the statistical method marginal at best. The distribution of the Older postcaldera basalt is different spatially from and largely unrelated to the distribution of the Younger postcaldera basalt (see Section III). Combining the data sets in cluster analyses is not valid. Moreover, Connor and Hill (1994) use only the age (partially), and the spatial location of volcanic events. They do not include all aspects of the data variance (for example location, age, magma volume, eruption type, relationship to local structure). Their statistical analyses are underdetermined for cluster analyses, and their calculations are likely to be significantly different if extended to multivariate space. Connor and Hill (1994) also treat each volcanic event independently, and weight equally spatially separated volcanic centers and volcanic centers in recognized age-correlated clusters (secondary control of the distribution of volcanic events).

Perhaps the most important weakness of the spatial distribution models is the assumption that the location of past volcanic events constrains the location of future events. Careful examination of the patterns of the *sequences* of past volcanic events shows that this is not always a valid assumption (Crowe et al. 1994). Examination of the sequence of the location of past volcanic events shows that there is little consistency in the patterns of the location of individual volcanic events relative to the location of the immediately preceding volcanic event (Fig. 7.20). There is a tendency for events to occur in the CFVZ and secondarily in the Crater Flat topographic basin. However, the jump directions or lengths of the *changes* in location of one event to the next event are not systematic. Thus, there is an inherent danger of over interpreting the composite patterns of past events in attempts to constrain the location of future volcanic events.

d. Structural Models for E2: The second approach used to estimate E2 is an assessment of structural models for the location of volcanic centers in the YMR. This approach overlaps partly with the spatial distribution models but brings a slightly different perspective. The spatial distribution models are established entirely on the distribution of volcanic events. In contrast, the approach used for structural models attempts first, to identify structural features in the YMR, and second, to relate the spatial patterns of volcanic events to the structural features.

Table 7.14 lists the current range of identified structural models in the YMR and the strengths and weaknesses of each model. Two interpretations emerge immediately from examination of the structural models. First, there are two classes of models. These include: 1) structural models where the enclosing zone must be expanded to allow for intersection of the repository, and 2) structural models that include the repository and part or all of the controlled area in the zone. Most of the structural models fall into the first category. Second, the structural models cannot be considered independent of E1. Selection of some structural models eliminates individual or groups of volcanic centers from inclusion in the events used to estimate E1. This reduces the recurrence rate for most models (Wallmann et al. 1993; Wallmann 1994), and is described further in the final part of Section VII.

Fig. 7.20. Plot of the sequence of Pliocene and Quaternary volcanic events in the YMR. The events are plotted with brackets that are equal in length to the *maximum* cluster length in the YMR (13 km) and are centered at the volcanic events or cluster. The brackets represent possible directions of expansion of clusters or dikes following the modern stress field (northeast or southwest). The orientation of the brackets is controlled by the direction of alignment of multiple centers or vent-fissure systems. The event locations jump nonsystematically through time. The only area of overlap of events is in the Crater Flat basin.

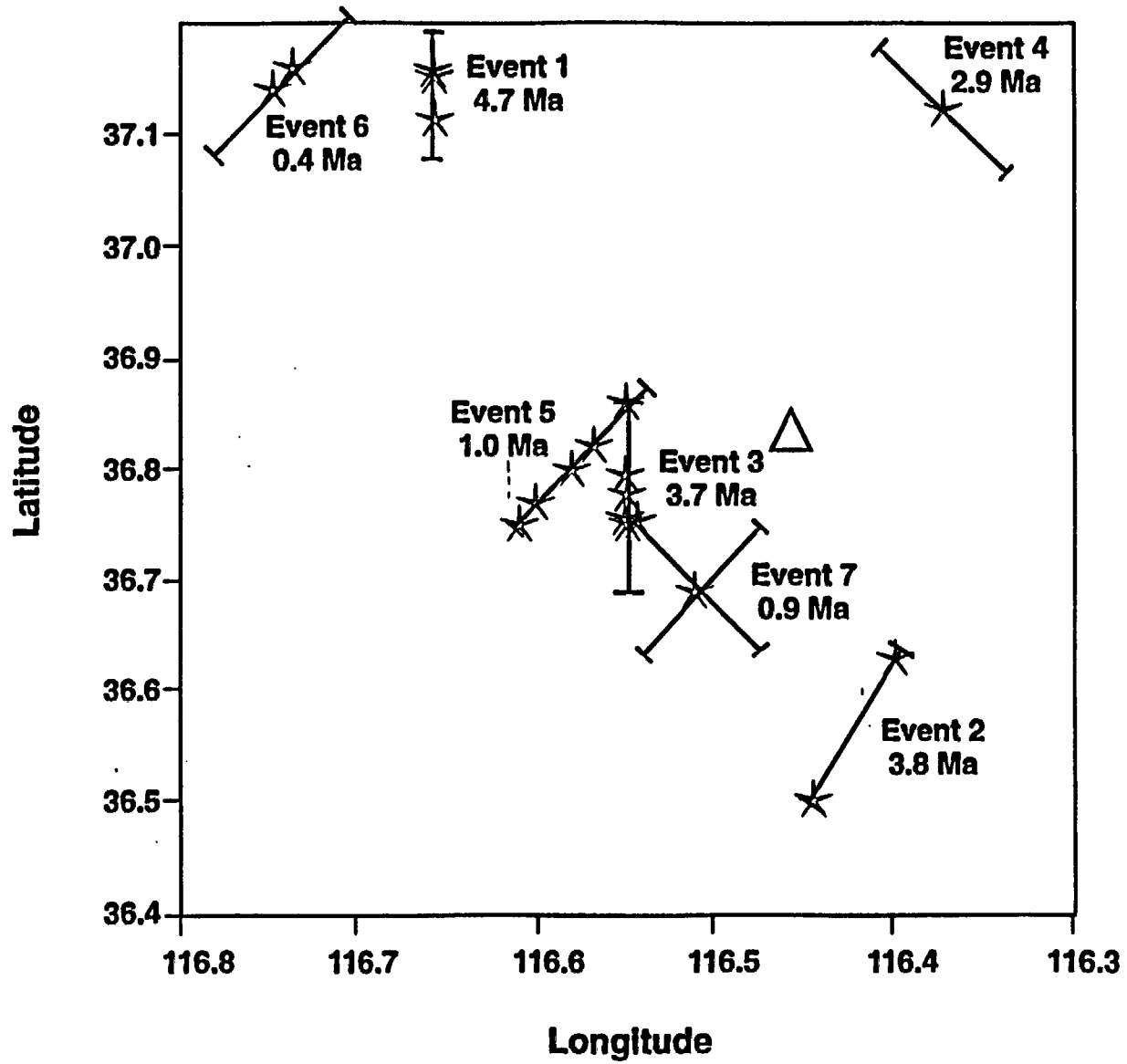


Table 17.14. Alternative Structural Models for the Distribution of Pliocene and Quaternary Volcanic Centers in the YMR.

Structural Model	Evidence for Model	Evidence Against Model	Subsets or Alternative Models
<p>Model 1: Crater Flat Volcanic Zone (Quaternary). This structural model is based on the definition of the Crater Flat volcanic zone of Crowe and Perry (1989). The dimensions of the zone are defined from the distribution of Quaternary volcanic centers.</p>	<p><i>Supportive Evidence: northwest-trending linear distribution of volcanic vents, coincidence of the zone and vent alignment with the orientation of the surface of maximum eruption volumes, predominance of northwest structural trends in the Walker Lane structural zone, possible evidence of strike-slip offset of structural features in Paleozoic rocks, strike-slip pull-apart origin of Crater Flat.</i></p>	<p>Negative Evidence: small number of volcanic centers, distance of gap between Crater Flat and Sleeping Butte centers, secondary northeast alignment of vent clusters.</p>	<p>Alternative Submodels: <i>The Crater Flat centers and the Sleeping Butte centers may be located in separate structural zones.</i></p>
<p>Model 2: Crater Flat Volcanic Zone (YPB). Same as model 1 but the dimensions of the zone are defined by the distribution of the Pliocene and Quaternary volcanic centers of the Younger Post-caldera basalt.</p>	<p><i>Supportive Evidence: Same as Model 1.</i></p>	<p>Negative Evidence: Same as model 1, basalt of Buckboard Mesa is not included in the structural zone.</p>	<p>Alternative Submodels: <i>Same as Model 1, the aeromagnetic anomalies of the Amargosa Valley may also be in separate structural zones.</i></p>
<p>Model 3: Yucca Mountain Region. This is a non-structurally based zone defined by the distribution of Pliocene and Quaternary basalt centers of the YMR. It is similar to but slightly larger than the Area of Most Recent Volcanism of Smith et al. (1990).</p>	<p><i>Supportive Evidence: Model is based on the distribution of Pliocene and Quaternary volcanic centers in the YMR.</i></p>	<p>Negative Evidence: No structural basis for model.</p>	

Table 7.14 (cont)

<p>Model 4: Crater Flat Volcanic field: This zone assumes that the major control of the occurrence of basalt centers is the local Crater Flat volcanic field, which is the primary site of Pliocene and Quaternary basaltic volcanism.</p>	<p><i>Supportive Evidence: most of the Pliocene and Quaternary volcanic events have occurred in the Crater Flat basin, Crater Flat is the centroid of the distribution of units of the YPB, the Crater Flat basin may be a remaining area of active tectonism and maximum extension, Crater Flat basin was a site of Miocene basaltic volcanism.</i></p>	<p>Negative Evidence: Other basalt centers occur outside the Crater Flat basin, the linear north-northwest alignment of basalt centers is oblique to the north-south elongation of the Crater Flat basin.</p>	<p>Alternative Submodels: Each group of volcanic rocks may record a separate volcanic field. These include the Crater Flat, Amargosa, Black Mountain and Buckboard fields.</p>
<p>Model 5: Strike-Slip Structural Control: Model A. This structural model is based on the inference that the alignment of basalt centers parallels a concealed northwest-trending right-slip fault of the Walker Lane structural system. The model has been described by Schweickert (1989).</p>	<p><i>Supportive Evidence: linear northwest alignment of basaltic volcanic centers, proposed offset of structural features of Paleozoic rocks, Walker Lane structural setting, clockwise rotation of field magnetization directions of the Tiva Canyon Member, coincidence of the basalt centers with zone of maximum rotation of the magnetization directions, similar structural bounds may be defined for Miocene basaltic volcanism (Older basalt of Crater Flat, aeromagnetic anomaly of VH-2).</i></p>	<p>Negative Evidence: Strike-slip fault is not expressed at the surface, there is not always a strong correlation between strike-slip faults and sites of Quaternary volcanism in the basin-range.</p>	<p>Alternative Submodels: The Thirsty Mesa/Sleeping Butte centers and the aeromagnetic anomalies of the Amargosa Valley may be located on separate strike-slip faults and be unrelated to the Crater Flat basalt units.</p>

Table 7.14 (cont)

<p>Model 6: Strike Slip Structural Control: Model B. This structural model is based on the inference that the south-southeast edge of the Crater Flat basin is bounded by a north-northwest trending, right slip fault. The Pliocene and Quaternary basalt centers are inferred to have ascended along this fault zone and diverted to the northeast (maximum compressive stress direction).</p>	<p><i>Supportive Evidence: steep gravity gradient paralleling proposed strike-slip fault, presence of north-northwest trending right-slip fault in the arcuate ridge at the south end of Crater Flat, clockwise rotation of field magnetization directions of the Tiva Canyon member, structural models of Crater Flat basin.</i></p>	<p>Negative Evidence: Bare Mountain fault shows predominately dip-slip offset, basalt centers do not occur on the Bare Mountain fault, no correlation between volume of basalt centers and proximity to proposed bounding strike-slip fault.</p>	<p>Alternative Submodels: Same as model 5.</p>
<p>Model 7: Stress-field Dike: Quaternary centers. This structural model assumes basalt magma ascended along a concealed structure defined by the northwest orientation of vents of the CFVZ. The feeder dike or dikes following this structure and diverted at shallow depths to follow the maximum compressive stress direction. The direction of dike propagation is either to the north-northeast or south-southwest.</p>	<p><i>Supportive Evidence: coincidence of the zone of maximum erupted volume of magma with the CFVZ, symmetrical distribution of vents about northwest-trending vent locations, cluster length of the Quaternary basalt of Crater Flat exceeds maximum likely dike length.</i></p>	<p>Negative Evidence: multiple dikes are required only for the Quaternary basalt of Crater Flat, no recognized correlation between center chemistry and proposed dike systems, does not explain the distribution of all basalt centers.</p>	<p>Alternative Submodels: This model is a subset of the strike-slip models.</p>

Table 7.14 (cont)

<p>Model 8: Stress-field Dike: Pliocene and Quaternary centers. This model is identical to model 7. The dimensions of the structural zone are defined by the distribution of Pliocene and Quaternary volcanic centers.</p>	<p><i>Supportive Evidence: Same as model 8, aeromagnetic anomalies of Amargosa Valley may be analogous to the Quaternary basalt centers of Crater Flat, and formed basalt centers only at the ends of the dikes.</i></p>	<p>Negative Evidence: Does not explain the occurrence of the basalt of Buckboard Mesa.</p>	<p>Alternative Submodels: May form three separate structural systems including the aeromagnetic anomalies of Amargosa Valley, the Crater Flat volcanic field, and the Thirsty Mesa/Sleeping Butte centers.</p>
<p>Model 9: Chain model. Basalt centers follow northeast-trending chains and the chains form zones of higher risk for future volcanic events (Smith et al. 1990).</p>	<p><i>Supportive Evidence: northeast-trends of clusters of contemporaneous volcanic centers, parallelism of northeast trends of clusters to bedrock faults of Yucca Mountain, analog comparison to other basaltic volcanic fields.</i></p>	<p>Negative Evidence: risk zones are unsuccessful as predictors of future events, basalt of the YPB do not follow existing faults, dimensions of chains from analog volcanic fields exceed maximum cluster lengths of centers in the YMR, structural trends different for alignments of the Thirsty Mesa and basalt of southeast Crater Flat (north trending), longer chains occur only in alluvial basins, Lathrop Wells and Buckboard Mesa centers do not form chains, northeast trends are secondary to northwest trends.</p>	

Table 7.14 (cont)

<p>Model 10: Pull-Apart Basin: The Crater Flat basin is a pull-apart basin located at the termination of northwest-trending, strike-slip faults of the Walker Lane structural system. The basin is a tectonic basin and the basalt centers occur along extensional structures of the basin (Fridrich and Price 1992).</p>	<p><i>Supportive Evidence: discontinuous northwest-trending faults of the Crater Flat area, multiple basalt cycles of the Crater Flat basin (10.5 Ma and Pliocene and Quaternary), gravity data showing steep, northwest-trending gradients, clockwise rotation of field magnetization directions of the Tiva Canyon Member, Walker Lane structural setting.</i></p>	<p>Negative Evidence: the occurrence of basalt centers is not confined to the pull-apart basins, limited continuity of northwest-trending fault systems.</p>	
<p>Model 11: Caldera Model. The Crater Flat basin is a structural depression formed by multiple, coalesced caldera collapses associated with eruption of the Crater Flat tuff. Basalt centers are inferred to follow the ring-fracture system of the caldera complex (Carr, 1990).</p>	<p><i>Supportive Evidence: Crater Flat basin is located on the south part of the southwest Nevada volcanic field, basalt centers are located commonly along ring-fracture zones of caldera complexes, basalt of Buckboard mesa is located on the ring-fracture of the Timber Mountain caldera, dike of Solatario Canyon and extensions may follow ring-fracture zone.</i></p>	<p>Negative Evidence: caldera origin of the basin is controversial, basalt centers occur beyond the confines of the Crater Flat basin, basalt centers occur across the caldera floor and resurgent dome and are not confined to the ring-fracture zone.</p>	

Table 7.14 (cont)

<p>Model 12: Northeast Structural Zone: The YMR is located in a diffuse northeast trending, tectonic-volcanic rift zone. Sites of basaltic volcanism are more common in the zone than outside the zone; composite model proposed by Carr (1984; 1990; Kawich-Greenwater Rift zone, and Wright 1989; Amargosa Desert Rift zone).</p>	<p><i>Supportive Evidence:</i> northeast-trending zone of closely spaced, normal faulting, orientation of caldera centers in the southwest Nevada volcanic field, northeast trending structural trough that is delineated partly by gravity data, concentration of basaltic volcanic centers in the northeast-trending structural zone.</p>	<p>Negative Evidence: structural zones may be a composite of multiple different structures, basalt centers are present both in and outside the structural zone, northwest linear alignment of basalt centers occur within the northeast-trending zone.</p>	
<p>Model 13: Crater Flat and Buckboard Mesa volcanic zone: The basalt centers of Crater Flat and the basalt of Buckboard Mesa form a northeast trending zone that extends through the potential Yucca Mountain site (proposed by Smith et al. 1990 and Naumann et al. 1992).</p>	<p><i>Supportive Evidence:</i> local northeast trends of basalt vents, in Crater Flat, existence of the basalt centers of Crater Flat, and Buckboard Mesa.</p>	<p>Negative Evidence: Distance of separation between the Crater Flat basalt centers and the basalt of Buckboard Mesa, interruption of the northeast-trends by oblique structures of the Timber Mountain-Oasis Valley caldera complex, northwest-trending vent alignments of the basalt of Buckboard Mesa, no basalt centers between Crater Flat and Buckboard Mesa.</p>	

Table 7.15 is a summary of disruption ratios (E2) established from the structural models of Table 7.14. The minimum disruption ratio (column E2 area of Table 7.15) is estimated through assuming a 6 km² repository area located in the structural zone. Structural models that do not include the potential repository site (12 of the 16 structural models of Table 7.14) are expanded to include the site (column "Forced Intersection" of Table 7.15). These structural zones are expanded by increasing the dimensions of each zone to the northeast and southwest while still preserving the geometric shape of the zone. The column labeled "Likelihood Intersection" on Table 7.15 is a judgmental assessment of how likely the required expansion is for each model from the perspective of the structural zone and the spatial dispersion of volcanic events in the structural zone. For most cases the likelihood of intersection is low. Intersection is judged to be unlikely for four cases. Cases 4 and 4a require dike lengths that exceed representative lengths to result in intersection. Cases 10 and 10a are for structures that do not intersect the potential Yucca Mountain site. For one case, the caldera model (model 11 of Table 7.14), the likelihood of intersection is judged to be moderate because the inferred structure extends to the boundaries of the potential Yucca Mountain site. The models labeled high in column are structural models that include (without expansion) the potential Yucca Mountain site. The column labeled "E2 Intersection" on Table 7.15 is the disruption ratio (E2) for the expanded structural zone. The columns labeled "E2 Interior" and "E2 Front" are weighted values of the E2 intersection column using the frequency of occurrence of volcanic events in alluvial basins, range fronts, and range interiors (data summarized on Table 7.2). The median estimates of E2 for forced intersection, range interior, and range front plus range interior models are respectively, $4.6 \pm 4.4 \times 10^{-3}$, $6.9 \pm 6.6 \times 10^{-4}$, and $1.1 \pm 1.1 \times 10^{-4}$ (all from Table 7.15).

Evaluation of the estimates of E2 from Table 7.15 requires some degree of subjective judgment. First, a judgment must be made about the structural viability of the geometry of structural models that are expanded to intersect the potential repository site. If the geometry of intersection is not realistic, the estimates of Table 7.15 are worse case estimates. Second, a judgment must be made of how reasonable the structural models are for the Yucca Mountain setting. The majority of structural models form zones that do not include the potential repository or the controlled area. This statement is consistent with the geologic record of the YMR. During the past 4.8 Ma, there has been intermittent basaltic volcanism in the basins of the Amargosa Valley, Crater Flat, Timber Mountain caldera depression, and the south edge of the Black Mountain highland. None of the volcanic events occurred in the potential repository or controlled area of Yucca Mountain. The required subjective judgment is whether the models are sufficiently valid to conclude that Yucca Mountain is not and will continue not to be located in the structural zones.

Four of the structural models of Table 7.15 include the potential Yucca Mountain site. The mean estimates of E2 for only the four models (intersection, range interior, and range front plus range interior models) are respectively: $3.1 \pm 1.1 \times 10^{-3}$, $5.2 \pm 1.6 \times 10^{-4}$, and $8.7 \pm 2.7 \times 10^{-4}$. These estimates are smaller than and exhibit less variance than the median estimates of all other structural models. The data show that the northeast-trending models do not give larger estimates for the disruption ratio, and are not worse or even worst case models for the YMR (compare with Smith et al. 1990; Ho, 1992). The only inconsistency with that statement is for the chain model of Smith et al. (1990). There are two lines of evidence why the chain length model proposed by Smith et al. (1990) is not a viable model. First, the maximum chain lengths used by Smith et al. (1990) are taken from the Reville and Fortification volcanic fields. These fields are unrelated to the volcanic rocks of the YMR. We assign a chain length for the chain model of Table 7.15 using the longest observed cluster length of volcanic centers in the YMR (13 km). The dispersion of volcanic vents using this cluster length is 1/2 of the length (6.5 km) since a dike could propagate *either* southwest or northeast. The 6.5 km half-length is too short to result in penetration of the repository. Second, even if the assumption is accepted that longer chain lengths are feasible, penetration of the repository would result from N-NE propagation of volcanic clusters for only a small component of the total length of the CFVZ (approximately 10% of the zone). The disruption probability of the chain models of Table 7.15 is weighted for the area of the structural model that could

propagate directly toward the potential repository site. These cases are highlighted on Table 7.15 because this treatment of the data may be regarded as controversial.

Table 7.15. Estimations of E2 for Structural Models of the Yucca Mountain Region.

Model Number	Name	Time Interval	Intersection repository	Area (km ²)	Forced Intersection	Likelihood Intersection	E2 Intersection	E2 Interior	E2 Front
Model 1	CFVZ	1.00	no	1100	1310	Low	4.6E-03	6.9E-04	1.2E-03
Model 2	CFVZ	3.85	no	1350	1450	Low	4.1E-03	6.2E-04	1.0E-03
Model 3	YMR/AMRV	4.80	yes	2180	2180	High	2.7E-03	4.1E-04	6.9E-04
Model 4	CFVF	3.75	no	220	400	Unlikely	1.5E-02	2.2E-03	3.7E-03
Model 4a	CFVF with AV	3.85	no	750	750	Unlikely	8.0E-03	1.2E-03	2.0E-03
Model 5	Strike Slip	1.00	no	1100	1310	Low	4.6E-03	6.9E-04	1.1E-03
Model 6	Strike Slip	4.80	no	1350	1450	Low	4.1E-03	6.2E-04	1.0E-03
Model 7	Stress-Dike	1.00	no	1100	1310	Low	4.6E-03	6.9E-04	1.1E-03
Model 8	Stress-Dike	4.80	no	1350	1450	Low	4.1E-03	6.2E-04	1.0E-03
Model 9	Chain Model	3.75	no	390	450	Low	2.7E-03	4.0E-04	6.7E-04
Model 9a	Chain Model	3.85	no	500	690	Low	7.8E-04	1.2E-04	2.0E-04
Model 10	Puff-Apart	3.75	no	390	450	Unlikely	1.3E-02	2.0E-03	3.3E-03
Model 10a	Puff-Apart	3.85	no	500	690	Unlikely	8.7E-03	1.3E-03	2.2E-03
Model 11	Caldera	3.75	no	220	400	Moderate	1.5E-02	2.2E-03	3.7E-03
Model 12	Kawich Rift	3.75	yes	1700	1700	High	3.5E-03	5.3E-04	8.8E-04
Model 12a	12 with AV	3.85	yes	2250	2250	High	2.7E-03	4.0E-04	6.7E-04
Model 13	NESZ	3.75	yes	1200	1200	High	5.0E-03	7.5E-04	1.2E-03
				Statistics (all models)	Mean		6.1E-03	9.1E-04	1.5E-03
					Median		4.6E-03	6.9E-04	1.1E-03
					Geomean		4.8E-03	7.2E-04	1.2E-03
					StdDev		4.4E-03	6.6E-04	1.1E-03
				Statistics (Intersection models)	Mean		3.5E-03	5.2E-04	8.7E-04
					Median		3.1E-03	4.7E-04	7.8E-04
					Geomean		3.4E-03	5.0E-04	8.4E-04
					Std Dev		1.1E-03	1.6E-04	2.7E-04

c. Analog Basaltic Volcanic Fields of the Basin and Range Province

Additional insight can be gained on bounds for the disruption ratio for the YMR through comparisons with the spatial distribution of volcanic centers in basaltic volcanic fields of the basin and range province. The analog fields used for comparison are the same as those used for the analog assessments of E1: the Lunar Crater and Cima volcanic fields. Each field has a sufficient number of centers to evaluate the spatial variability of the locations of basaltic volcanic centers. Moreover, the large number of volcanic events at both fields provides a better definition than the YMR of the dispersion of vents in a volcanic field.

Fig. 7.21 is a plot of the location of volcanic vents in the Lunar Crater field. The locations are shown as x,y coordinates transposed from the latitude and longitude of the vents. Mercator projections are not used for these data because of the relatively small size of the area, and the detail of the intra-field distribution of vents is not important. What is important is the geometry of the volcanic fields, the dispersion of vents in the fields, and comparison with the distribution of basaltic volcanic centers in the YMR.

The distribution of volcanic vents in the Lunar Crater volcanic field is structurally controlled (Fig. 7.21). There are 82 identified vents of probable Quaternary age and the vents are distributed along north-northeast trending alignments (Crowe et al. 1986) parallel to the elongation of the volcanic field (Fig. 7.21; see also Scott and Trask, 1970). The feeder dikes for the field must be predominately parallel to controlling structure of the volcanic field. The volcanic field occupies an area of about 260 km.² Exploratory data analyses show that the locations of the vents (latitude and longitude) deviate slightly from a normal distribution, but there are no identified outliers in the data set. Several methods are used to evaluate the spatial variability of the vent distribution. The major points of interest are the shape of the basaltic field and the degree of dispersion of the vents; the detailed distribution of vents is of lesser importance. Fig. 7.21 shows the centroid of the vent distribution (95 % confidence interval), and bivariate gaussian ellipsoids were drawn in a separate calculation at the 90 and 95 percent confidence intervals. The ellipsoids are elongate parallel to the elongation direction of the volcanic field, reflecting the northeast structural control of vent locations. The width of the volcanic field is 10.5 km at the location of the vent centroid. The 90 % ellipsoid bounds approximately the distribution of vents in the field (Fig. 7.21). The half-width of the 90 % ellipsoid at the position of the centroid is 5.25 km (orthogonal to the field elongation). The half-width of the 95 % ellipsoid at the position of the vent centroid is 7.3 km. The half-length of the ellipsoid drawn through the centroid is 29 km. These dimensions provide approximate measures of the shape and dispersion of vents in the Lunar Crater volcanic field.

There are several complicating factors that must be considered for observations of the vent distributions in the Lunar Crater volcanic field. First, construction of bivariate gaussian ellipsoids assumes a normal distribution of volcanic vents. The actual vent distribution deviates somewhat from a normal distribution. Second, there are time-space migration patterns in the location of eruptive vents in the Lunar Crater volcanic field. The general pattern is a decrease in the age of the centers from southwest to northeast (Scott and Trask 1971; Crowe et al. 1986; Bergman et al. 1985). This will increase slightly the degree of vent dispersion parallel to the direction of migration, but should have a minor effect on field width.

The same calculations can be made for the Cima volcanic field in the Mojave desert of California (Dohrenwend et al. 1986, Crowe et al. 1992). Fig. 7.22 is similar to Fig. 7.21 and shows the distribution of Quaternary volcanic vents in the southwest part of the Cima volcanic field. The centroid of the vent distribution (95 % confidence interval) and bivariate gaussian ellipsoids are drawn at confidence intervals of 90 and 95%. The distribution of volcanic events in the Cima volcanic field is less strongly controlled structurally than the Lunar Crater volcanic field. The former field is elongate slightly in a northeast

Fig. 7.21. Distribution of volcanic vents in the Lunar Crater volcanic field. The vent locations are the latitude and longitude of the vents converted to an x-y grid for plotting. The data *have not* been converted to Mercator projections because of the small size of the map. The small ellipse in the center of the field is vent centroid for all vents. The larger ellipses are the bivariate gaussian ellipsoids drawn at confidence intervals of 90 and 95%.

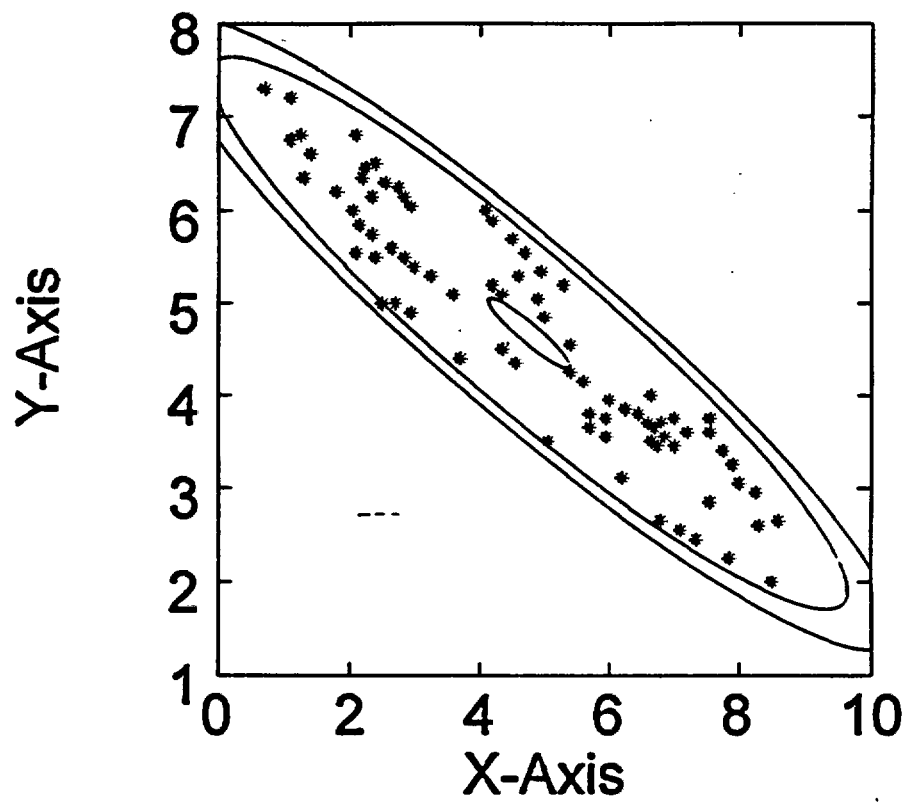
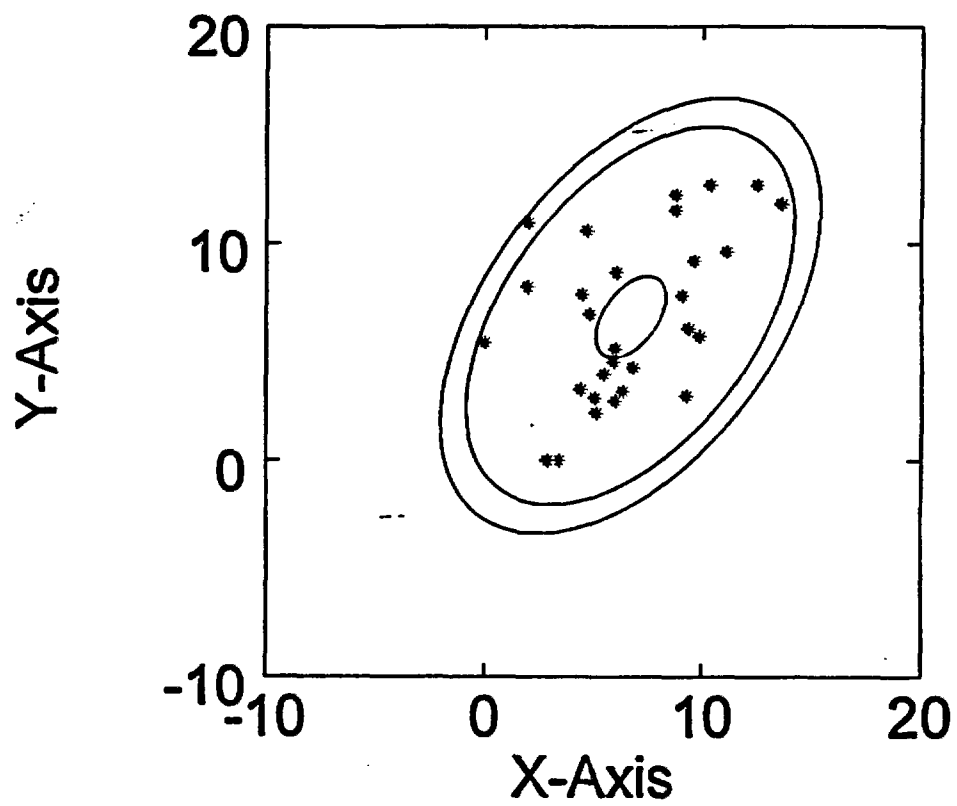


Fig. 7.22 Distribution of volcanic vents in the Cima volcanic field. The figure is identical to Fig. 7.21 but drawn for volcanic events in the Cima volcanic field.



direction as shown by the vent centroid and bivariate gaussian ellipsoids. The half-width of the 90 percentile confidence interval for the bivariate gaussian ellipsoid is 4.8 km; the half-width of the 95 percentile confidence interval drawn through the vent centroid is 5.4 km.

What is the significance of the analog descriptions of the Lunar Crater and Cima volcanic fields? The calculations are not intended to provide statistically significant descriptions of the spatial distribution of volcanic vents in the fields. However, the calculations for the Lunar Crater and Cima volcanic fields illustrate two important points that have application to the YMR. First, there are a large number of Quaternary vents in these active volcanic fields. The number of Quaternary basaltic centers in the fields exceeds the number of centers in the YMR by a factor of 4 (Cima volcanic field) to greater than a factor of 10 (Lunar Crater volcanic field). The number of vents is sufficient to assume that the vent dispersion is representative of the behavior of large, high cone density volcanic fields. Second, Fig. 7.23 is a plot of the distribution of volcanic centers in the Yucca Mountain region, and shows the half-width and half-length dimensions of the 95% bivariate gaussian ellipsoid for the Lunar Crater volcanic field (the Cima volcanic field is not shown since it is smaller than the Lunar Crater field). The plotted dimensions of the Lunar Crater volcanic field are centered on the vent centroid drawn from the distribution of Pliocene and Quaternary volcanic centers; the long dimension of the field is oriented parallel to the CFVZ. The dispersion of vents in the Lunar Crater volcanic field is insufficient, when superimposed on the YMR, to overlap the potential Yucca Mountain site. The width of the Lunar Crater volcanic field drawn at the 95% ellipsoid (14.6 km) is only slightly greater than the degree of north-northeast dispersion of clustered volcanic centers in the YMR (longest cluster = 13 km).

e. Simulation Modeling: E2 the Disruption Probability: Risk simulation is used to attempt to define the distribution of E2, the disruption probability, in probability space. Fig. 7.24 shows the distribution of E2 (dimensionless) using different combination of published, spatial and structural estimates for the YMR (Tables 7.13 and 7.14). Defining limits for E2 in probability space is more difficult than for E1, and only approximate limits can be identified. The vertical line labeled "controlled area" on Fig. 7.24 is the ratio of the repository area (6 km^2) to the controlled area (86 km^2). Estimates of E2 must lie to the right of that line since Pliocene and Quaternary volcanic activity is centered in Crater Flat, and there has been no volcanism in the controlled-area since the Miocene. The lines labeled "Cima volcanic field" and "Lunar Volcanic field" on Fig. 7-24 are the disruption probability obtained by locating a 6 km^2 repository in the interior of the respective volcanic fields. Logically, the disruption ratio for the YMR should be located to the right of the disruption ratios for the Cima and Lunar fields because the potential repository site is not located *inside* the zones of most spatial and structural models. The potential sites included in some spatial and structural models but because the cone density (centers km^{-2}) in the YMR is low, these models are located well to the right of the disruption ratios for the Cima and Lunar volcanic fields (see enclosed pattern of NESZ on Fig. 7-24). Finally, the vertical line labeled "Outlier" on Fig. 7-24 identifies the approximate position of estimates identified as outliers using exploratory data analyses (box, stem and leaf and probability plots). All disruption ratios to the left of the line are outliers or far outliers. This line provides a less subjective method for identifying natural variations in the data distribution.

The judgment could be made that the outlier values of Fig. 7-24 should not be included in estimations of the disruption ratio (E2). Spatial models that approach or exceed the disruption ratio for the Lunar Crater and Cima volcanic field appear unrealistic, given the greater number of basaltic centers in the volcanic fields versus the YMR. Moreover, judgment concerning the suitability of the outlier values is dependent partly on the acceptance or rejection of structural models for the tectonic setting of Yucca Mountain. The majority of geologic, and structural data for the YMR appear consistent with the CFVZ being a preferential zone of Pliocene and Quaternary basaltic volcanism. The fundamental evidence in support of the observation is simply the spatial distribution of volcanic events. Additionally, newly refined structural models of the Crater Flat basin provide increased support for the existence of a strike-slip bounded, pull-apart basin that has and may continue to bound the occurrence of both Paleocene

and Neogene basaltic volcanic activity (C. Fridrich, written communication, 1994). The significance of the

Fig. 7.23. Plot of the distribution of Pliocene and Quaternary volcanic events in the Yucca Mountain region with the event centroid drawn at a 90% confidence interval. The Quaternary part of the Lunar Crater volcanic field is centered in the event centroid and its long axis is oriented parallel to the CFVZ.

UTMEAST

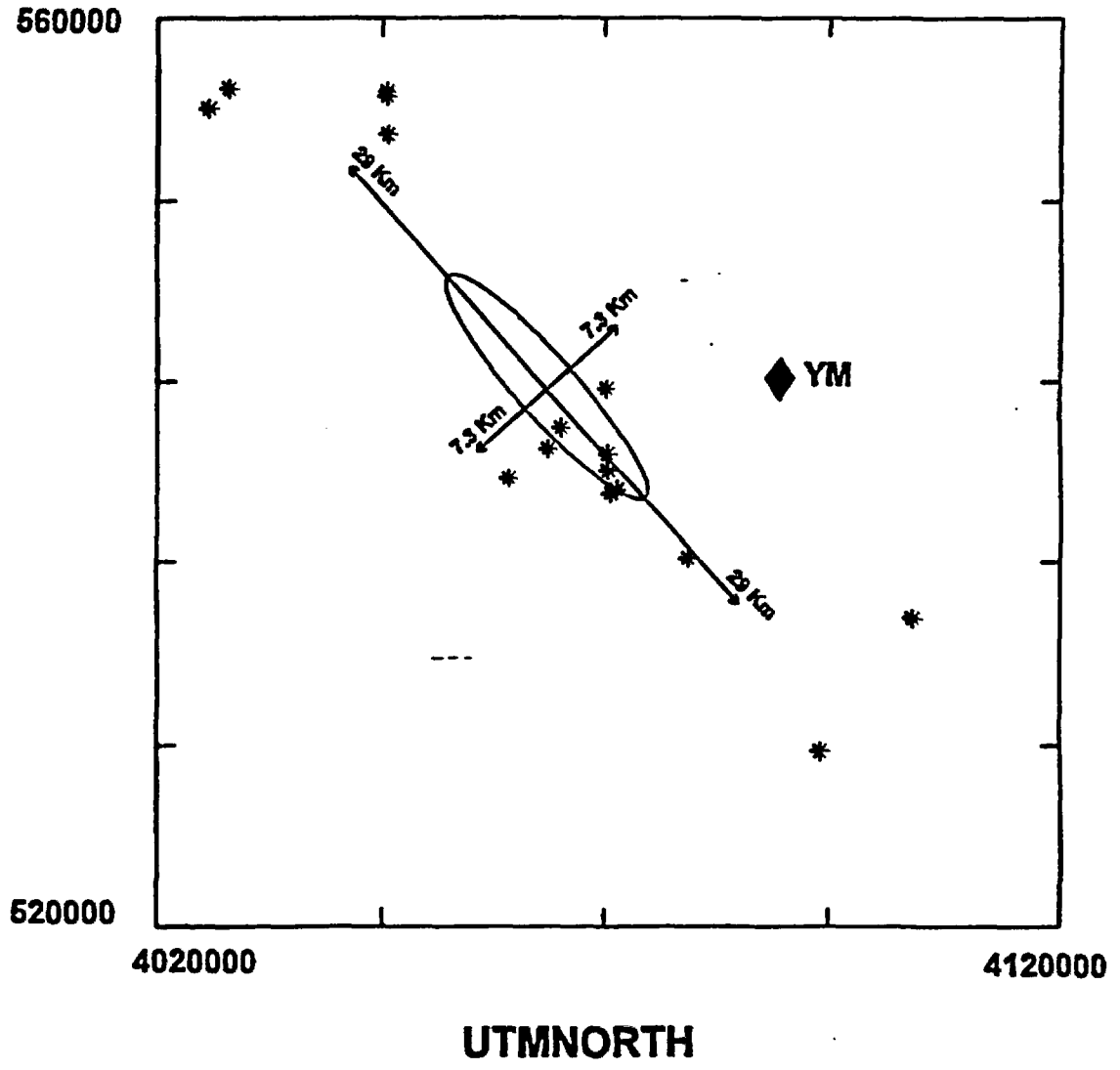
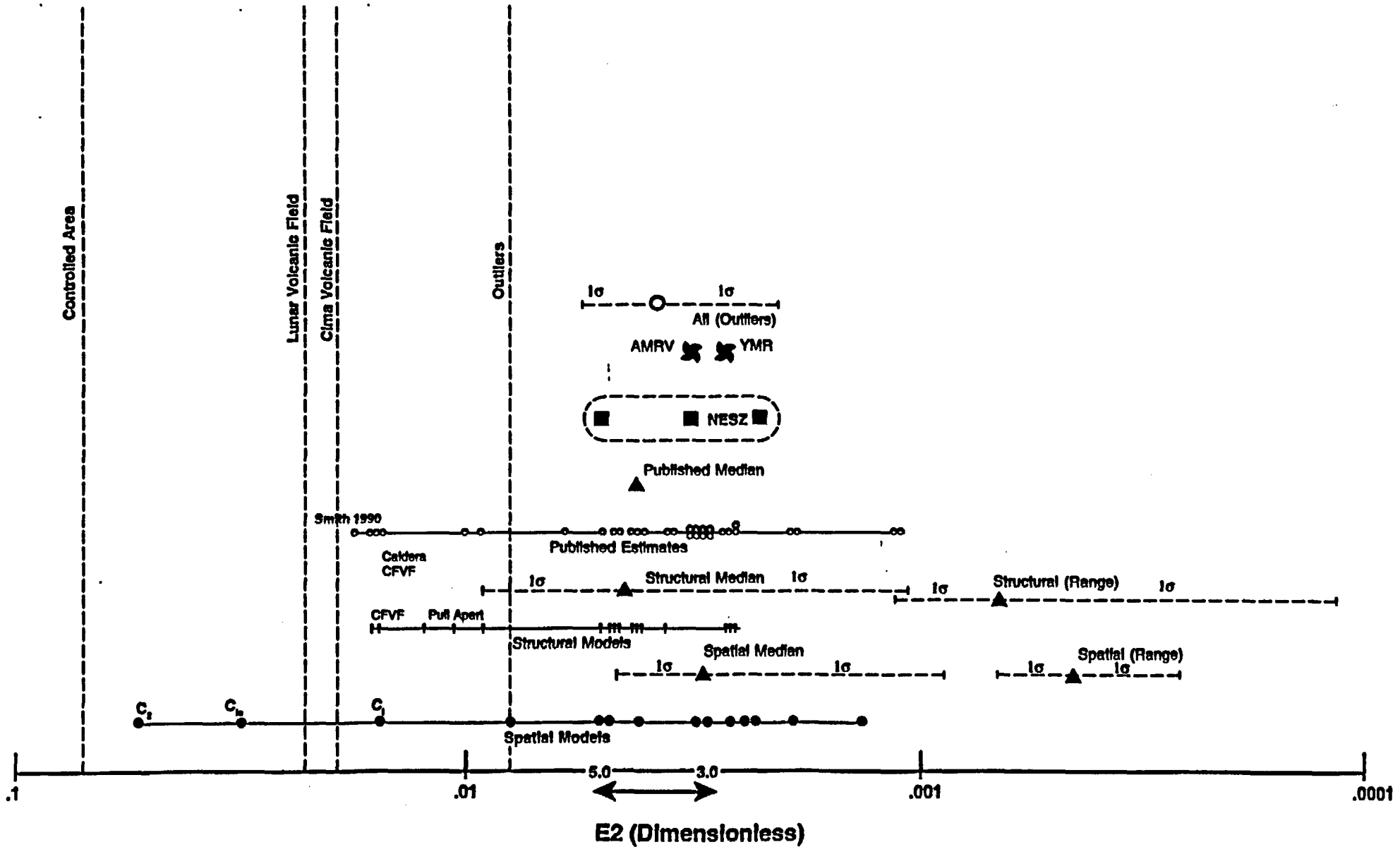


Fig. 7.24. Distribution of E2, the disruption probability in probability space. The x-axis is a long scale of E2 (dimensionless) and the y-axis has no scale. It is used to provide plotting space for the overlapping estimates of the disruption ratio. The vertical line labeled "Outliers" is the position of estimates identified as outliers using exploratory data analyses. All points to the left of the line are outliers or far outliers. The vertical lines labeled "Lunar volcanic Field" and "Cima volcanic field" are the estimate of the disruption probability if a 6 km² repository were randomly located in the respective fields. The vertical line labeled "Controlled Area" is the ratio of the controlled area to the potential repository site.



pull-apart basin is twofold. First, the potential Yucca Mountain site is located outside the structural basin. Second, the basin boundaries appear to limit both the distribution and degree of north-northeast dispersion of sites of Pliocene and Quaternary basaltic volcanism. Thus sites of basaltic volcanism, in the vicinity of Crater Flat, appear to occur only within the structural boundaries of the pull-apart basin.

We have chosen to not exclude the outlier estimates of E2 from the risk analyses for two reasons. First, we prefer not to exclude any information at this stage of studies. Second, alternative structural models exist supporting northeast trends in the distribution of volcanic events, both in the orientation of age-correlated centers and in the alignment of vents. The evidence that these trends extend to or through the potential Yucca Mountain site is admittedly weak, but cannot be disproved with the limited number of volcanic events in the YMR.

The disruption ratios determined from spatial and structural models group between values of 3.0 to 5.0×10^{-3} (Fig. 7.24). The set of structural models that include the potential Yucca Mountain site (labeled NESZ and AMRV on Fig. 7.24) give ratios for E2 that are also between 3.0 to 5.0×10^{-3} . Finally, if the estimates of all models of E2 are weighted for the tendency of basalt centers to occur in alluvial basins versus range fronts or range interiors, almost all estimates of the probability of disruption (E2) are $< 10^{-3}$ (Fig. 7.24).

A simulation matrix was constructed using five sets of model estimations of E2, with each model subdivided into two cases (Table 7.16). The models include: (1) all published estimates of E2, (2) edited estimates of all published estimates (outlier estimates removed), (3) spatial models, (4) outlier edited spatial models, (5) structural models from Table 7.14 (these data are not edited for outliers because the data are not strongly skewed), and (6) intersection models that include the potential Yucca Mountain site (Tables 7.13 and 7.14). Subclasses for each model include: (1) estimates of E2 for intersection or forced intersection models, and (2) estimates of E2 for range interiors. Because it is difficult to identify bounds for E2, the data are modeled as a normal distribution using the median and standard deviation estimates from the data tables. All simulations were run for 10,000 sampling iterations using the Latin-Hypercube sampling method.

The results of the simulation modeling are shown on Table 7.17. Intersection models (mean estimates) range from 4.6×10^{-3} (structural models) to 2.8×10^{-3} (outlier-removed, spatial models). Range interior models (mean estimates) range from 6.9×10^{-4} (structural models) to 4.3×10^{-4} (outlier-removed, spatial models). A subset of cumulative probability curves (intersection models) generated from the simulation modeling using the simulation matrix are shown on Fig. 7.25. The cumulative probability curves for the range interior models are not shown. They are identical to the intersection models, but are shifted to lower disruption ratios. The median estimates of the cumulative distribution curves cluster in a narrow range (2.8 to 4.6×10^{-3} ; see expected values of Fig. 7.25). The curves differ primarily in the spread or uncertainty of the distributions (Fig. 7.26). The uncertainty is largest for the spatial model (with outliers) and smallest for the subset of intersection models that include the repository (NE models of Fig. 7.25). The 50 percentile estimate of the structural models is *larger* than the 50 percentile estimate for the spatial model but the distribution of the spatial model is much wider. Finally, the cumulative probability curves for the edited spatial and published models plot very close to the NE models (the curves partly overlap).

Table 7.16. Simulation Matrix for E2, the Disruption Probability.

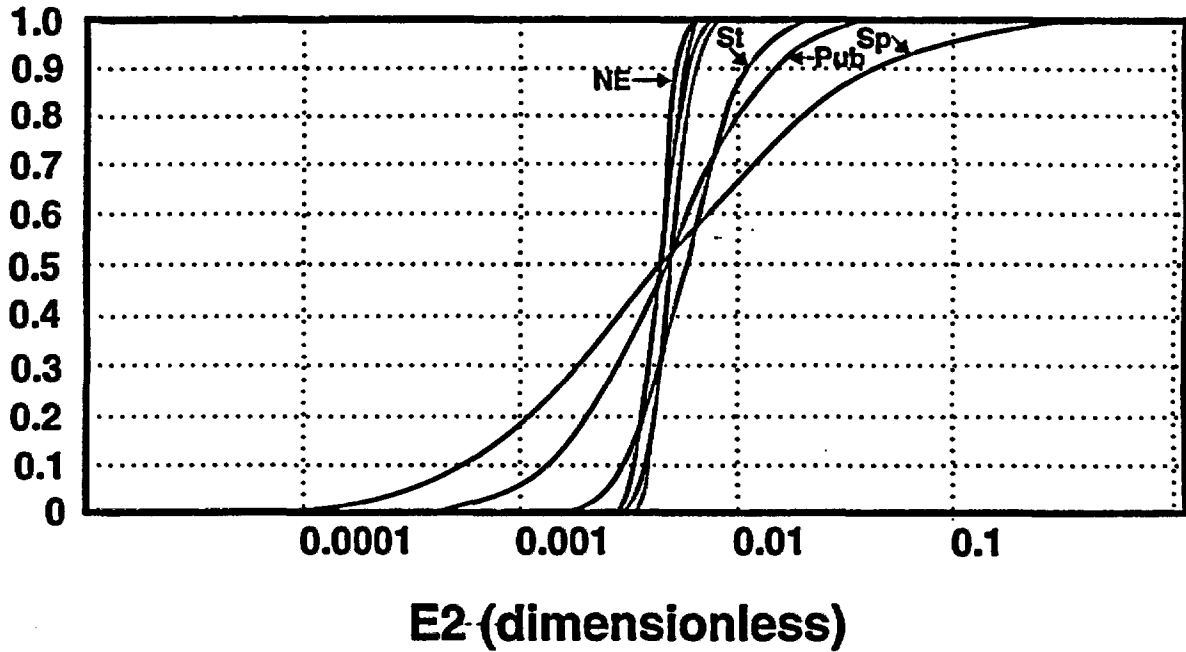
Disruption Model (E2)	Median	Std Deviation	Skewness	Simulation (mean, 1 σ)
All Published Estimates				
Intersection	4.1E-03	7.9E-03	2.2	4.1E-03
Range Interior	6.2E-04	1.3E-03	2.2	6.2E-04
All Published (no outliers)				
Intersection	3.8E-03	1.8E-03	1.3	3.8E-03
Range Interior	5.7E-04	2.6E-04	1.3	5.7E-04
Spatial Distribution Models				
Intersection	3.1E-03	1.5E-02	2.6	3.1E-03
Range Interior	4.6E-04	2.2E-03	2.6	4.6E-04
Spatial Distribution (no outliers)				
Intersection	2.8E-03	1.8E-03	1.6	2.8E-03
Range	4.3E-04	2.7E-04	1.6	4.3E-04
Structural Models				
Intersection	4.6E-03	4.4E-03	1.2	4.6E-03
Range Interior	6.9E-04	6.6E-04	1.2	6.9E-04
Intersection Models				
Intersection	3.1E-03	1.1E-03	1.3	3.1E-03
Range Interior	4.7E-04	1.6E-04	1.3	4.7E-04

Table 7.17. Simulation Results for E2, the Probability of Magmatic Disruption.

Simulation	Published Estimates Intersection	Published Estimates Range	Published Estimates Intersection (no outliers)	Published Estimates Range (no outliers)
Minimum	-2.8E-02	-5.0E-03	-2.9E-03	-5.1E-04
10 percent	-6.9E-03	-1.1E-03	1.5E-03	2.3E-04
Mean	4.1E-03	6.2E-04	3.8E-03	5.7E-04
90 percent	1.4E-02	2.4E-03	6.0E-03	9.0E-04
Maximum	3.7E-02	7.2E-03	1.0E-02	1.6E-03
Simulation	Spatial Models Intersection	Spatial Models Range	Spatial Models Intersection (no outliers)	Spatial Models Range (no outliers)
Minimum	-5.7E-02	-8.2E-03	-3.9E-03	-5.9E-04
10 percent	-1.6E-02	-2.4E-03	5.5E-04	8.3E-05
Mean	3.1E-03	4.7E-04	2.8E-03	4.3E-04
90 percent	2.2E-02	3.3E-03	5.1E-03	7.7E-04
Maximum	6.5E-02	9.6E-03	9.7E-03	1.5E-03
Simulation	Structural Models Intersection	Structural Models Range	Direct Intersection	Direct Intersection Range
Minimum	-1.2E-02	-2.0E-03	-1.0E-03	-1.5E-04
10 percent	-1.1E-03	-1.6E-04	1.8E-03	2.6E-04
Mean	4.6E-03	6.9E-04	3.1E-03	4.7E-04
90 percent	1.0E-02	1.5E-03	4.5E-03	6.8E-04
Maximum	2.3E-02	3.3E-03	7.7E-03	1.1E-03

Fig. 7.25. Cumulative probability curves for E2 generated from the simulation matrix of Table 7.16.

Simulation Results: E2

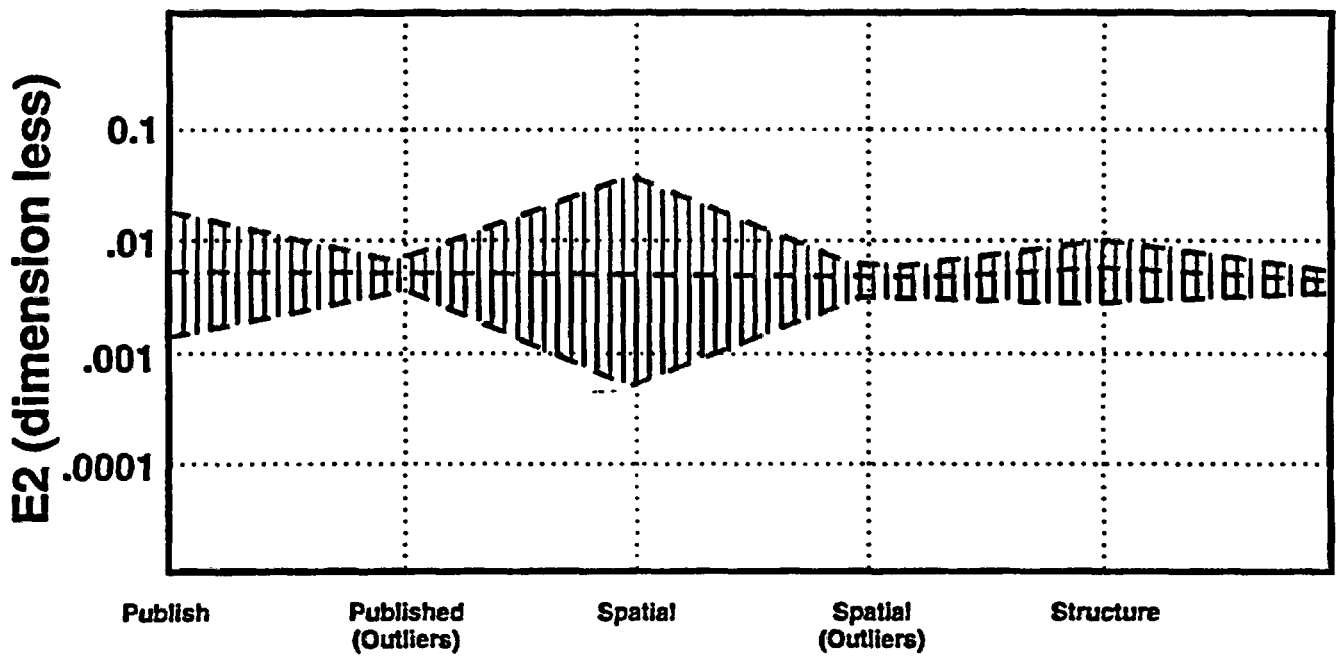


Expected Value

All Published $4.1E^{-3}$
Published (outliers) $3.8E^{-3}$
All Spatial $3.1E^{-3}$
Spatial (outliers) $2.8E^{-3}$
Structural $4.6E^{-3}$
NE Trend $3.1E^{-3}$

Fig. 7.26 Risk simulation summary for the probability of disruption of the repository showing variations in uncertainty for the 10 percentile, mean, and 90 percentile estimates.

Risk Summary: E2intersect



Top - - - - 90 per %

Center - - - - Mean

Bottom - - - - 10 per %

E. Probability of Magmatic Disruption of the Potential Repository

The cumulative distribution curves for E1 and E2 can be combined through risk simulation to give the cumulative distribution curves for estimates of the probability of magmatic disruption of the repository, the controlled area, and the Yucca Mountain region ($\Pr(E2 \text{ given } E1)\Pr(E1)$). We attempt to define a range of cumulative distribution curves for the probability of magmatic disruption by assembling three sets of models. For the first model, two fixed estimates for E2 are used (intersection and range intersection), and E1 is varied using the estimates from Tables 7.5 and 7.6. For the second model, a single distribution is used for E1, and E2 is varied using the range of simulation modeling from Table 7.17. Finally, the third model examines the variability in E1 *required* by selection of individual models of E2. The exponential equation for the conditional probability of magmatic disruption is approximately linear for $t = 1$ to 10,000 yrs so the cumulative distribution curves can be combined by simple multiplication.

Table 7.18 is the simulation matrix and expected values for estimations of the probability of magmatic disruption of the repository. The models used for E1 are the preferred models using homogeneous and nonhomogeneous Poisson distributions for the volcanic cycle (event and stress-dike) and Quaternary accelerated intervals (event and stress-dike). Also included in the recurrence models are the minimum and maximum estimations from Tables 7.5 and 7.6. The simulations were run with 10,000 iterations using Latin-Hypercube sampling. The recurrence estimates are modeled as trigen distributions using the most likely values for the mid-point estimate (except minimum and maximum simulations), the Quaternary field limit as the 5 percentile lower bound (1.1×10^{-5} events yr^{-1}), and the regulatory perspective as the 10 percentile upper bound (5×10^{-7} events yr^{-1}). The two fixed estimates for E2 are simulated as normal distributions (median, standard deviation) using the summary statistics for the structural models from Table 7.14. The minimum and maximum estimates used in the simulation are the maximum estimate (worst case) and minimum estimate (best case) from Tables 7.5 and 7.6. This simulation matrix is designed to examine the sensitivity of the probability of magmatic disruption to different recurrence models.

Table 7.19 shows the mean, 10 and 96 percentile, and maximum and minimum estimates for the risk simulation using homogeneous Poisson models. Only the homogeneous Poisson model is shown because the estimates for the nonhomogeneous model are nearly identical. The mean estimates using simulation modeling based on the probability matrix are bracketed by the minimum and maximum models of Table 7.19 (2.1×10^{-8} to 2.6×10^{-8} events yr^{-1} for intersection). There is only a narrow range of mean estimates, showing that there is limited variability in the probability of magmatic disruption with different recurrence models (E1). The mean estimates for homogeneous and nonhomogeneous Poisson models are identical ($2.3 \pm 0.2 \times 10^{-8}$ events yr^{-1}). Fig. 7.27 shows the cumulative probability curves for the minimum and maximum homogeneous Poisson models of Table 7.19. This figure provides an approximation of the sensitivity or uncertainty of the probability of magmatic disruption controlled by alternative recurrence models.

Judgment is required to assess whether it is reasonable to weight the probability of magmatic disruption by the frequency of formation of basaltic volcanic centers in range interiors. Table 7.19 shows that the mean estimates of cumulative probability curves for volcanic events in range interiors varies from 3.2×10^{-9} to 3.9×10^{-9} events yr^{-1} . The probability of magmatic disruption of the controlled area is larger than the probability of magmatic disruption of the repository by a factor of 13.5. The probability of magmatic disruption of the YMR is \geq to the probability of disruption of the controlled area.

Table 7.20 is the second simulation matrix, and it is designed to assess the variability of the probability of magmatic disruption with different estimates of E2. The simulation uses a single distribution for E1 and a range of estimates for E2. The E1 is modeled as a trigen distribution using the median estimate from the

Table 7.18. Simulation Matrix for Homogeneous and Nonhomogeneous Poisson Recurrence Models of E1 using Fixed Estimates of E2.

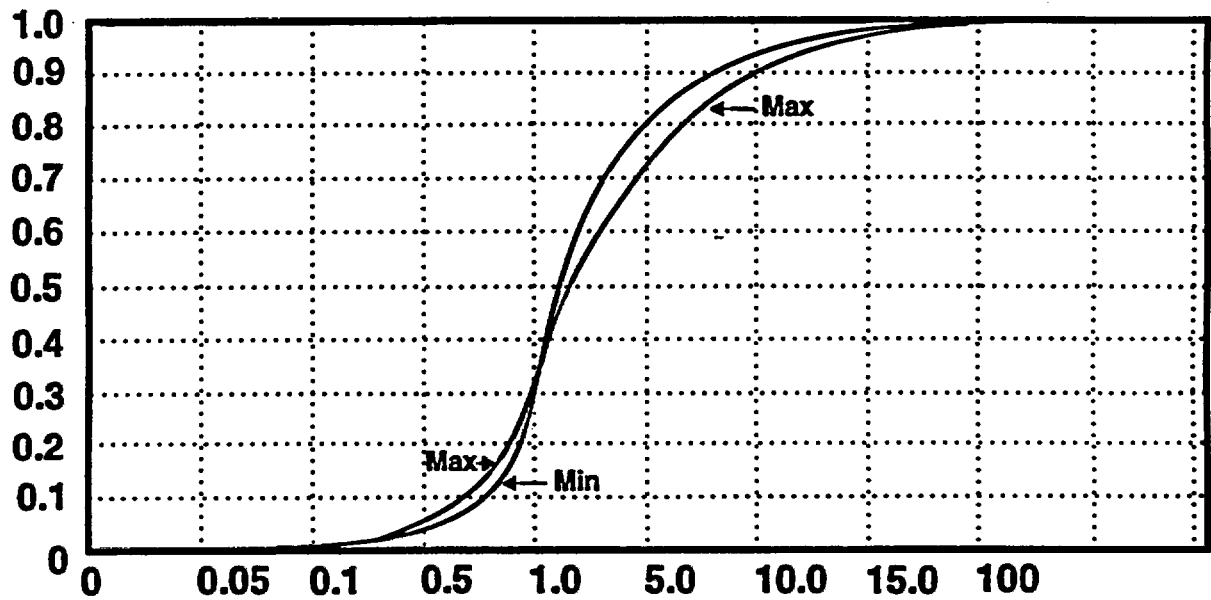
Simulation Matrix E1 Model	Trigen Homogeneous	Trigen Nonhomogeneous	Trigen E2Intersect	Normal E2Range
Vol Cycle Event	4.8E-06	4.8E-06	4.6E-03	6.9E-04
Vol Cycle Stress Dike	4.7E-06	4.7E-06	4.6E-03	6.9E-04
Quat Accel Events	5.3E-06	5.0E-06	4.6E-03	6.9E-04
Quat Accel Stress Dike	5.2E-06	4.8E-06	4.6E-03	6.9E-04
Minimum	4.6E-06	4.6E-06	4.6E-03	6.9E-04
Maximum	5.7E-06	5.7E-06	4.6E-03	6.9E-04
Simulation Expected Values	Homogeneous Pr(intersect)	Nonhomogeneous Pr(intersect)	Homogeneous Pr(range)	Nonhomogeneous Pr(range)
Vol Cycle Event	2.2E-08	2.2E-08	3.3E-09	3.2E-09
Vol Cycle Stress Dike	2.1E-08	2.1E-08	3.2E-09	3.2E-09
Quat Accel Events	2.4E-08	2.3E-08	3.7E-09	3.4E-09
Quat Accel Stress Dike	2.4E-08	2.2E-08	3.5E-09	3.3E-09
Minimum	2.1E-08	2.1E-08	3.2E-09	3.2E-09
Maximum	2.6E-08	2.6E-08	3.9E-09	3.9E-09
Summary Statistics				
Mean	2.3E-08	2.3E-08	3.5E-09	3.4E-09
Std Deviation	0.2E-08	0.2E-08	0.3E-09	0.3E-09

Table 7.19: Simulation Results of Homogeneous Poisson Models for the Probability of Magmatic Disruption of the Repository (Pr(E2 given E1)Pr(E1)).

Simulation Results						
Homogeneous Poisson	Cycle Event	Cycle Dike	Quat Events	Quat Dikes	Minimum	Maximum
Minimum=	-2.04E-07	-2.22E-07	-2.66E-07	-2.35E-07	-2.31E-07	-2.09E-07
10Perc=	-2.29E-08	-2.19E-08	-2.74E-08	-2.64E-08	-2.14E-08	-3.05E-08
Mean=	2.18E-08	2.17E-08	2.46E-08	2.34E-08	2.13E-08	2.62E-08
90Perc=	8.30E-08	8.31E-08	9.21E-08	8.85E-08	8.14E-08	9.87E-08
Maximum=	3.63E-07	3.13E-07	3.40E-07	3.92E-07	3.66E-07	3.86E-07

Fig. 7.27 Cumulative probability distribution curves for the simulation matrix of Table 7.19. Fixed estimates of E2 are used for intersection and range interior models for a range of homogeneous Poisson models of the recurrence rate. The probability distribution curves are not shown for nonhomogeneous Poisson models because the results are similar.

Simulation Results: E2 Fixed



$\Pr(E_2 \text{ given } E1)\Pr(E1)$
Events yr⁻¹ x 10⁻⁶

most likely value of Table 7.5. A lower bound of 1.1×10^{-5} events yr^{-1} (95 percentile) is used with an upper bound of 5.0×10^{-7} events yr^{-1} (10 percentile; Simulation Three of Table 7.5). The estimates used for E2 are the median and standard deviation from the summary statistics for the intersection, and range interior columns for the structural, the spatial, and the spatial models with outliers removed (estimates from Tables 7.13 and 7.15). The minimum and maximum estimates were assigned from the smallest and largest estimates from *all* estimates of Tables 7.13 and 7.15. A standard deviation of 50% of the estimate was assumed for the distribution models of the minimum (best case) and maximum (worst case) estimates.

The mean estimates of the probability of magmatic disruption of the repository are similar to the estimates for the first simulation matrix (intersection and range models; Fig. 7.28). The estimates range from 1.3 to 2.2×10^{-8} events yr^{-1} for the intersection models and 1.9 to 3.4×10^{-9} events yr^{-1} for the range intersection models (Table 7.21). However, the minimum and maximum estimates are much more variable for the second simulation matrix than the first simulation matrix (Fig. 7.28). The minimum estimates of the probability of magmatic disruption (intersection models) range from 3.8×10^{-9} to 6.9×10^{-9} events yr^{-1} (Table 7.21). The maximum estimate is identical to the range of the first simulation matrix for the spatial models with outliers removed (2.4×10^{-8} events yr^{-1} ; Table 7.21). However, an estimate for the probability of magmatic disruption of the repository of 7.3×10^{-8} events yr^{-1} was obtained from the maximum estimates (worse cases) of the structural and spatial models. These are the largest estimations of the probability of magmatic disruption of the potential repository of any published probability calculations (except the worst case of Ho 1992). The variability in the maximum estimates is controlled by the large values of E2 for a small set of spatial and structural models (Tables 7.13 and 7.15; Fig. 7.28). These models are identified as having significant effects on the sensitivity of estimations of the probability of magmatic disruption of the repository. They must be examined more carefully, and this examination leads to the consideration of the third probability matrix.

The conditional probability model used for risk assessment assumes independence of probability attributes. However, there are indirect controls placed on the recurrence rate from the selection of spatial and structural models for E2. These limits are an effect of the exclusion of some volcanic events because of the smaller or restricted area (compared to the YMR) of specific spatial or structural models of E2. This effect is not considered in estimations of the probability of magmatic disruption *if E1 and E2 are estimated independently* (Crowe et al. 1994; Wallmann 1994). The effect on the probability of magmatic disruption is largest for disruption models that give the highest disruption probabilities (spatially restricted models), and is zero for disruption models that include all volcanic events in the YMR.

Table 7.22 is a probability matrix where E1 is adjusted for individual spatial and structural models for E2 (column "E1 Adjusted" of Table 7.22). The adjusted estimates of E1 are combined with estimates for E2 to give the probability of magmatic disruption of the repository. The adjustments to E1 are made by *not including* volcanic events in the recurrence rate calculations if they *are not included* in the area of the disruption ratio. The adjusted estimates of E1 for Table 7.21 are made only for the most likely models

Table 7.20: Simulation Matrix for the Probability of Magmatic Disruption of the Repository using Median, Minimum, and Maximum Estimates of E2 and a Fixed Estimate of E1.

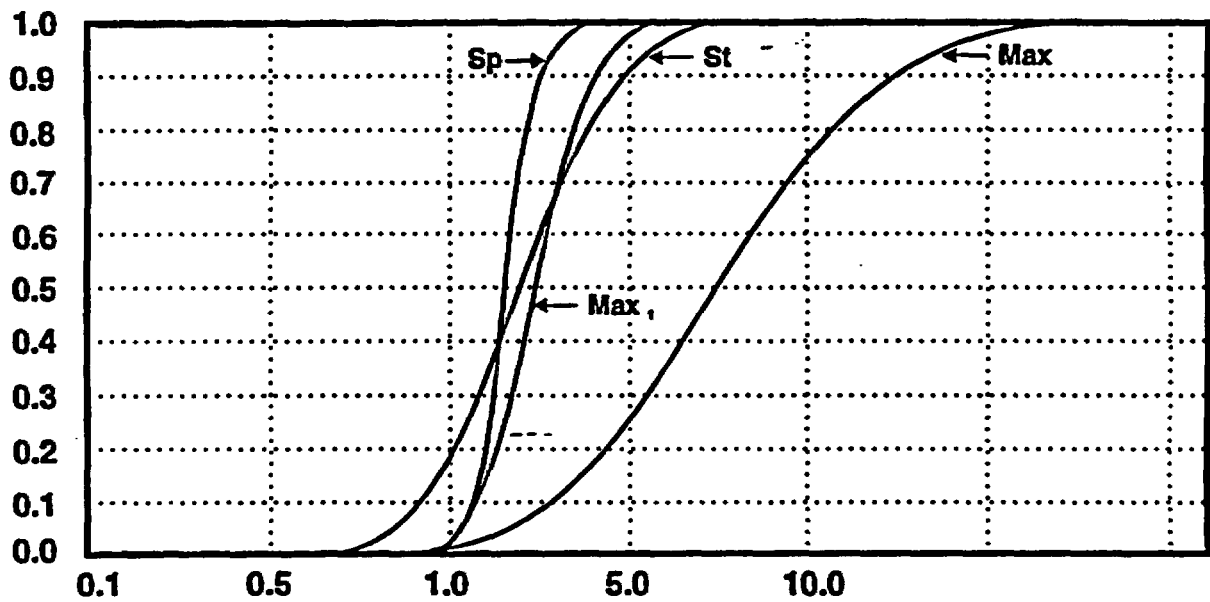
E2 Models	E1	Intersect	Range	Minimum	Maximum
Structural	4.9E-06	4.6E-03	6.90E-04	7.8E-04	1.5E-02
<i>Pr(disrupt)</i>		2.2E-08	3.4E-09	3.8E-09	7.3E-08
Spatial	4.9E-06	3.1E-03	4.6E-04	1.4E-03	1.5E-02
<i>Pr(disrupt)</i>		1.5E-08	2.2E-09	6.9E-09	7.3E-08
Spatial (outliers)	4.9E-06	2.6E-03	3.9E-04	1.40E-03	5.0E-03
<i>Pr(disrupt)</i>		1.3E-08	1.9E-09	6.9E-09	2.4E-08

Table 7.22: Simulation Results for the Probability of Magmatic Disruption of a Repository using the Probability Matrix of Table 7.21.

Structural Models	Intersection	Range	Minimum	Maximum
<i>Minimum=</i>	-5.8E-08	-8.6E-09	-4.4E-09	-6.7E-08
<i>10Perc=</i>	-5.0E-09	-7.7E-10	1.4E-09	2.6E-08
<i>Mean=</i>	2.2E-08	3.4E-09	3.8E-09	7.3E-08
<i>90Perc=</i>	5.0E-08	7.5E-09	6.3E-09	1.2E-07
<i>Maximum=</i>	1.0E-07	1.6E-08	1.1E-08	2.1E-07
Spatial Models (all data)				
	Intersection	Range	Minimum	Maximum
<i>Minimum=</i>	-1.4E-08	-1.2E-08	-7.0E-09	-6.6E-08
<i>10Perc=</i>	5.7E-09	-2.3E-09	2.4E-09	2.6E-08
<i>Mean=</i>	1.5E-08	2.3E-09	6.9E-09	7.3E-08
<i>90Perc=</i>	2.5E-08	6.9E-09	1.1E-08	1.2E-07
<i>Maximum=</i>	4.8E-08	1.6E-08	2.1E-08	2.2E-07
Spatial Models (all data)				
	Intersection	Range	Minimum	Maximum
<i>Minimum=</i>	-1.0E-08	-1.3E-09	-6.2E-09	-2.8E-08
<i>10Perc=</i>	5.2E-09	7.8E-10	2.4E-09	8.7E-09
<i>Mean=</i>	1.3E-08	1.9E-09	6.9E-09	2.4E-08
<i>90Perc=</i>	2.0E-08	3.1E-09	1.1E-08	4.1E-08
<i>Maximum=</i>	3.7E-08	5.7E-09	1.9E-08	7.7E-08

Fig. 7.28. Cumulative probability distribution curves for the probability of magmatic disruption of the repository using a fixed estimate of E1, and varying models for E2.

Simulation Results: Intersection Models



Expected Value

Structural 2.25×10^{-6}

Spatial 1.5×10^{-6}

Maximum 7.3×10^{-6}

Maximum 2.4×10^{-6}
(outliers)

established from homogeneous Poisson event counts. We have not re-estimated E1 for all recurrence models because the recurrence models show limited variability.

Careful examination of Table 7.22 shows two features. First, the median estimate is slightly smaller than median estimates for the probability of magmatic disruption of the repository for E2 Tables (7.19 and 7.21). However, the difference is small and is not significant (standard deviations overlap). Second, Table 7.22 provides a more realistic basis for identifying worse case estimates for the probability of magmatic disruption. The column labeled "Z score" is the standardized variable of the intersection column and can be used to identify data that are more than 1σ from the median. There are two cases where the z-score is greater than 1: Cluster 1 and 1a of the spatial models. These cases are highlighted in Table 7.22, and are identified as sensitive models for the estimates of the probability of magmatic disruption of the repository.

Table 7.22. Probability of magmatic disruption of the repository where the recurrence rate (E1) is adjusted for individual spatial and structural models of E2.

Spatial Models	E2	E1 Adjusted	Pr(E2 given E1)Pr(E1)		Range
			Intersection	Z Score	
Cluster 1 (3.7)	1.5E-02	2.6E-06	4.01E-08	1.4	6.0E-09
Cluster 1a (3.85)	8.0E-03	2.3E-06	1.9E-08	0.0	2.8E-09
CFVZ (4.8)	4.1E-03	3.7E-06	1.5E-08	-0.1	2.3E-09
NESZ (3.85)	5.0E-03	3.6E-06	1.8E-08	0.0	2.7E-09
Cluster 1a (1.0)	1.5E-02	5.0E-06	7.5E-08	3.6	1.1E-08
CFVZ (1.0)	4.6E-03	6.0E-06	2.7E-08	0.6	4.1E-09
Structural Models					
CFVZ (1.0)	4.6E-03	6.0E-06	2.7E-08	0.6	4.1E-09
CFVZ (4.8)	4.1E-03	2.5E-06	1.0E-08	-0.5	1.5E-09
YMR (4.8)	2.7E-03	2.5E-06	6.9E-09	-0.7	1.0E-09
CFV Field (3.75)	1.5E-02	1.6E-06	2.4E-08	0.4	3.6E-09
CFV Field + AV	8.0E-03	2.3E-06	1.9E-08	0.0	2.8E-09
Strike Slip (1.0)	4.6E-03	6.0E-06	2.7E-08	0.6	4.1E-09
Strike Slip (4.8)	4.1E-03	2.3E-06	9.5E-09	-0.5	1.4E-09
Stress-Dike (1.0)	4.6E-03	2.7E-06	1.2E-08	-0.4	1.8E-09
Chain Model (3.7)	2.7E-03	1.6E-06	4.3E-09	-0.9	6.4E-10
Chain Model (3.85)	7.8E-04	2.1E-06	1.6E-09	-1.0	2.4E-10
Pull-Apart (3.7)	1.3E-02	1.6E-06	2.1E-08	0.2	3.2E-09
Pull-Apart (3.85)	8.7E-03	2.1E-06	1.8E-08	0.0	2.7E-09
Caldera (3.75)	1.5E-02	1.6E-06	2.4E-08	0.4	3.6E-09
Kawich Rift (3.7)	3.5E-03	1.6E-06	5.6E-09	-0.8	8.5E-10
Kawich Rift (3.85)	2.7E-03	2.1E-06	5.5E-09	-0.8	8.3E-10
NESZ (3.7)	5.0E-03	1.9E-06	9.4E-09	-0.6	1.4E-09
	Summary	Mean	1.9E-08		2.9E-09
	Statistics	Median	1.8E-08		2.7E-09
		Geomean	1.5E-08		2.2E-09
		StDev	1.6E-08		2.1E-09
		Skewness	2.2		2.2
		Minimum	1.6E-09		2.4E-10
		Maximum	7.5E-08		1.1E-08

F. Discussion: Probability of Magmatic Disruption

The conditional probability of magmatic disruption has been examined for a range of alternative models of the recurrence rate, and spatial and structural models of the distribution of volcanic centers in the YMR. The median estimates using both statistical descriptors and risk simulation are slightly greater than 10^{-8} events yr^{-1} for simple intersection models, and generally less than 10^{-8} for models weighted by the likelihood of volcanic events in range interiors. Cumulative probability distributions, constructed through simulation modeling, are presented for a range of alternative recurrence and disruption models. These curves provide the best representation of the uncertainty of the data distributions. The cumulative probability distributions for the recurrence rate (E1) are bounded by regulatory perspectives and observations of rates of basaltic volcanic events in Quaternary volcanic fields. The mid-point estimates of the recurrence rate show a limited range of variation for multiple alternative models (time-series, homogeneous and nonhomogeneous Poisson, and models of magma output rate). The cumulative probability distributions for the disruption probability (E2) are more difficult to bound. The data show a relatively narrow range of median estimates but with significance variance. The data distribution for E2 is

affected strongly by the existence of a subset of spatial and structural models that give high disruption probabilities ($\approx 10^{-2}$).

What is the significance of the present status of probability studies? The data summarized in this section supports previous judgments by the DOE (EA 1986; SCP 1988; ESSE 1992) that volcanism is not a disqualifying condition for the potential Yucca Mountain site. The basis for that judgment is the low probability of disruption of the potential repository. The median probability of disruption using both homogeneous and nonhomogeneous Poisson recurrence models and the median estimate of disruption models is $2.3 \pm 0.8 \times 10^{-8}$ events yr^{-1} for intersection of the repository. The median estimate of the probability of magmatic disruption for models weighted by the likelihood of the occurrence of volcanic events in range interiors is $3.5 \pm 0.3 \times 10^{-9}$ events yr^{-1} . The mean probability of disruption from simulation modeling using a mean estimate of recurrence models, and median estimates of disruption models is $1.7 \pm 0.5 \times 10^{-8}$ events yr^{-1} for intersection, and $2.5 \pm 0.8 \times 10^{-9}$ events yr^{-1} for intersection weighted by the likelihood of volcanic events in range interiors. Finally, the median probability of disruption of the repository is $1.8 \pm 3.2 \times 10^{-8}$ events yr^{-1} for intersection models and $2.7 \pm 4.7 \times 10^{-9}$ events yr^{-1} for range intersection models for estimates where E1 is adjusted for individual spatial and structural models. Two worse case estimates for the E1 are identified from the adjusted probability matrix, and are 7.5 to 4.0×10^{-8} events yr^{-1} . These estimates correspond to cluster models of volcanic events in Crater Flat (Pliocene and Quaternary) that have a low likelihood of resulting in disruption of the potential repository.

The probability estimates exceed 10^{-8} events yr^{-1} for the controlled area and the YMR. Therefore, studies will have to be conducted of the effects of eruptive and intrusive activity near the potential repository site. The probability of disruption of the potential repository approaches or is less than 10^{-8} events yr^{-1} if the probability is weighted for the reduced likelihood of event occurrence in range interiors. However, several lines of evidence suggest that studies will still be required of the effects of magmatic disruption of the repository. First, the criterion of an occurrence probability of 10^{-8} events yr^{-1} is currently being reviewed. Second, it is unclear what percentile position on a cumulative probability curve must be less than 10^{-8} events yr^{-1} . Thus the standards are ambiguous for judging the significance of probability estimations and cannot be easily applied. ---

The range of estimates of the probability of magmatic disruption for this report is nearly identical to estimates of the probability of magmatic disruption of the repository by Crowe et al. (1982; Crowe 1986; Wallmann et al. 1993; Wallmann 1994; Connor and Hill 1994; and Crowe et al. 1994). The only published calculations with different probability estimates are Ho (1992). However, Ho's calculations cannot easily be compared with other calculations (see discussion of Section VI). He used recurrence rates for the YMR and applied them to an area of 75 km^2 (less than the size of the controlled area) extending north of the Lathrop Wells volcanic center. He did not examine the variability in E1 required by assumptions used to estimate E2. The calculations of Ho (1992) are correct mathematically but are physically implausible. Justification for his worst case model would require evidence that future volcanic events, defined as the recurrence rate of formation of a new volcanic center in the YMR, could occur only in the identified 75 km^2 area. Existing evidence provides no support for that model.

The framework calculations for probability studies are now well developed. It will be relatively easy to reassess probability estimates should new results change assumptions for models of E1 or E2. The cumulative probability distributions for the probability of magmatic disruption can be readily modified using the systematic procedures of risk simulation. Three observations are made using insight gained from risk simulations. First, the recurrence rate of volcanic events (E1) is relatively well constrained in probability space. The range of probability estimates using alternative recurrence models is not large, and the probability of magmatic disruption does not vary significantly with different models of E1. Second, simulation modeling of E2, the disruption probability, shows that the cumulative distributions are sensitive to a small number of spatial and structural models. It is logical to focus future site characterization studies on assessments of the applicability of these models. Third, we have made only limited attempts to assess

the likelihood of acceptance of alternative models of E1 and E2. Logically, there is a ranking that could be developed for the alternative models, and this ranking could be applied to risk simulation. Ranking of models is probably most important for E2 and of lesser importance for E1. The model ranking could be readily implemented through application of formal procedures of expert knowledge.

Some insight into the magnitude of the probability of magmatic disruption of the potential repository in the YMR can be gained by examination of analog volcanic fields. Probabilistic assessments can be compared by estimating the probability of intersection of a 6 km² area randomly placed in the interior of the Lunar Crater and Cima volcanic fields. The area of the Lunar Crater volcanic field (Quaternary part of the field) is about 260 km². The probability of random intersection of a six km² area in the field is about 0.023. There are 82 vents forming 28 clusters in the Lunar Crater volcanic field. Recurrence rates (homogeneous Poisson model) for the Lunar Crater volcanic field are about 4.5 x 10⁻⁵ to 1.1 x 10⁻⁵ events yr⁻¹ (Crowe et al. 1992; 1994). The probability of magmatic disruption of a 6 km² area in the Lunar Crater volcanic field is 1.0x 10⁻⁶ to 2.5 x 10⁻⁷ events yr⁻¹. The area of the Quaternary part of the Cima volcanic field is about 160 km². The probability of random intersection of a 6 km² area in the field is about .037. There are 28 volcanic centers forming 22 volcanic clusters in the Cima volcanic field. The recurrence rate of volcanic events (homogeneous Poisson model) in the Cima volcanic field is about 1.4 to 1.1 x 10⁻⁵ events yr⁻¹. The probability of disruption of a 6 km² area in the Cima volcanic field is about 4 to 5 x 10⁻⁷ events yr⁻¹. These probability estimates (4 x 10⁻⁷ to 1 x 10⁻⁶ events yr⁻¹) represent an upper bound to the disruption probability that is useful to compare with the probabilistic assessments for the YMR region. The probability of repository disruption in a large and active basaltic volcanic field is relatively low (< 1 in one million per year) for two reasons. First, volcanic events even in large and active volcanic fields are infrequent. The recurrence times between volcanic events for very active basaltic volcanic fields are relatively long (20,000 to 90,000 yrs) compared to the 10,000 yr isolation period of radioactive waste. Second, a volcanic event must occur in or near a potential repository to result in immediate release of radioactive waste. The Lunar Crater field has more than an order of magnitude greater number of Quaternary volcanic events than the YMR. The Cima volcanic field has more Quaternary events than the YMR by a factor of four. The potential repository site in Yucca Mountain is not located inside most spatial and structural zones. The structural models that include the potential site have a very low cone density per km². Both the disruption ratio and the probability of magmatic disruption must be less in the YMR than in the Lunar Crater and Cima volcanic fields. By comparison with analog volcanic fields, simple logic requires that the probability of magmatic disruption of the potential Yucca Mountain site must be less than about 5 x 10⁻⁷ events yr⁻¹. This limit could be inferred *without* site characterization studies.

Finally, the probability tables and cumulative probability distributions for E1, E2 and Pr(E2 give E1)Pr(E1) are not necessarily the data that will be used in regulatory documents. The DOE may or may not choose to modify the probability estimates and the cumulative probability distributions in response to regulatory perspectives.

V. REFERENCES

- Bacon C. R., "Time-Predictable Bimodal Volcanism in the Coso range, California," *Geology* 10, 65-69 (1982).
- Bergman, S. C. "Petrogenetic Aspects of Alkali Basaltic Lavas and Included Megacrysts and Nodules from the Lunar Crater Volcanic Field, Nevada, USA," PhD. Dissertation, Princeton University, 432 pp. (1982).
- Bruce, P. M., and H. E. Huppert, "Solidification and Melting Along Dykes by the Laminar Flow of Basaltic Magma," in M. P. Ryan (ed. Magma Transport and Storage, John Wiley and Sons, 88-101 (1990).

Champion, D. E., "Volcanic episodes near Yucca Mountain as determined by paleomagnetic studies at Lathrop Wells, Crater Flat, and Sleeping Butte, Nevada," *Proceedings, High Level Radioactive Waste Management, American Nuclear Society*, 61-67 (1991).

Champion, D. E., Oral Presentation to the United States Nuclear Waste Technical Review Board, Panel on Structural Geology and Geoen지니어ing, Meeting on Volcanism, Las Vegas, Nevada (September 14, 1992).

Carr, W. J., "Regional structural setting of Yucca Mountain, southwestern Nevada, and late Cenozoic rates of tectonic activity in part of the southwestern great basin, Nevada and California," U.S. Geological Survey Open-File Report 84-854, 109 pp. (1984).

Carr, W. J., "Styles of extension in the Nevada Test Site region, southern Walker Lane Belt; An integration of volcano-tectonic and detachment fault models," *in Basin and Range Extensional Tectonics near the latitude of Las Vegas, Nevada*, B. P. Wernicke, ed., Geological Society of America Memoir 176, 283-303 (1990).

Clemen, R.T., *Making Hard Decisions*, PWS-Kent Publishing Company, Boston, MA, 557 p. (1991).

Cressie, N. A. C., *Statistics for Spatial Data*, John Wiley and Sons, New York, NY, 900 pp. (1991).

Crowe, B. M., "Volcanic hazard assessment for disposal of high-level radioactive waste," in *Recent Tectonics: Impact on Society*, National Academy Press, Washington, D.C., Chap. 16, 247-260 (1986).

Crowe, B. M., "Basaltic Volcanic Episodes of the YMR," *High Level Radioactive Waste Management, International Conference, April 8-12, 1990* 1, 65-73 (1990).

Crowe, B. M., M. E. Johnson, and R. J. Beckman, "Calculation of the probability of volcanic disruption of a high-level radioactive waste repository within southern Nevada, USA," *Radioactive Waste Management* 3, 167-190 (1982).

Crowe, B. M., D. T. Vaniman, and W. J. Carr, "Status of volcanic hazard studies for the Nevada Nuclear Waste Storage Investigations," Los Alamos National Laboratory report LA-9325-MS (1983a).

Crowe, B. M., S. Self, D. Vaniman, R. Amos, and F. Perry, "Aspects of potential magmatic disruption of a high-level radioactive waste repository in southern Nevada," *Journal of Geology* 91, 259-276 (1983b).

Crowe, B. M., K. H. Wohletz, D. T. Vaniman, E. Gladney, and N. Bower, "Status of volcanic hazard studies for the Nevada Nuclear Waste Storage Investigations," Los Alamos National Laboratory report LA-9325-MS, VOL. II (1986).

Crowe, B., C. Harrington, L. McFadden, F. Perry, S. Wells, B. Turrin, and D. Champion, "Preliminary geologic map of the Lathrop Wells volcanic center," Los Alamos National Laboratory report LA-UR-88-4155 (1988).

Crowe, B. M., B. Turrin, S. Wells, F. Perry, L. McFadden, C. Renault, D. Champion, and C. Harrington, "Volcanic hazard studies for the Yucca Mountain project," in *Waste Management '89* 1, 485-492 (1989).

Crowe, B. M., R. Picard, G. Valentine, and F. V. Perry, "Recurrence Models of Volcanic Events: Applications to Volcanic Risk Assessment," *High level Radioactive Waste management: Proceedings of the Third International Conference Las Vegas, Nevada, April 12-16* 2, 2344-2355 (1992).

Crowe, B. M., and W. J. Carr, "Preliminary assessment of the risk of volcanism at a proposed nuclear waste repository in the southern Great Basin," U.S. Geological Survey Open-File Report 80-375, 15 pp. (1980).

Crowe, B. M., and F. V. Perry, "Volcanic probability calculations for the Yucca Mountain site: Estimation of volcanic rates," *Proceedings Nuclear Waste Isolation in the Unsaturated Zone, Focus '89*, American Nuclear Society, 326-334 (1989).

Crowe, B. M., and F. V. Perry, "Preliminary geologic map of the Sleeping butte volcanic centers," Los Alamos National Laboratory report LA-12101-MS, 11 pp. (1991).

Crowe, B. M., F. V. Perry, and G. A. Valentine, "Simulation Modeling of the Probability of Magmatic Disruption of the Potential Yucca Mountain Site," American Nuclear Society Focus93 (in press).

Connor C. B., "Cinder Cone Clustering in the TransMexican Volcanic Belt Implications for Structural and Petrologic Models," *Journal of Geophysical Research* 95 (B12), 19,395-19,405 (1990).

Connor C. B., and B. E. Hill, "Estimating the Probability of Volcanic Disruption of the Candidate Yucca Mountain Repository Using Spatially and Temporally Non Homogeneous Poisson Models," American Nuclear Society Focus93 (in press).

Davis, J. C., Statistics and Data Analysis in Geology, Second Edition, John Wiley and Sons, New York, NY, 646 pp. (1986).

Delaney, P. T., "Heat Transfer During emplacement and cooling of mafic dykes," in H. C. Hall, and W. F. Fahrig (eds.) Mafic Dike Swarms, Geol. Assoc. Canada Spec. Pap. 34, 31-46 (1987).

Delaney P. T., and D. D. Pollard, "Solidification of Basaltic Magma During Flow in a Dike," *American Journal of Science* 242, 856-887 (1982).

Devore, J. L. Probability and Statistics for Engineering and the Sciences, Second Edition, Brooks/Cole Publishing Company, Monterey, CA, 672 pp. (1987).

DOE (U.S. Department of Energy), "Environmental Assessment: Yucca Mountain Site, Nevada Research and Development Area, Nevada," DOE/RW-0073, Office of Civilian Radioactive Waste Management, Washington D.C. (1986).

DOE (U.S. Department of Energy), "Site Characterization Plan, Yucca Mountain Site, Nevada Research and Development Area, Nevada," DOE/RW-0199, Office of Civilian Radioactive Waste Management, Washington D.C. (1988).

Dohrenwend, J. C., L. D. McFadden, B. D. Turrin, and S. G. Wells, "K-Ar dating of the Cima volcanic field, eastern Mojave desert, California: Late Cenozoic volcanic history and landscape evolution," *Geology* 12, 163-167 (1984).

Dohrenwend, J. C., S. G. Wells, and B. D. Turrin, "Degradation of Quaternary cinder cones in the Cima volcanic field, Mojave, Desert, California," *Geological Society of America Bulletin* 97, 421-427 (1986).

Foland, K. A., and S. C. Bergman, "Temporal and Spatial Distribution of Basaltic Volcanism in the Pancake and Reveille Ranges North of Yucca Mountain," *Proceedings, High Level Radioactive Waste Management, American Nuclear Society*, 2, 2366-2371 (1992).

- Fridrich, C. and J. Price, "Tectonic framework of Crater Flat basin, adjacent to Yucca Mountain Nevada: A preliminary report," *Abstract Geological Society America* 23, A189 (1992).
- Frizzel, V. A., and J. Shulters, "Geologic map of the Nevada Test Site," U.S. Geol. Surv., Misc. Invest. Series, Map I-2046 (1990).
- Harris, A. G., J. E. Repetski, J. L. Clayton, J. A. Grow, M. D. Carr, and T. A. Davis, "Results from 1991 Wildcat Wells near Yucca Mountain, Nevada," *Geological Society of America Abstracts with Programs*, 24, 17 (1992).
- Hasenaka, T., and I. S. E. Carmichael, "The Cinder Cones of Michoacan-Guanajuato, Central Mexico: Their Age, Volume, Distribution, and Magma Discharge Rate," *Journal Volcanology Geothermal Research* 25, 105-124 (1985).
- Ho, C. H., E. I. Smith, D. L. Feurbach, and T. R. Naumann, "Eruptive probability calculation for the Yucca Mountain site, USA: statistical estimation of recurrence rates," *Bulletin of Volcanology* 54, 50-56 (1991).
- Ho, C. H., "Time trend analysis of basaltic volcanism for the Yucca Mountain site," *Journal Volcanology Geothermal Research* 46, 61-72 (1991).
- Ho, C. H., "Risk Assessment for the Yucca Mountain High-Level Nuclear Repository Site: Estimation of Volcanic Disruption," *Mathematical Geology* 24 (4) 347-364 (1992).
- Kane, M. F., and R. E. Bracken, "Aeromagnetic Map of Yucca Mountain and Surrounding Regions, Southwest Nevada," U.S. Geol. Surv., Open-File Report 83-616, 19 pp. (1983).
- Katz, M., and A. Boettcher, "The Cima Volcanic Field," in Fiefe, D. L., and A. R. Brown (eds.) *Geology and Mineral Wealth of the California Desert*, Santa Ana, California South Coast Geologic Society, 236-241 (1980).
- King, C. Y., "Volume Predictability of Historical Eruptions at Kilauea and Mauna Loa Volcanoes," *Journal Volcanology Geothermal Research* 38, 281-285 (1989).
- Kuntz, M. A., D. E. Champion, E. C. Spiker, R. H. Lefebure, "Contrasting Magma Types and Steady-State, Volume-Predictable Basaltic Volcanism Along the Great Rift, Idaho," *Geological Society of America* 97, 579-594 (1986).
- Langenheim, V. E., S. F. Carle, D. A. Ponce, and J. D. Philips, "Revision of an aeromagnetic survey of the Lathrop Wells area, Nevada," U.S. Geol. Surv., Open-File Report 91-46, 17 pp. (1991).
- Lister, J. R., and R. C. Kerr, "Fluid-Mechanical Models of Crack Propagation and Their Application to Magma Transport in Dykes," *Journal of Geophysical Research* 96, 10,049-10,077 (1991).
- Megil, R.E., An introduction to risk analysis, PennWell Books, Tulsa, OK, 274 p. (1984).
- Minor, S. A., D. A. Sawyer, R. R. Wahl, V. A. Frizzel Jr., S. P. Schilling, R. G. Warren, P. P. Orkild, F. A. Coe, M. R. Hudson, R. J. Fleck M. A. Lanphere, W. C. Swadley, and J. C. Cole, "Preliminary Geologic Map of the Pahute Mesa 30' X 40' Quadrangle, Nevada," U. S. Geol. Surv. Open-File Report 93-299, (1993).

- Newendorp, P.D. Decision analysis for petroleum exploration, PennWell Books, Tulsa, OK, 668 p. (1974).
- Nauman, T. R., D. L. Feuerbach, and E. I. Smith, "Structural control of Pliocene volcanism in the vicinity of the Nevada Test Site, Nevada: An example from Buckboard Mesa," *Abstract Geological Society of America* 23 (2) 82 (1991).
- Perry, F. V., and B. M. Crowe, "Geochemical Evidence for Waning Magmatism and Polycyclic Volcanism at Crater Flat, Nevada," *High Level Radioactive Waste Management: Proceedings of the Third International Conference Las Vegas, NV, April 12-16* 2, 2344-2355 (1992).
- Peterson, D. W., "Volcanoes: Tectonic Setting and Impact on Society," in Active Tectonics, National Academy Press, Washington D.C., Chap. 15, 231-245 (1986).
- Schweickert, R. A., "Evidence for a Concealed Dextral Strike-Slip Fault Beneath Crater Flat, Nevada," *Geological Society of America Abstracts with Programs*, p. A90 (1989).
- Scott, D. H., and N. J. Trask, "Geology of the Lunar Crater Volcanic Field, Nye County, Nevada," U.S. Geological Survey Prof. Pap. 599-I, 36 pp. (1971).
- Sinnock, S. and R. G. Easterling, "Empirically Determined Uncertainty in Potassium-Argon Ages for Plio-Pleistocene Basalts from Crater Flat, Nye County, Nevada," Sandia National Laboratories, SAND82-2441, 17 pp. (1982).
- Settle, M., "The Structure and Emplacement of Cinder Cone Fields," *American Journal of Science* 279, 1089-1107 (1980).
- Shaw, H., "The Fracture Mechanisms of Magma Transport from the Mantle to the Surface," in Physics of Magmatic Transport, R. B. Hargraves, ed., Princeton University Press, 201-264 (1980).
- Shaw, H. R., "Uniqueness of volcanic systems," U.S. Geological Survey Prof. Pap. 1350, p. 1357-1394 (1987).
- Sheridan, M. F. "A Monte Carlo Technique to Estimate the Probability of Volcanic Dikes," *Proceedings, High Level Radioactive Waste Management, American Nuclear Society*, 2, 2033-2038 (1992).
- Smith, E. I., D. L. Feuerbach, T. R. Naumann, and J. E. Faulds, "The area of most recent volcanism near Yucca Mountain, Nevada: implications for volcanic risk assessment," *Proc. Int. Topical Meeting, High-Level Radioactive Waste Management, American Nuclear Society* 1, 81-90 (1990).
- Smith, R. L., and R. G. Luedke, "Potentially active volcanic lineaments and loci in western conterminous United States," in *Explosive Volcanism: Inception, Evolution and Hazards*, Geophysics Study Committee, National Research Council, National Academy Press, Washington D.C., 47-66 (1984).
- Stieltjes, L. and P. Moutou, "A statistical and probabilistic study of the historic activity of Piton de la Fournaise, Reunion Island, Indian Ocean," in A. R. McBirney (ed.), *Piton de la Fournaise Volcanic, Reunion Island, Journal of Volcanology Geothermal Research* 36, 67-86 (1987).
- Tuckwell H. C., Elementary Applications of Probability Theory, Chapman and Hall, New York, NY, 255 pp., (1988).

- Turrin, B. D., D. Champion, and R. J. Fleck, " $^{40}\text{Ar}/^{39}\text{Ar}$ age of the Lathrop Wells volcanic center, Yucca Mountain, Nevada," *Science* **253**, 654-657 (1991).
- Turrin, B. D., D. E. Champion, and R. J. Fleck, "Measuring the age of the Lathrop Wells volcanic center at Yucca Mountain," *Science* **257**, 556-558 (1992).
- Turrin, B. C. Oral Presentation to the United States Nuclear Waste Technical Review Board, Panel on Structural Geology and Geoengineering, Meeting on Volcanism, Las Vegas, Nevada (September 14, 1992).
- Valentine, G. A., B. M. Crowe, and F. V. Perry, "Physical processes and Effects of Magmatism in the Yucca Mountain Region," *Proceedings, High Level Radioactive Waste Management, American Nuclear Society*, **3**, 2344-2355 (1992).
- Vaniman, D. T., and B. M. Crowe, "Geology and petrology of the basalts of Crater Flat: Applications to volcanic risk assessment for the Nevada Nuclear Waste Storage Investigations," Los Alamos National Laboratory report LA-8845-MS, 67 pp. (1981).
- Vaniman, D. T., B. M. Crowe and E. S. Gladney, "Petrology and Geochemistry of Hawaiite Lavas From Crater Flat, Nevada," *Contributions in Mineralogy and Petrology* **80**, 341-357 (1982).
- Wadge G., "Steady state volcanism: Evidence from eruption histories of polygenetic volcanoes," *Journal of Geophysical Research* **87**, 4035-4039 (1982).
- Wallmann, P. C. I. Miller, and R. Kossik, "Assessment of Volcanic and Tectonic Hazards to High Level Radioactive Waste Repositories," *Proceedings High Level Radioactive Waste Management, American Nuclear Society* **4**, 188-195 (1993).
- Wallmann P. C., "A Technique for Calculation of the Probability of Dikes Intersecting a Repository," *American Nuclear Society Focus* (in press).
- Walpole, R. E., and R. H. Myers, Probability and Statistics for Engineers and Scientists, Fifth Edition, Macmillan Publishing Company, New York, NY, (1993).
- Wells, S. G., L. D. McFadden, C. E. Renault, B. D. Turrin, and B. M. Crowe, "A geomorphic assessment of Quaternary volcanism in the Yucca Mountain area, Nevada Test Site, southern Nevada: Implications for the proposed high-level radioactive waste repository," *Geology* **18**, 549-553 (1990).
- Wells, S. G., B. M. Crowe, and L. D. McFadden, "Measuring the Age of the Lathrop Wells Volcanic Center at Yucca Mountain," *Science* **257**, 555-558 (1992).
- Whitney, J. W., and R. R. Shroba, "Comment and Reply on Geomorphic Assessment of late Quaternary Volcanism in the Yucca Mountain Area, Southern Nevada: Implications for the Proposed High-Level Radioactive Waste Repository," *Geology* **June**, 661-662 (1991).
- Wilshire, H. G., McGuire, A. V., Noller, J. S., and B. D. Turrin, "Petrology of lower crustal and upper mantle xenoliths from the Cima volcanic field, California," *Journal of Petrology* **32** 169-200 (1991).
- Wilson, L. and J. W. Head, "Ascent and Eruption of Basaltic Magma on the Earth and Moon," *Journal of Geophysical Research* **86**, 2971-3001 (1981).
- Wood, C. A., and J. Kienle, *Volcanoes of North America*, Cambridge University Press, Cambridge (1990).

Wright, L. A., "Overview of the Role of Strike-Slip and Normal Faulting in the Neogene History of the Region Northeast of Death Valley, California-Nevada," Nevada Bureau of Mines Open-File 89-1.

Yunker, J. L., W. B., Andrews, G. A. Fasano, C. C. Herrington, S. R. Mattson, R. C. Murray, L. B. Ballou, M. A. Revelli, L. E. Shephard, W. W. Dudley, D. T. Hoxie, R. J. Herbst, E. A. Patera, B. R. Judd, J. A. Docka, and L. D. Rickertsen, "Report of the Early Site Suitability Evaluation of the Potential Repository Site at Yucca Mountain, Nevada," Science Applications International Corporation Report SAIC-91/8000 (1992).